Chapter 4
Physical Factors of the Environment

Physical influences from the environment on biological systems are considered an energetic, as well as an informational input. This chapter therefore on the one hand refers to the biophysical basis of sensory systems, and on the other hand to the input of energy. This energy input can occur either by a specific mechanism of absorption, for example in the case of photosynthesis, where the energy of photons is transformed into chemical energy, or it can be absorbed in an unspecific way, randomly modifying molecules or directly dissipating in the form of heat.

Beside aspects of sensory physiology, these interactions therefore concern the fields of environmental biophysics especially problems of radiation protection, as well as medical physics in respect of therapeutic and diagnostic use of physical influences.

In order to affect the molecular structures of a biological organism, the input energy must overcome the activation energy of a particular biochemical reaction or molecular displacement. Regardless of whether this energy input is sufficient for this or not, in any case this interaction finally ends in thermal motion, or using the language of phenomenological thermodynamics: in entropy dissipation. This eventually leads to a greater or smaller increase of the temperature in the system, and possibly to thermal effects.

Already in 1817 Theodor Grotthuss and John W. Draper stated that only that light which really is absorbed by a system can bring about a photochemical change. This circumstance has been generalized as the so-called *Grotthuss–Draper principle*, whereby it is not the energy penetrating the organism which is effective, but that part of the energy that is actually absorbed by the system. Investigations into the mechanism of molecular interaction, which forms the basis of all questions of the influence of any physical input into a biological system, therefore start with the question: how and where is this kind of energy absorbed? Eventually it must be clarified whether particular changes are induced by the absorbed energy, and how these influence the biological system.

In any case the relation must be considered between the absorbed energy, and the energy of thermic noise (kT, resp. RT, see Sect. 2.1.5). This question, however, cannot be answered in a general way. The prerequisite is knowledge of the particular molecular absorption mechanism. In many sensory systems special mechanisms are

R. Glaser, *Biophysics*,
DOI 10.1007/978-3-642-25212-9_4, © Springer-Verlag Berlin Heidelberg 2012

developed to overcome thermal noise. Conversely, a particular noise can even increase the sensibility of a sensory system through stochastic resonance (see Sect. 3.1.5).

As a peculiarity of biological systems particular cascades of amplification exist. Very small amounts of energy, occasionally being absorbed at particular targets, can significantly influence biological mechanisms of control, and eventually will be expressed in a macroscopically visible way. The place of interaction in this case does not need to be a specific receptor, but possibly it could be a crucial point in the network of reactions. An example of this is the induction of mutations by ionizing radiation. In this case a single modification of a DNA molecule could lead to dramatic consequences in the system. Even if the theory of biological amplification was first developed in radiation biology, it is crucial also for a number of other physical influences.

In this context it should be noted that organisms have adapted through evolution to all physical parameters of their environment. In this sense, for example, the development of double-stranded DNA could be considered as a precaution against single-strand breaks caused by ionizing radiation from the natural environment. Additionally, a large number of mechanisms have been developed to repair these kinds of damage. In this context the problem is relevant, how does the range of completely new environmental influences caused by man affect life today. This is a topical problem of environmental biophysics concerning especially electromagnetic influences of power lines and various radio frequency-emitting devices.

Further Reading

On environmental biophysics in general: Campbell and Norman 1998.

4.1 Temperature

In Sect. 2.1.5 the Arrhenius equation was introduced to describe the temperature dependence of chemical reactions. We learned that all elementary reaction steps will be accelerated by an increase in temperature helping to overcome the corresponding activation energies. In this way, even concentrations of metabolites in a steady-state system can be changed. Degree and direction of these changes depends on the extent to which two opposing fluxes are affected by temperature alterations. If for example, in an open system the temperature dependence of the rate of decomposition resp. of the efflux of a certain component is predominant then with rising temperature the corresponding steady-state concentration decreases, and vice versa. It follows that in complex systems, an increase in temperature can lead to an increase, as well as to a decrease in the overall activity. An optimum of temperature therefore exists for all biological functions.

There are two possible strategies that the biological system may use to handle temperature changes in the environment. On the one hand there exist various mechanisms of protection against the results of dangerous heating or cooling, and on the other hand some organisms achieve a constant temperature in their body, which is more or less independent of the temperature of the environment. Both of

these mechanisms require a precise system of thermoreceptors. In homeothermic animals, such as birds and mammals, but also in some poikilothermic organisms a particular mechanism of thermoregulation exists.

Let us first consider the systems of *temperature sensation*. Some animals possess a particular receptor system for infrared light, such as for example some snakes (*Boa constrictor*, *Crotalus atrox*) and insects (fire beetles, mosquitoes) which aid them in hunting, feeding, and overall survival. As much as is known to date is that these organs do not contain specific quantum receptors for infrared, but in these sensors the IR radiation is transformed into temperature changes of particular thermosensitive membranes. It has been calculated that for example thethermosensitive membrane in the pit organ of snakes already activates at temperature alterations of 0.003–0.01 K. The threshold for temperature perception in the receptors of human skin is only in the range of about 0.06 K.

A particular kind of temperature response is *thermotaxis*, the oriented movement of organisms in a thermal gradient. This kind of behavior can be seen in various organizational levels from bacteria (*Escherichia coli*) to more highly organized organisms (*Caenorhabditis elegans*); its molecular mechanisms, however, remain largely unknown.

Recent research, however, allows some insights into the molecular basis of thermoreception itself. In general two different types of thermosensitive molecules have been found. The members of one family are temperature-dependent RNA molecules, forming a special kind of *riboswitch*, which have been found in bacteria and in cells of many other organisms. In *E. coli* for example, these molecules are responsible for the activation of enzymes for the synthesis of new phospholipids, for regulation of the expression of heatshock proteins, etc. In the particular case of *E. coli* the metabolism is activated if the bacterium is transferred from a cold environment into a warm homeothermic organism.

The other type of thermoreceptor molecules are membrane-located proteins, such as for example some of the so-called TRPV-transport proteins, which usually are cation channels, located in the membrane of various cells everywhere in the living world (TRP stands for "transient receptor potential," V indicates a vallinoid-sensitive subfamily). These molecules are not only distributed in skin and various endothelial cells, but they are especially responsible for thermoreception in neurons. Recently they have also been found in the thermosensitive membrane of the pit organs of rattle snakes.

A characteristic of both types of thermosensitive molecules is their property to achieve particular structural conformations always in a quite close temperature range. In this case the RNA riboswitches will be activated, resp. the gating mechanisms of the protein channels change their transport properties. Recently it was shown that the pathway for temperature-dependent activation of TRP channels is distinct from those for ligand- and voltage-dependent activation and involves the pore turret. The pore turret therefore, is an important part of the heat activation machinery of this molecule.

As an example, Fig. 4.1 shows the abrupt change of the permeability of a thermosensitive cation channel TRPV4 at 24°C, which is characterized by the average current in a patch-clamp experiment. As explained in Sect. 2.1.5, the Q_{10}-parameter is

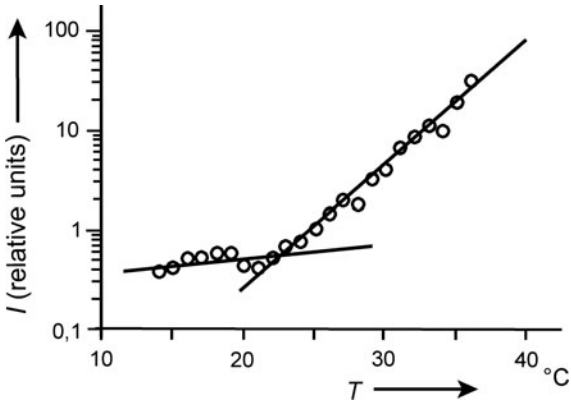

Fig. 4.1 Heat-activated average current (normalized to that at 25°C) in a temperature-sensitive TRPV4-channel. The lower slope exhibited $Q_{10} = 1.6$; the higher slope $Q_{10} = 19.1$. From the intersection of these two lines, the threshold temperature was estimated to be 24°C. In Fig. 2.4 the same data are demonstrated in an Arrhenius plot (Data from Watanabe et al. 2002)

an indicator for the increase of a reaction rate in the temperature range of 10 K. For biochemical reactions this factor usually amounts to around 2. This is in fact also the case for this transport protein in the temperature range below 24°C. At higher temperatures, however, this factor abruptly increases up to 19.2. Small temperature elevations therefore dramatically increase the transport rate of this channel.

Thermosensitive cells usually contain a large amount and diversity of such molecules. Each of these kinds of receptor molecules operates over a specific temperature range and also in a specific way. In some cases biochemical reactions as a whole exhibit a so-called *non-Arrhenius* behavior. This means that an increasing activity is seen in one, and a decreasing activity in another temperature region, caused by the combined action of cold and warm receptors. Of course, this contradiction to the Arrhenius rule is only apparent, because in fact each class of these molecules behaves exactly according to the rule, but one changes the process in one direction, while the other changes it in the opposite direction.

Thermoregulation itself is controlled by these thermoreceptors which are distributed everywhere in the body. In Fig. 4.2 the system of thermoreception in men is illustrated schematically, starting at the molecular thermosensors in thermoreceptor cells and finally leading to psycho-physiological reactions in the brain. This scheme illustrates the noise reduction of this system by averaging over a large number of receptors, the local consequences of thermoreception in each position (the system of thermosensitive riboswitches is not included), and finally the information processing in the hypothalamus. For minimal temperature changes, only the local reactions will be activated without sending the signal to the cortex. This means that various physiological regulations are possible even without a conscious feeling of warmth or cold.

The regulation of temperature in the body in general is considered a steady-state system composed of heat production through metabolism on the one hand, and heat dissipation into the environment on the other hand. In Fig. 4.3 different forms of heat transport between an organism and its environment are illustrated. In general, a distinction has to be made between conduction, convection, radiation, and heat loss due to evaporation of water. It is possible to define a thermal flux ($\mathbf{J}_Q$) which is the thermal energy that is exchanged per unit of time across a particular area of the surface.

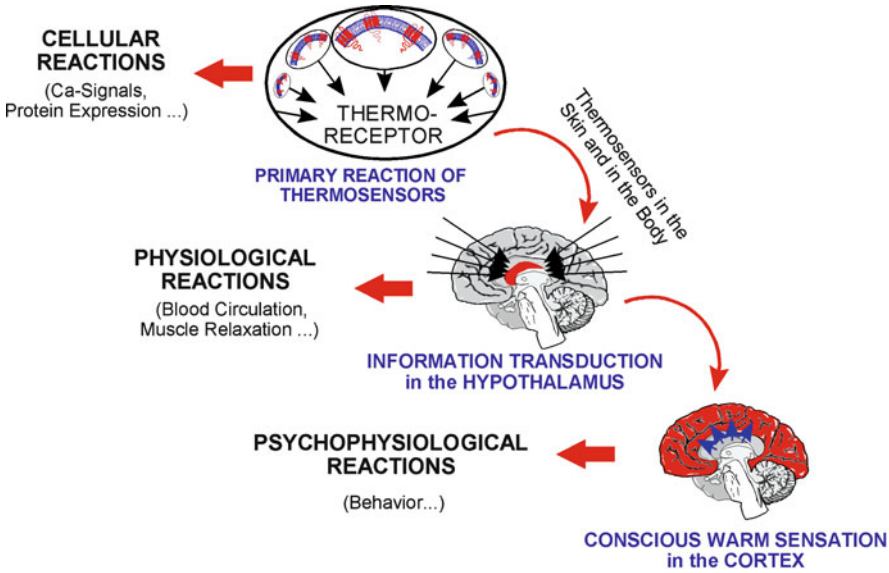

Fig. 4.2 A schematic illustration of the steps in the hierarchic system of neuronal thermosensation, starting from molecular reactions in thermoreceptor cells, up to the information center in the hypothalamus, leading under some conditions to a conscious warm sensation. In each of these steps, filtering is accomplished to reduce noise, and each step is sensitive to physiological influences. Other thermally sensitive effects, such as variation in expression of heat shock protein or effects of thermoregulatory changes in blood flow, are possible at each stage of thermoregulation (After Foster and Glaser 2007 modified)

Thermal conductivity is governed by *Fourier's law*, an equation which corresponds to the first Fick's law, which was used to calculate the diffusion of a substance (see Sect. 3.3.1, Eq. 3.131). For a temperature gradient in the x-direction, the heat flux $\mathbf{J}_{Qc}$ (in J m^{-2}) can be calculated by the following equation:

$$\mathbf{J}_{Qc} = -\lambda \frac{\mathrm{d}T}{\mathrm{d}x} \tag{4.1}$$

The negative sign indicates the direction of the thermal flux from higher to lower temperature. The factor λ in this equation is the *thermal conductivity*, also called *thermal coefficient*. It has the measuring unit J m^{-1} s^{-1} K^{-1}, accordingly: Wm^{-1} K^{-1}. In Table 4.1 some examples of thermal conductivity are listed. The data shows the good thermal insulating properties of a layer of fat.

Relating to the diffusion of substances the heat flux can also be included into the flux matrix (Sect. 3.1.3, Eq. 3.58), and consequently it can be coupled with the transport of matter, the so-called thermodiffusion.

If the stationary heat flux (Eq. 4.1) is not of interest, but the time dependence of the temperature at a particular point in a heat-conducting medium, than in

Table 4.1 Thermal conductivity for various tissues and other biological materials (After Precht et al. 1955)

	Thermal conductivity [J m^{-1} $s^{-1}K^{-1}$]
Tissue in vitro	
Human skin: epidermis and corium	0.34
Epidermis (pig)	0.21
Fat (pig)	0.17
Muscle (pig)	0.46
Living tissues in situ	
Human skin, poor blood flow	0.31. . .0.33
Human skin, strong blood flow	1.5
Human muscle, no blood flow	0.46
Human muscle, normal blood flow	0.53
Human muscle, strong blood flow	0.63
Hair and feathers	
Wool (loose)	0.024
Feathers	0.024
Rabbit fur	0.025
Other substances	
Air	0.023
Water (20°C)	0.59
Silver	420

correspondence to the second Fick's law (Eq. 3.132), the second deviation of the temperature is included:

$$\frac{\partial T}{\partial t} = \frac{\lambda}{\rho C} \nabla^2 T \tag{4.2}$$

In contrast to Eq. 4.1, here the three-dimensional temperature gradient is considered. The Nabla operator (∇) stands for grad T, i.e., for deviation of T with respect to x, y, and z. The operator ∇^2 means the second derivation, the same as: div grad T. This equation contains the specific heat capacity (C) which in biological tissue amounts to approximately 3,600 Jkg^{-1} K^{-1}, and the density (ρ in kg m^{-3}).

Convection allows a very intensive heat transport at physiological temperatures. As shown in Fig. 4.3, convection in homoiothermic animals is mediated internally through blood circulation, and externally through the flow of air or water. At constant flow, the amount of heat transported by convection is proportional to the temperature differences between the two phases. The flow rate on the one hand, and the geometric conditions of the boundary layer on the other are crucial for the effectiveness of this kind of heat transfer. The level of convection depends on the thickness of unstirred layers of air or water near the body, and on the flow behavior at the boundary layer (see Sect. 3.7.1). This insulating layer in some cases is improved artificially by hairs or feathers.

Thermal radiation is an electromagnetic radiation in the Terra-Hertz or IR frequency range (see the spectrum in Fig. 4.32). To investigate thermal radiation, a so-called *black body* is used. This is a physical body that will completely absorb

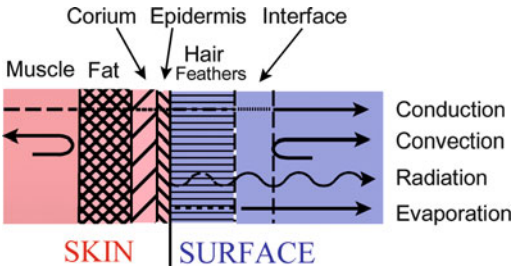

Fig. 4.3 Various forms of heat transport between the body and its environment

all of the infrared radiant energy that falls on it, and correspondingly changed its temperature. The black body is also suitable for measuring the radiation which is emitted by an object at a given temperature. In contrast to the other kinds of heat transfer, thermal radiation does not depend on the temperature difference between the body and the environment but rather on the absolute temperature of the emitting body itself, whereas the temperature (T) occurs in the fourth power. The amount of heat emitted by a black body ($\mathbf{J}_{QR}$) obeys the *Stefan–Boltzmann law*.

$$\mathbf{J}_{QR} = \sigma T^4 \tag{4.3}$$

The proportionality constant is $\sigma = 5.67 \cdot 10^{-8}$ $\mathrm{Wm^{-2}\ K^{-4}}$. Additionally, a correction factor is used if the surface of real bodies does not behave like a black body. For the surface of biological objects it lies between 0.9 and 1. The value depends on the pigmentation of the organism.

Evaporation of water is an important mechanism of temperature regulation of animals living in air. The evaporation of 1 g of water will cause the body to lose about 2.4 kJ. The rate of evaporation depends on the surface structure, on the wind velocity, and on the difference in the vapor pressure between the surface of the body and the surroundings. Because the vapor pressure is temperature dependent, evaporation can still take place when the air is saturated with moisture provided that the ambient temperature is below the body temperature.

For a number of problems in the field of occupational health and safety, as well as in various kinds of therapeutic treatment the overall temperature balance in the human body is of interest. What is the temperature increase in a particular part of the body if it is exposed for example to ultrasound, or to high-frequency electromagnetic fields, or other kinds of energy input (see Sects. 4.3.5, 4.7)? In 1948 Harry H. Pennes developed the so-called *bioheat equation*, which is an expression of the heat balance in the body as the result of internal and external heat exchange.

In its general form this equation can be written as follows:

$$C\frac{\partial T}{\partial t} = \frac{\lambda}{\rho}\nabla^2 T + SAR + \Phi - B(T - T_B) \tag{4.4}$$

The first term in the sum corresponds to the heat conduction (Eq. 4.2). The second summand reflects the heat input from outside, whereas SAR means *specific*

absorption rate (for more detail see Sect. 4.7.1). $\mathbf{\Phi}$ is the Rayleigh dissipation function (see Sect. 3.1.4, Eq. 3.64), and represents the heat production by metabolism. The last negative term concerns the heat acquisition by blood circulation. This in fact is a quite complex expression, including various anatomical and hemorheological properties. All the summands in Eq. 4.4 have the measure Wkg^{-1}.

This equation can be solved only using particular assumptions of the included parameters. It becomes even more complex if it is considered that the parameters C, λ, and ρ in fact are space-dependent functions.

Further Reading

General aspects: Ahlborn 2004; Foster and Glaser 2007; Hirata et al. 2009; molecular aspects: Digel et al. 2008; Yang et al. 2010; thermoreception in snakes: De Cock Buning 1983; Gracheva et al. 2010.

4.2 Pressure

Pressure, in addition to other influences on systems in equilibrium, is governed by the *Le Chatelier principle*. It states that if a system at equilibrium experiences a change in various conditions (e.g., concentration, temperature, volume, or pressure), then it shifts to counteract the imposed change. This reaction scheme was mentioned in Sects. 2.2.3 and 2.3.2 in context with processes of self-assembly of supramolecular structures. The thermodynamic explanation of Le Chatelier's principle is provided by the Gibbs equation (see Sect. 3.1.2, e.g., Eq. 3.29). Amongst other factors, this equation indicates the shift of the energy of the system as the result of pressure alterations.

Simply put, pressure will change the volume of gas-filled cavities in biological systems. Another mechanism involves the pressure dependence of the solubility of gases in the various aqueous phases such as blood and tissue. Le Chatelier's principle in this case is reflected in the circumstance that the volume of the mixed phases liquid + gas is larger than the gas dissolved in the liquid. The reversible effect is well known as the exsolution of carbon dioxide when opening a bottle of sparkling mineral water.

These kinds of pressure effects occur already at moderate degrees of pressure alterations. They are important for problems in occupational medicine and sports. The reduced oxygen solubility in the blood which occurs for example at great heights, is particularly important for alpinists and pilots. This oxygen deficit can be compensated for by an increase in the partial pressure of oxygen in the inspired air. If humans remain under an increased pressure, for example in the case of divers, the reverse effect occurs, namely an increase in the amount of dissolved gas in the blood. At greater depth this may lead to a dangerous shift in the proportions of dissolved gases. In the case of a fast return to normal atmospheric pressure, especially following a long stay at great depth, gas bubbles are formed in the blood (mainly N_2). This can cause aeroembolism, which is also called the bends

or *Caisson disease*. In general, the term *barotrauma* is used to denote various kinds of physiological damage caused by pressure alterations.

Another mechanism of pressure interaction involves different changes in the partial mole volume of various reaction components. This also leads to a shift of the equilibrium distribution according to Le Chatelier's principle. The range of pressure changes that affect this mechanism without participating gas phases is much higher than that for the cases mentioned earlier. This mechanism forms the basis of the so-called *high-pressure biotechnology*, which has been developed in recent decades. It is an interdisciplinary field of science in which pressure is applied to biological systems in order to address a wide range of issues of relevance to biochemistry, biophysics, biotechnology, and the environment.

The ecological aspect of pressure influences arises from the fact that 70% of the surface of the earth is covered by oceans with an average depth of 3,800 m. Fifty percent of the surface of our planet is covered by water at least 4,000 m deep. In fact this is the depth with the greatest number of different species. Considering that at an increase in depth of 10 m the pressure increases by about 0.1 MPa, deep-sea organisms live under conditions where the hydrostatic pressure can be as high as 100 MPa. Some organisms are called *piezophiles*, i.e., they are especially adapted for life under conditions of high pressure. So for example deep-sea microbes have been isolated from both cold and hot deep-sea environments which for their growth indicate an upper pressure limit of 130 MPa. In processes of high-pressure biotechnology the applications of pressure extend even up to 600–800 MPa, and sometimes higher. The word *piezophysiology* was proposed to describe the unique cellular responses to high pressure in living cells.

Since the early 1990s high pressure has been used also as a nonthermal method in the commercial processing of foods. The term *pascalization* was introduced for a method of pressure preservation in contrast to heat treatment of food by *pasteurization*. It turned out to be an effective approach for inactivating microbes and viruses. In some cases high-pressure treatments may cause changes which are not observed under other conditions.

What are the molecular mechanisms of these processes? As already mentioned in Sects. 2.2.3 and 2.3.2, mainly the water structure and the corresponding hydrophobic reactions are responsible for these processes. As illustrated in Fig. 2.19 the degree of orientation of the water molecules strongly influences its partial mole volume. In the case of highly condensed or coiled macromolecules the amount of bound, and therefore structured water molecules is lower than in the case of loosely packed or uncoiled macromolecules. The same concerns supramolecular structures like membranes, cytoskeleton, microtubules, etc. According to Le Chatelier's principle the application of pressure shifts the equilibrium toward higher structured water, i.e., to the condition of lower organized macromolecules. Thus, all these macromolecular and supramolecular structures that are stuck together by hydrophobic interactions will be destabilized under extremely high pressure conditions. Life in the deep sea is possible only if this risk is compensated for by special adaptations. For example, in this regard, it was found that the actin and other

proteins from deep-sea fishes have unique amino acid substitutions in comparison to those of non deep-sea fishes.

High-pressure biotechnology exploits the possibility to optimize biochemical reactions using structural peculiarities of these molecules. In this way some enzyme activities can be substantially elevated by increases in pressure.

Further Reading

Bartlett 2010; Péqueux and Gilles 1985; Winter 2003.

4.3 Mechanical Oscillations

Mechanical oscillations, on one hand, can influence biological systems directly by an input of considerable energy; on the other hand, they can be recorded by animals with the help of highly specified receptors and serve as physical carriers of information. Oscillations in the air at frequencies between 16 Hz and 20 kHz are perceived by humans as sound. Low-frequency oscillations (lower than 20 Hz) are called *infrasound*, while high-frequency oscillations (higher than 20 kHz) are called *ultrasound*. Besides this, vibrations can also influence biological systems by direct contact with vibrating materials at various frequencies. Because of these peculiarities, these kinds of vibrations will be considered in a separate chapter.

4.3.1 Vibration

Biological effects of vibration, on one hand, are of particular interest in occupational medicine; on the other hand, they are used in various kinds of medical treatments and for training aspects in sports. Vibrating seats of tractors, trucks, cars, etc., which create whole body oscillations, as well as the use of various vibrating handheld machineries, which create vibrations of the arms and hands, are considered as possible sources of occupational diseases. Whole body vibrating devices are used for therapeutic purposes to treat particular body parts affected by sports injuries.

If the body is treated by harmonic oscillation with the angular frequency ω, the displacement $x(t)$ occurs in the form:

$$x = x_{\max} \sin \omega t \tag{4.5}$$

where x_{max} is the amplitude of this oscillation. Deriving this equation in respect to the time (t), the function for the vibration velocity $\mathbf{v}(t)$ is obtained by:

$$\mathrm{v} = \frac{\mathrm{d}x}{\mathrm{d}t} = \omega\, x_{\max} \cos \omega t = \mathrm{v}_{\max} \cos \omega t \tag{4.6}$$

These equations, though, represent only a simplified case. The vibrations usually occur in all directions, i.e., the derivatives of x, y, and z should also be considered.

In order to evaluate its influence on living systems, the energy input of this vibration is required. This is a function of the acceleration (a), resulting from the second derivation of Eq. 4.5:

$$a = \ddot{x} = -x_{\max}\omega^2 \sin\omega \tag{4.7}$$

with a peak acceleration:

$$a_{\max} = x_{\max}\omega^2 \tag{4.8}$$

Usually, the total vibration exposure for sinusoidal oscillations is expressed by RMS (root-mean-square) given by:

$$a_{\mathrm{RMS}} = \frac{a_{\max}}{\sqrt{2}} \tag{4.9}$$

In the case of a time variable intensity of the exposition, the root-mean-square of the frequency weighted, a_{RMS}, is evaluated, where t_D is the duration of the exposition:

$$a_W = \sqrt{\frac{1}{t_D}\int_0^{t_D} a_{\mathrm{RMS}}^2(t)\mathrm{d}t} \tag{4.10}$$

The use of frequency weighted exposition results from differences in the biological effectiveness of vibrations. For this, a frequency-dependent evaluation factor is introduced, based on empirical values (Fig. 4.4). There are only slight variations when applied to the whole body or only to parts of the body, like the arms and hands. This curve shows that for biological systems, the most effective frequencies are in the region of about 10 Hz.

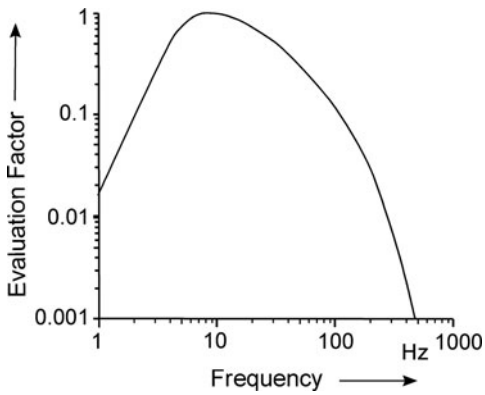

Fig. 4.4 Evaluation factor indicating the relative sensibility of human body to vibrations in dependence of the frequency

Another problem consists in determining the kind of mechanical coupling used to link the body to the oscillating materials and transmitting the vibration to its different parts. As an example, Fig. 4.5 shows the movement of the head, shoulders, and hips of a person sitting on a vertically vibrating seat. The relation between the amplitude of vibration of the specific points of the body and the amplitude of vibration of the support is depicted on the ordinate. This demonstrates that the amplitudes of vibration in different parts of the body are different and a function of frequency. At frequencies below 2 Hz, the body simply follows the movement of the seat, i.e., the degree of amplification is about 1. When the applied frequency is approximate to the resonance frequency or equals it, the amplitude of the enforced oscillation is greater than that of the seat. Even at the fundamental resonance frequency of a human body of about 5 Hz, differences are observed between vibrations of head, shoulder, and hip. This is the frequency at the maximal displacement of all three reference points. The head, furthermore, shows a second maximum of vibration amplitude at about 20 Hz. A further increase in the external frequency leads to a decrease in the coupling efficiency up to 0, at $\omega \Rightarrow \infty$.

The biophysical evaluation of possible mechanical influences on cells and organs, like muscles, joints, and bones, requires analytical models based on data of viscoelastic properties of the tissue. The oscillation of a mechanical system can be treated analog to the electrical oscillations of an RCL circuit (see also Sect. 3.5.3). Similar to these approaches, complex parameters are used to describe damping and elastic parameters of these mechanical systems. In analogy to electrical systems, a *mechanical impedance* of the system can be defined. It is the relation between vibrational force and vibrational velocity.

In practice, the quantitative evaluation of possible exposition of humans in vibrating devices is quite complicated. In most cases, the vibration does not consist of only simple sinus waves, but rather a sum of many frequencies differing in

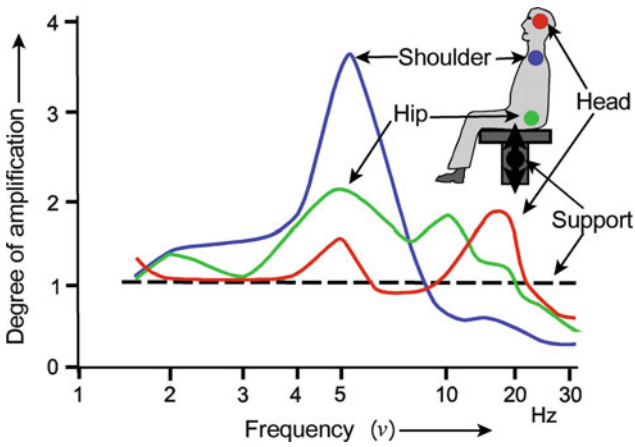

Fig. 4.5 The amplification factor for vertical oscillations at various points of the body of a man sitting on a vibrating support as a function of frequency (Redrawn from Dieckmann 1984)

amplitude as well as in phase. Using Fourier analysis, these can be regarded as a sum of many sinusoidal oscillations. On the other hand, the biological influence of vibration cannot be calculated simply by physical models, using passive mechanical properties of anatomical constituents of the body. It must be taken into account that forces are generated by the muscles actively trying to compensate the external stress. This, however, in some cases, can lead to an opposite effect, namely, to an additional strain on the joints. In general, one must take into consideration that the mechanical impedances of parts of the body are influenced by neurophysiological processes.

As already mentioned, the biological effects of vibration find applications not only in occupational medicine but, to some extent, also in therapeutics, rehabilitation, and preventive medicine, as well as in sports and in prevention of degenerative effects due to loss of weight in men. Vibration exercises activate the muscles, induce warm-up effects, and help to improve flexibility. In general, as an effect of vibration, muscles and tendons tend to elongate initially (stretch phase), followed by a period of shortening (shortening phase). Vibration, therefore, can be characterized by a cyclic transition between eccentric and concentric muscle contractions. In the same manner, it acts on joints and bones, while strain energy density or fluid flow may serve as osteogenic stimuli. Vibration can affect muscle perfusion and increase the metabolic demands of the contracting musculature. These reactions are partly stimulated by mechanoreceptors, such as *Meissner corpuscles*, which are most responsive around 40 Hz, and the *Vater-Pacini corpuscles*, in the frequency region of 100 Hz and above.

The question whether these frequencies are detrimental in the sense of occupational protection or helpful regarding therapy or sports apparently depends on the intensity, duration, and the kind of exposure. The long-term biological effects of whole body vibrations consist mostly of wear of the joints. Continuous use of vibrating handheld machinery or exposure to other kinds of local vibrations may cause the hand-arm vibration syndrome or the *Raynaud's phenomenon*, a vasospastic disorder causing discoloration of the fingers, toes, and occasionally other extremities.

The frequency range below 2 Hz shows some neurophysiological peculiarities. At these extremely low frequencies, the effects of vibration cannot be simply attributed to mechanical processes. This applies, for example, to the occurrence of *kinetosis*. Particularly, a frequency of 0.3 Hz causes seasickness. All these conditions are caused by neurophysiological influences and are induced by the vestibular system that detects accelerations of the head. This can lead to variations in blood circulation, along with all subsequent physiological consequences.

The mechanisms by which humans and animals can perceive vibrations are a special field of research. Humans, for example, can detect a frequency of 200 Hz with an amplitude of only 0.1 μm! The sensibility of insects and spiders can be several orders of amplitude higher.

For water-gliding insects that hunt for objects fallen on the surface of relatively still ponds, the surface waves act as important signals. The propagation of these waves, its velocity and frequency are functions of surface tension and density of water. The typical frequencies are in the range of 10–100 Hz and the propagation speed between 0.3 and 0.5 m/s.

Further Reading

Arnason et al. 2002; Fritz 1998, HVDI 2057 2002; Mansfield 2005; Rittweger 2010; Rossing and Fletcher 2004; Wilson 1994.

4.3.2 Sound

Sound consists of longitudinal, i.e., compression, waves transmitted through solids, liquids, or gases. This leads to periodic deviations in pressure from that at the equilibrium. As a result of this pressure oscillation (p in N m^{-2} = Pa), a certain *particle displacement* (Δx) occurs, with a *particle velocity* v_P, and, therefore, an energy dissipation. The power density of sound is termed *sound intensity* (I in W/m^2). The physical link between these parameters is given by the *acoustic impedance* (Z in N s m^{-3} = Pa s m^{-1}), which itself appears as a function of frequency. These parameters are linked by the following relations:

$$p = \rho v_S \omega \Delta x = Z\omega\Delta x = Zv_p \tag{4.11}$$

and

$$I = Zv_p^2 = \frac{p^2}{Z} \tag{4.12}$$

where ρ is the density of the medium (in kg m^{-3}) and v_S is the speed of sound, distinct from the particle velocity v_P. The values of these parameters for air and water at 20°C are listed in Table 4.2. The parameters of soft tissue are similar to that of water, whereas the speed of sound in bone is much greater.

To characterize the sound intensity, a unit that was first applied in the Bell Telephone Laboratories to characterize the quality of telephone transmission is used. A *Bell* was defined as the base-10 logarithm of the ratio of the measured power to a reference power. Later, the *decibel* (dB) was used, which was ten times the base-10 logarithm of the ratio of measured power to reference.

This parameter, which is used widely in engineering techniques, coincides with experiences in the physiology of sensory reception. At the end of the nineteenth century, the physiologist Ernst Heinrich Weber found that alterations of external signals are perceived more sensitively the lower the absolute intensity of the signal is. Later, the psychologist Gustav Fechner elaborated the theoretical interpretation of this connection and formulated the logarithmic relation between stimulus and perception. This is the so-called Weber–Fechner law, which is valid for all kinds of sense organs.

Table 4.2 Acoustically relevant parameters of air and water

Medium	Density (ρ) [kg m^{-3}]	Speed of sound (v_S) [m s^{-1}]	Acoustic impedance (Z) [N s m^{-3}]
Air	1.204	343	413.5
Water	$1 \cdot 10^3$	1 440	$1.44 \cdot 10^6$

According to these considerations, the *sound level* (L), which is measured in dB according to the intensity relation (I/I_0), is defined as follows:

$$L = 10 \log \frac{I}{I_0} = 10 \log \frac{p^2}{p_0^2} = 20 \log \frac{p}{p_0} \tag{4.13}$$

The introduction of p^2 instead of I corresponds to Eq. 4.12.

This relation requires the reference parameters I_0 and p_0. For this, the human hearing threshold level of 1,000 Hz was used as the reference frequency (see Fig. 4.6). The values for these parameters are $I_0 = 10^{-12}$ Wm^{-2} and $p_0 = 2{\cdot}10^{-5}$ Pa.

Figure 4.6 shows a frequency diagram of human auditory sense. The sound level (L in dB) and the sound pressure (p in Pa) are plotted against the frequency. To characterize the sensibility of the human ear at all frequencies, furthermore, the unit *phon* is introduced. By definition, one phon is the apparent loudness of a sound equal to 1 dB of a sound having a frequency of 1,000 Hz. As an example, in Fig. 4.6, the 60-phon curve is shown crossing the frequency of 1,000 Hz at the level of 60 dB. Similarly, the 0-phon curve is plotted, indicating the auditory threshold at all frequencies.

This indicates that a 50 Hz sound, for example, with an objective sound intensity level of 120 dB, subjectively seems to have the same loudness as a 1 kHz sound of only 60 dB. The phon unit, therefore, is a subjective measure which is related to a normal human ear.

It is, however, useful to evaluate not only various *pure tones* (sinus waves) but also *sounds* (true musical tones with overtones) and *noise* (random mixture of various frequencies). This evaluation depends not only on the loudness but also on the duration of the sound. Sounds with a duration less than 1 s will be subjectively underestimated.

Furthermore, a simple measurement of an overall sound intensity in dB is too crude to be used for practical environmental protection because of the broad

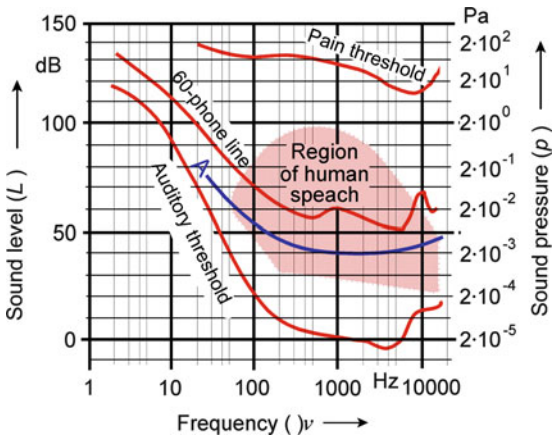

Fig. 4.6 Response of human ear to sound intensity. The curves are extended up to the frequencies of infrasound ($\nu < 20$ Hz) according to data from Møller 1984. A-40-phon weighting scale as in Fig. 4.7

variations of the character of noise. Usually, weighing scales are used to measure a particular noise (Fig. 4.7). These scales are determined empirically and fixed by standardization. They are always normalized for 1 kHz and take into account the frequency dependence of the sensibility of the human ear. With the help of these scales, it is possible to take into account the lower sensibility of the human ear to frequencies that are lower or higher than 1 kHz. Of course, such scales are dependent on the real character of the measured noise and on the question being asked. There are differences in the frequency mixture, depending on whether the noise comes from engines, from a discotheque, from traffic, or from other sources. It also makes a difference as to whether the noise limits of a workplace in a factory, in an apartment, or in a hospital are to be determined. Mostly, the weighing scale A (Fig. 4.7) is used. It particularly takes into account the low sensibility of the human ear to lower frequencies (Fig. 4.6), and not so much to the higher ones. A very flat scale B (not drawn) is not used anymore. Instead, the C-scale is used for noise in a very broad frequency range. The SI-scale considers particularly the disturbances in human communication. In Fig. 4.6, the parameters are shown according to the scale A to indicate its similarity to the sensibility of the human ear.

Figure 4.8 shows some examples of noise production from various sources. It has been known for a long time that in case of permanent exposure, vegetative diseases may possibly occur at 60 dB. The level of dangerous noise at low

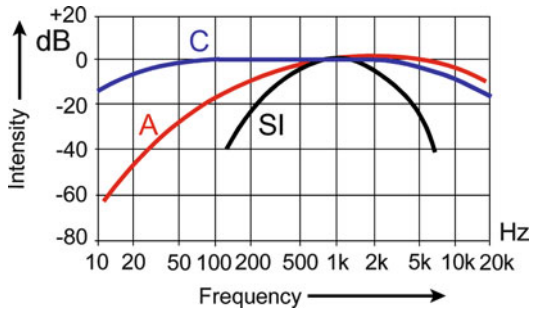

Fig. 4.7 Weighting scales for practical noise measurement (description in the text)

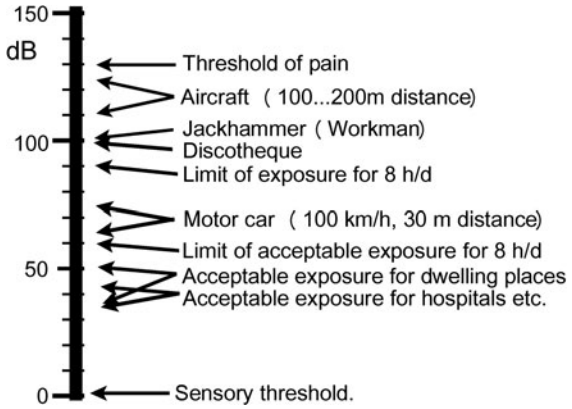

Fig. 4.8 Examples of noise production from various sources

frequencies is 80 dB and at high frequencies is 90 dB. Sound intensities that can induce acute injury lie above this region.

From the legal point of view, noise is a sound which is able to disturb, endanger, or significantly discriminate or cause inconvenience to neighbors or anybody else.

Further Reading

Everest and Pohlmann 2009; Rossing and Fletcher 2004; Wilson 1994

4.3.3 The Biophysics of Hearing

Anatomically, the ear can be divided into three parts: outer, middle, and inner (see Fig. 4.9). The eardrum, or the tympanic membrane, separates the outer ear from the inner ear, and both are air filled. The middle ear contains three ear ossicles (*malleus, incus, stapes*), which transmit the vibration from the eardrum to the oval window. The cochlea is a part of the inner ear, which also includes the vestibular apparatus, a sense organ for gravity and motion (not included in Fig. 4.9). The cochlea is a spiraled, hollow, conical chamber of bone, containing the *scala vestibuli* and the *scala tympani*, which are connected together at the top by the *helicotrema*. Both are filled with a sodium-rich perilymph. The scala tympani terminates at the round window. Between these two scales is located the scala media (see also Fig. 4.15), which contains the *organ of Corti* having hair cells that are vibration-sensible elements. The scala media as well as the vestibular apparatus is filled with potassium-rich endolymph.

The human ear as well as the ears of other vertebrates are amazingly optimized organs. This concerns not only the astonishing sensibility, the noise suppression, and the property to analyze the sound, but also its angular localization. All these properties are the result of an interplay of at least four components, each of them with particular mechanisms requiring different biophysical approaches, not including the neuronal sound analysis in the brain:

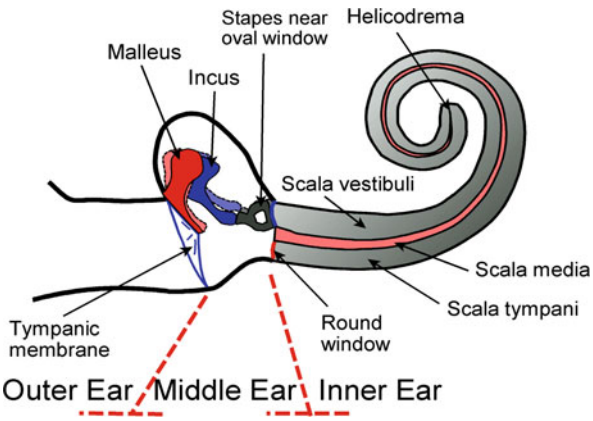

Fig. 4.9 Schematic illustration of the human ear consisting of the air-filled outer and middle ear, with the eardrum in between, and the inner ear, filled with perilymph (*scala vestibuli* and *scala tympani*)

- The outer ear, as an amplifier with particular frequency and angular characteristics
- The middle ear, as an adjustable impedance transducer, transforming vibrations of air in vibrations of a kind of an aqueous medium
- The cochlea, where traveling waves appear with frequency-specific maxima at particular locations
- The organ of Corti with hair cells as sensible noise-reducing elements, transducing vibrations into coded nerve impulses.

In this way, biophysical approaches are essentially applied to various different levels of organization, from laws of phenomenological acoustics up to various considerations at the cellular and the molecular level.

The *outer ear* consists of the pinna, the concha, and the auditory meatus. The human outer ear selectively concentrates the sound pressure by 30- to 100-fold at frequencies between 2 and 3 kHz. This corresponds to the frequency range of the human voice (see Fig. 4.6). At the same time, this amplification reduces the noise of other frequency bands. These characteristic frequencies of sound acceleration and filtering, and correspondingly also the anatomical structure of the outer ear, are optimized in various animals in different ways corresponding to conditions of their life.

Furthermore, the sensibility of the human outer ear, and even to a larger extent that of other animals, depends on the direction from where the sound comes. In general, however, the process of sound localization is based on the analysis of the time delay in which the sound reaches the two ears and on the evaluation of the differences in the corresponding intensities. Humans are able to localize a source of sound with an angular resolution of 3°. This means that the minimal time resolution of the differences of arriving auditory signals must be about 35 μs. In fact, the conversion of a mechanical stimulus into an electrical potential in the hair cells of the inner ear lasted as little as 10 μs. In fact, the entire process of angular sound localization occurs in the temporal lobe of the brain.

To differentiate between neurobiological and purely biomechanical mechanisms of sound analysis, the following experiments can be instructive. Two pure tones are transmitted by a headphone. In the first case, both of them are simultaneously transmitted into both earpieces, whereas in the second case, one tone is transmitted into the right and the other into the left earpiece. If both tones are mistuned, having nearly the same frequency, first-order beats occur, i.e., the amplitude of the resulting tone becomes low frequency modulated. This sort of mistuned sound is recognized if both tones are fed together into both earphones. In this way, a so-called first-order beat results, which is sensed in the inner ear. In contrast to this, tones with nearly harmonic frequencies, i.e., mistuned fourth or third, etc., produce *beats of the second order*, namely, a sort of frequency modulation. In this case, recognition is also possible if each tone is fed only into one of the two earphones, while no physical interference of the tones can occur. They come together only in the brain.

The *middle ear* is considered to be an impedance transformer, transmitting the air sound of the outer ear into sound of the aqueous medium of the inner ear. The acoustic impedance (Z) of the lymph in the inner ear, resembling that of water, is nearly four orders of magnitude larger than that of air. Equations 4.11 and 4.12 (Sect. 4.3.2) show the interdependence of sound intensity (I), pressure (p), and

particle displacement (Δx) with this parameter (Z). The amplitude of low pressure and large displacement in air, therefore, should be transformed into vibrations of an aqueous medium with high pressure and low displacement amplitude.

As the simplest approach to calculate this efficiency of the impedance transformation, a mechanical lever arm system can be considered (Fig. 4.10). The force from the vibrating eardrum that results from the product of pressure and area ($F_T = p_T A_T$) is boosted by the ossicles represented by the malleus lever (l_1) and the incus–stapes (l_2) lever arms in the relation l_1/l_2 and transmitted via stapes to the oval window. This produces a pressure: $p_o = F_T(l_1/l_2)/A_o$.

These considerations lead to the following relation of the pressure amplification in the middle ear:

$$\frac{p_o}{p_t} = \frac{A_t}{A_o}\frac{l_1}{l_2} \tag{4.14}$$

In Table 4.3, characteristic parameters of this system, as depicted in Fig. 4.10, are listed for humans and various animals of different sizes. An analysis of these data indicates that the absolute size of the auditory ossicles as well of the tympanic membrane and the oval windows corresponds in an isometric relation to the size of the animals (see Sect. 3.8). The transformer ratio (p_o/p_t), however, seems to be more or less independent of the size and ranges between 30 and 80.

This system of the auditory ossicles clearly indicates specific frequency characteristics of transmission. Their dimensions and mass as well as their mechanical inertia allows to calculate the maximal frequency limits of transmission (v_{lim}) (see Table 4.3), which correspond to the physiologically and behaviorally measured values.

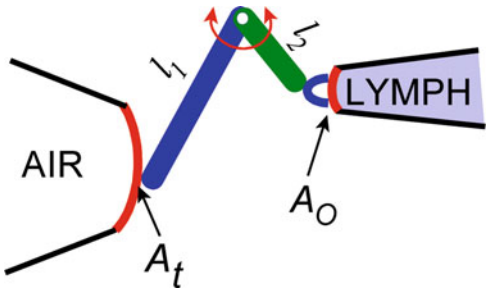

Fig. 4.10 Schematic illustration of the force acceleration in the middle ear between the tympanic membrane (A_t) and the oval window (A_o) by the malleus (*blue*, l_1) and the incus–stape (*green*, l_2) lever arms as a mechanical system (for corresponding values, see Table 4.3)

Table 4.3 Mechanical parameters of the middle ear of human and various animals corresponding to Fig. 4.10 (Data from Hemilä et al. 1995)

	A_t [mm^2]	A_o [mm^2]	l_1 [mm]	l_2 [mm]	p_o/p_t	v_{lim} [kHz]
Human	633	298	624	446	3,209	20
Indian elephant	454	136	163	85	6,409	10
Cattle	511	266	897	331	5,206	35
Dog	633	196	816	256	1,030	45
Rabbit	282	134	500	208	5,051	69
Mouse	422	15	200	52	108	92

As a result, our knowledge about the anatomy and physiology of the middle ear is improved, based inter alia on realistic 3D anatomical data from high-resolution CT scan. Obviously, the lever arm ratio of the middle ear ossicles is variable and, therefore, indicates a frequency-dependent transmission quality. Furthermore, the efficiency of this system is regulated by two small muscles that trigger the transmission by loud noise to protect the inner ear.

These circumstances are taken into account in new models, using the finite element method. The most significant development in these models is the inclusion of the function of ligaments and tendons in the middle ear as well as the properties of the external ear canal. These models allow to evaluate the static and dynamic behavior of middle ear components and to simulate various pathologic alterations.

The actual sound detection takes place in the *inner ear*. Early on, it had been found that the auditory nerve transmits so-called microphonic potentials, i.e., electrical vibrations analog to the received sound. These effects, however, are generated passively as a result of vibrations of the inner ear as inhomogeneous dielectrics. It remains unclear as to whether this has any physiological relevance.

In 1863, Hermann von Helmholtz proposed a resonance model to explain the frequency analysis of the inner ear. He postulated that the basilar membrane at particular locations along its extension shows resonance properties at various frequencies. For this kind of resonance, however, there is no experimental evidence. Nevertheless, his single-point theory of auditory perception, i.e., the idea that various positions in the basilar membrane would be sensible to particular frequencies, has been confirmed by George von Békésy (Nobel prize winner 1961), even though in quite a different way.

The sound, transmitted by the ossicles of the middle ear to the oval window, spreads out very fast through the cochlea and is finally damped at its end at the round window. In fact, the basilar membrane exhibits very specific viscoelastic properties along its extension. In humans, it is 35-mm long and gets tenfold wider over this diameter away from the oval window. Likewise, its elastic properties change. As shown in Fig. 4.11, the stiffness of the basilar membrane is reduced by about 100-fold with increasing distance from the oval window.

Investigations into the vibration characteristics of this system are very complicated. Békésy's theory can be understood using the mechanistic model shown in Fig. 4.12. To represent the sound in the cochlea, a rigidly coupled pendulum transmits its movement to a rotatable rod to which other pendulums are fixed. They are made of balls fixed on rods of various lengths, reflecting the above-mentioned viscoelastic differences along the basilar membrane. The oscillating movements of the axle cause all of these pendulums to move simultaneously at a given frequency, which, in most cases, does not correspond to the resonance frequency of the individual pendulums. Additionally, the pendulums are coupled to one another in series by threads weighted with small ball bearings. The degree of coupling depends on the point of attachment of these threads.

This model demonstrates the following properties of the inner ear. The sound waves spread so rapidly in the perilymph fluid that, similar to the effect of the axle in the model, there is a simultaneous stimulation along the entire length of the membrane.

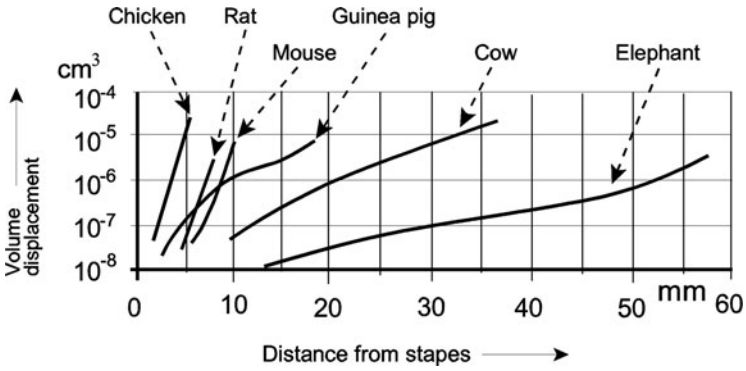

Fig. 4.11 The elasticity of the cochlear partition of various animals as a function of the distance from the stapes. As a measure, the volume displacement is used, produced in a 1-mm segment by a pressure of 1 cm of water (After Békésy, in Waterman and Morowitz 1965)

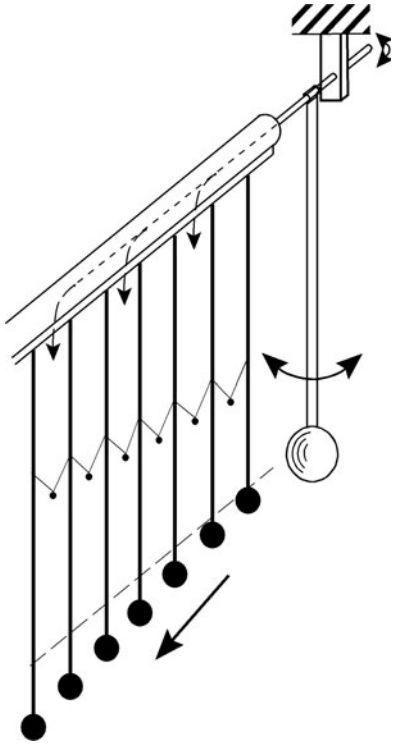

Fig. 4.12 Pendulum resonator model to demonstrate traveling waves in the inner ear (After Békésy, in Waterman and Morowitz 1965 modified)

The length and coupling of the pendulums correspond to the position-dependent viscoelastic properties of the basilar membrane. If this system is activated by a simple harmonic oscillation, traveling waves along the series of pendulums are generated, which always move from the stiffer to the more compliantly coupled pendulums. The

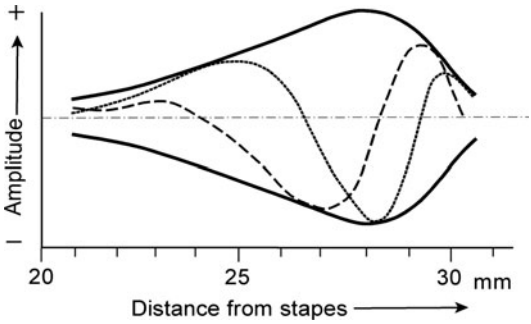

Fig. 4.13 Amplitude of cochlear vibration at two instances within a cycle and the corresponding envelope curve at a frequency of 200 Hz (After Békésy, in Waterman and Morowitz 1965)

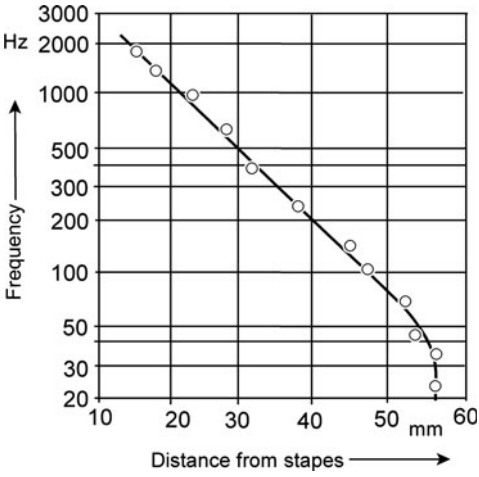

Fig. 4.14 Position of maximum stimulation along the cochlear partition in the inner ear of an elephant (After Békésy, in Waterman and Morowitz 1965)

amplitudes of these waves, however, are not constant. They reach their maxima at certain points of their movement in the direction of the arrow in Fig. 4.13, depending on the frequency of activation. Connecting these maxima, an *envelope curve* is obtained, the position of its maximum depending on the frequency of activation.

In fact, this model takes into consideration the plasto-elastic properties of the basilar membrane and the hydromechanics of the endolymph and the perilymph. It shows that the higher the frequency, the closer the maximum of this envelope curve to the oval window. Figure 4.14 indicates the positions of maximum stimulation along the cochlear partition as a function of frequency in the ear of an elephant. In the case of complicated tones, envelope curves have several maxima. At the points of maximal amplitude, the basilar membrane is deformed, which eventually leads to stimulations of the sensory cells. This mechanism can be considered as one particular step of frequency analysis.

The entire reception of the sound takes place in the *organ of Corti* (Fig. 4.15). In contrast to the anatomical-hydrodynamic and anatomical-mechanical approaches, which are used to explain the function of the middle ear and the traveling waves in

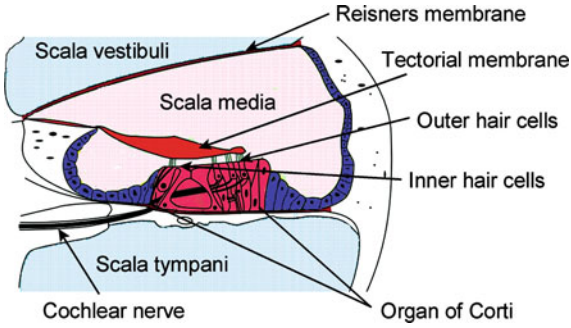

Fig. 4.15 Section of the human cochlea

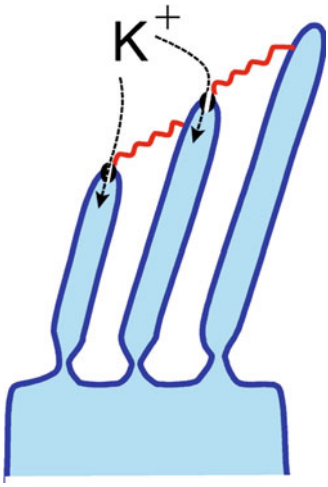

Fig. 4.16 Schematic illustration of the apical part of a hair cell with stereocilia, connected at the top by filaments (*red*). In the case of deflecting, these tip links mechanically open potassium-selective channels, which leads to depolarization of the corresponding cells

the cochlea, the processes in the organ of Corti have to be discussed on the cellular and the molecular level. The entire transformation of mechanical vibrations into coded nerve impulses is performed by the so-called hair cells. About 16,000 of them are located at the basilar membrane in the human ear. Hair cells are flask-shaped epithelial cells, containing 30 to hundreds of hair-like extensions, so-called *stereocilia*, in a hexagonal arrangement. These stereocilia differ in length and thickness. Some of them reach to the tectorial membrane on the opposite side of the cleft.

The basic mechanism to transform the vibration of the basilar and tectorial membranes into a neuronal signal is illustrated schematically in Fig. 4.16. Parallel to the plane of bilateral symmetry of the cochlea, the stereocilia are connected to each other at the tip by filamentous structures. In the case of bending, these tip links mechanically open cation-selective channels, leading to a depolarization of the cell. An erection of the stereocilia closes these channels again. In this way, a mechanical vibration is transformed into an electrochemical one with respect to electrical signals.

This simplified description indicates particular noise-reducing properties. The orientation of the stereocilia and their interconnection by their tip links show that

not all kinds of displacements of the stereocilia will cause depolarization, but only those that are directed in line with the filaments.

But this is only one aspect of the highly optimized system of sound reception. In fact, there are a number of other peculiarities. One of them is the enormous spread of the range of sensibility. At 1 kHz, the auditory threshold for pain (130 dB) corresponds to a sound pressure that is about 10^7 times larger than that of the sensory threshold (0 dB) (see Fig. 4.6). According to Eq. 4.11 (Sect. 4.3.2), the sound pressure should be proportional to the amplitude of the displacement (Δx). It was observed that at a threshold stimulus of 0 dB, the basilar membrane vibrates at an amplitude around 0.1 nm $= 10^{-10}$ m. Applying this proportionality, this would be 1 mm $= 10^{-3}$ m near the pain threshold! Vibrations of this intensity, however, would definitely destroy the organ of Corti. In fact, measurements show that even at this maximal intensity, the basilar membrane vibrates only around 10 nm.

One reason for this strongly nonlinear behavior is the regulatory role of the ossicle system in the middle ear as well as the wave propagation in the cochlea is a result of its particular viscoelastic structure. Furthermore, a nonlinear behavior occurs also in the hair cells. So, a negative hair-bundle stiffness at a particular area of bending has been observed. This means that in particular situations, an additional force will be activated, supporting the bending of the stereocilia. In fact, the hair bundles can perform work and, in this way, amplify their input. Experiments on isolated outer hair cells indicate that not only the hair bundles but, after electrical excitation, the cell body itself undergoes a striking change in its shape. Furthermore, active movement of the basilar membrane has been observed.

This indicates that the inner ear is not only a simple passive receptor organ. In fact, it becomes an energy-consuming generator of sound. It was found that the ear of humans and that of many animals can emanate sound continuously at one or more frequencies. This is called *otoacoustic emission*. There are two types of otoacoustic emissions: *spontaneous* and *evoked*. Evoked otoacoustic emissions occur after the application of a pure-tone stimulus. This is used as a simple, noninvasive test for hearing defects. Otoacoustic emission seems to be the result of a frequency-specific neuronal feedback system, which leads to an increase in the distinguishability of signal variations in the inner ear.

Further Reading

Middle ear: Zhao et al. 2009; inner ear: Bekesy 1960; Ramamoorthy et al. 2010; hair cells: Hudspeth 2008; otoacoustic emission: Lilaonitkul and Guinan 2009; biophysics of music: Roederer 2008; neurophysiological background: Purves et al. 2008.

4.3.4 Infrasound

Infrasound is considered an acoustic oscillation of frequencies below 20 Hz. Its definition, as being below the low-frequency limit of audible sound, is in fact misleading, as sound remains audible at frequencies down to 4 Hz for exposure

in an acoustic chamber and down to 1.5 Hz for earphone listening. Sometimes, infrasound leads to unspecific auditory sensations. Even clinking and overtones can be heard. In general, infrasound interacts with air-filled cavities in the human body, like lungs, nasal cavities, frontal sinus, middle ear, and gut. Therefore, a range of vibrational receptors exist in the body, of which the ear is the most sensitive for higher frequencies (see Fig. 4.6), whereas vibration and contact detectors dominate at lower frequencies (see Sect. 4.3.1).

Because of its large wavelength, infrasound has some special properties in relation to sounds of higher frequencies. For example, it is only poorly damped by stone walls, buildings, etc. It is, therefore, difficult to shield from this kind of noise. Sometimes, even in spaces with corresponding resonance frequencies, an amplification occurs. These, for example, are cars or housing spaces with a typical resonance frequency of 2–8 Hz.

In general, we are surrounded by a large scale of naturally occurring infrasound in the range of about 0.01–2 Hz. These frequencies eventually merge into fast fluctuations of barometric pressure. There are various natural sources of infrasound, like wind, waterfalls, volcanic eruptions, and ocean waves, i.e., any effects that lead to slow oscillations of the air. Some speculations assume that animals may perceive infrasonic waves passing through the earth indicating the onset of natural disasters like earthquakes or tsunamis. Some large animals such as elephants, hippopotamuses, rhinoceroses, and whales use low-frequency sound and infrasound for long-range communication.

In a technical context, infrasound is produced by vibrations of various engines. There is a considerable exposition to infrasound in cars, if the air stream induces internal resonances. Sometimes the 100-dB limit is exceeded. In recent years, special infrasound loudspeakers are used in discotheques in order to cause psychosomatic resonance in the participants. Because of the above-mentioned problems of shielding, they may considerably disturb the neighborhood.

Two types of biological influences of infrasound must be considered: direct physical injuries on one hand and psychophysical influences on the other. At high intensities, damage to the middle ear is to be expected. For a 24-h exposure of sound below 20 Hz, levels of 120–130 dB seem to be tolerable. These limits, however, prevent only direct physiological damage. Unfortunately, there are no clear national and international protection standards for infrasound including their psychophysical aspects. Usually, this is managed as a subset of general protection from noise.

Further Reading

Garstang 2004; Le Pichon et al. 2010; Leventhall 2007; Møller 1984.

4.3.5 Ultrasound

Ultrasound per definition is a mechanical wave at a frequency range between 16 kHz and 1 GHz. Sometimes, for frequencies higher than 1.6 GHz, the term

hypersound is used. Technically, ultrasound can be generated by electroacoustic converters. Because of its short wavelength, it can be focused by appropriate reflectors and diffraction lenses.

In gases, fluids, and correspondingly in most tissues, ultrasound consists of longitudinal waves, i.e., of periodic alterations of local pressure, where the particles horizontally move back and forth relative to the direction of the wave energy. In harder biological materials such as bones, the particles move at right angles to the direction of the wave propagation. In these cases, shear waves occur. Diagnostic use of ultrasound is based on its interaction with the tissue in the form of absorption and scattering. Absorption is due to translational and rotational vibration of biological macromolecules even if their frequency of ultrasound is much lower than their thermal vibration modes. Scattering is related to small inhomogeneities of visco-elastic properties. Strong scattering contributions are produced by small arterioles and the collagen meshwork of parenchymal tissues. The propagation speed of ultrasound in a tissue is typically assumed to be constant at 1,540 m/s, similar to that of water.

Figure 4.17 shows the relation between the frequency (ν) and the wavelength (λ) of ultrasound in air and aqueous media. So, for example, ultrasound of $\nu = 10$ MHz in tissues has a wavelength of 0.15 mm. This ensures a satisfactory resolution for sonographic images. It can be increased further by using ultrasound of higher frequencies; however, this will decrease its penetration into the body. In fatty tissues, for ultrasound of 0.8 MHz, a half-value thickness of penetration of 3.3 cm has been measured; in muscles, it amounts to only 2.1 cm. This parameter decreases with increasing frequencies.

For diagnostic sonography (ultrasonography) as an image-generating technique, ultrasound pulses of various bandwidths are used. In general, these applications can be divided into pulse-echo imaging techniques and Doppler techniques for studying blood flow or tissue movement. 2D images are obtained by sweeping the ultrasonic beam. This results in a 2D representation of a slice in the body. A series of adjacent 2D images can be integrated into a 3D image. In this way, even a live 3D image of the beating heart is possible to obtain.

In order to achieve a good resolution of the images, an optimum of frequency and bandwidth of the applied pulses must be determined as a typical compromise: To resolve targets lying close together, side by side at the same range, a narrow beam is necessary, which requires a wide pulse. Both are possible using higher frequencies. This, however, limits the depth of penetration. This is the reason why for prenatal observations and mammographic diagnostics, frequencies of only 1–5 MHz are used. Around 3 MHz is typical of abdominal applications in adults and around 5 MHz in children. In ophthalmologic diagnosis for the anterior chamber of the eye, 10–50 MHz are used, or even 100 MHz in very superficial applications, such as imaging the cornea.

Ultrasound-induced bioeffects are generally separated into thermal and nonthermal mechanisms. The absorption of ultrasonic energy means a reduction in its amplitude as it propagates through a medium. This represents its dissipation, i.e., the conversion of mechanical energy into heat. This energy dissipation is proportional to the ultrasound

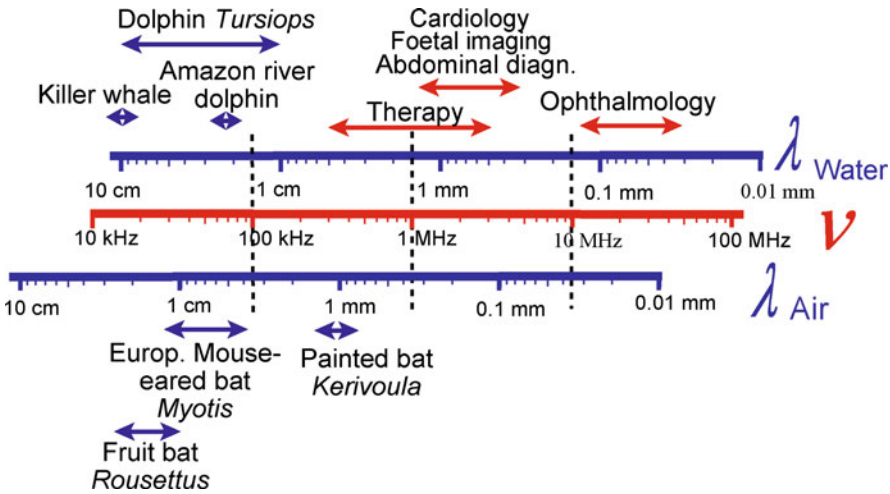

Fig. 4.17 Frequencies (ν), wavelengths in water (λ_{Water}) equivalent to that of soft tissue, and air (λ_{Air}) of ultrasound as well as regions of medical applications (*red arrows*) and animal sonar systems (*blue arrows*) (Data for animal frequencies from Withers 1992)

intensity, with respect to the square of its sound pressure (see Eq. 4.12), and to the absorption coefficient of the material, which increases with increasing frequency.

To characterize the temperature increase in the body resulting from ultrasound absorption, the term *diathermy* is used. This temperature increase takes place if the rate of heat production along the penetration of ultrasound is greater than the rate of heat removal. In general, the heat removal is governed by heat conduction. In a living body, the complex system of biorheological thermoregulation must be considered, including the acquisition of heat by blood circulation. This is governed by the bioheat equation of Harry H. Pennes, as discussed in Sect. 4.1 (Eq. 4.4).

Caused by diffraction, or reflection of ultrasound in the tissue, as well as by differences in blood supply, the amount of thermal effects can be heterogeneous. Hot spots may occur in the tissue, i.e., small locations of increased temperature (see a detailed discussion of possible sizes of them in Sect. 4.7.2).

The nonthermal mechanism of ultrasound interaction is mainly based on the effect of *cavitation*. Cavitation is the formation of gas-filled tiny bubbles as a result of alternating positive and negative pressures at particular spots in the medium. Homogeneous liquids have a considerable resistance to such an effect of disruption. In order to pull pure water apart in such a way that two parallel surfaces are formed, separated one from another, a negative pressure of about 1,500 MPa is required. However, only 150 MPa is sufficient to form a spherical cavity. Even lower local negative-pressure differences are required to induce cavitations in an inhomogeneous medium, such as a solution, suspension, or even a biological tissue.

These bubbles originate within materials at particular locations, so-called nucleation sites. In a complex medium such as a tissue, the exact nature of these nuclei of cavitation is not well understood. The occurrence of cavitation depends not only on the

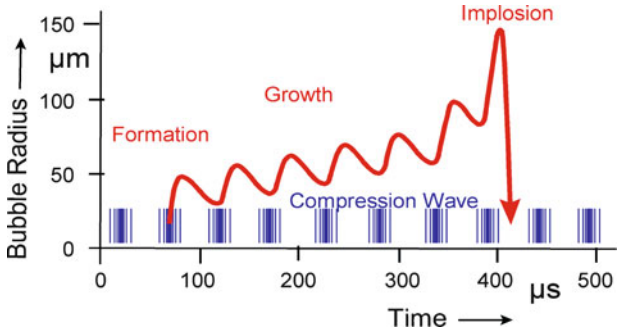

Fig. 4.18 Bubble growth and collapse during transient cavitation at a frequency of about 16 kHz (Redrawn from Suslick and Doktycz 1991)

concentration of these nuclei and on the intensity of ultrasound, but further more on some qualitative factors, such as frequency, field homogeneity (focused or unfocused ultrasound), and pulse parameters. For short pulses of ultrasound, cavitations in tissue have been observed at local pressure differences of above 10 MPa. To enhance the echogenicity of ultrasound in medical diagnostics, contrast agents are often used, indicating the preexistence of microbubbles. This, however, increases the possibility for ultrasound-induced cavitation and the potential for bioeffects. Cavitation can produce audible noise, leading finally to "boiling" of the liquid.

These cavities are filled by the gas which is dissolved in the liquid and by the vapor of the liquid itself. They may persist for several acoustic cycles. In this way, they expand to the sizes of their resonance radii, before collapsing violently during a single compression half cycle (Fig. 4.18). The sizes of these resonance radii depend on the medium and the frequency. So, for example, for argon bubbles in water, it amounts approximately to 4 μm at a frequency of 1 MHz and 80 μm at 50 kHz. The violent and rapid compression of the collapsing bubbles leads to an extremely large increase in the local temperature. The collapse of cavitation bubbles at 20 kHz is not completely adiabatic, and heat is lost from the bubbles to the surrounding liquid by means of conduction. At acoustic frequencies in the MHz region, however, the compression is so rapid that there is insufficient time for heat transfer to the liquid. The resulting temperature in the imploding cavity locally may increase to values of the order of several thousand degrees Kelvin, with a heating rate of about 10^{10} K/s and the corresponding pressure of hundreds of atmospheres.

These extreme conditions lead to the formation of hydroxyl radicals and hydrogen atoms. The formation of $^{\cdot}H$ and $^{\cdot}OH$ radicals as the primary products of sonolysis of water has been confirmed by electron spin resonance. These radicals either combine to form H_2, H_2O_2, and water or attack solute molecules, which are reduced or oxidized. In contrast to the radiolysis, where the primary products are hydrated electrons (see Sect. 4.9.2), in the course of sonolysis of water, these radicals are produced directly by thermal decomposition. In this respect, the definitions of "thermal" and "nonthermal" effects must be reconsidered. If an effect is called "thermal," then it is usually concerned with the consequences of

diathermal heating of macroscopic regions, and not the microscopic processes of thermal decomposition.

Besides this thermal theory of sonolysis, the possibility of an electrochemical effect also must be considered. This theory recently had been supported by investigations of long-living microbubbles, the collapse of which is slower and does not show a dramatic temperature increase. The microbubbles, in fact, contain surface charges and, correspondingly, show a ζ-potential at the gas–water interface (for ζ-potential, see Sect. 2.3.5). This ζ-potential is inversely proportional to the bubble size and increases with respect to the rate of shrinkage. The rate of movement of electrolyte ions of the corresponding electric double layer in water is not sufficiently high to counteract this increasing rate. Consequently, it is likely that some excess ions become trapped at the gas–water interface, which leads to an extreme accumulation of ions during the final stage of the collapse process. This might trigger generation of radicals via dispersion of the elevated chemical potential that has accumulated around the interface.

In biological systems, cavitation therefore leads to two kinds of effects: On one hand, the cavitation simply generates mechanical destructions of cell organelles and various supramolecular structures, and on the other hand, sonochemical effects need to be considered, i.e., consequences of the formation of reactive radicals.

Ultrasound is widely used in biotechnology and medicine. The range of frequency for therapeutic treatment is between 0.7 and 3.3 MHz (see Fig. 4.17). In contrast to diagnostic use, the optimization in therapeutics is oriented to maximal penetration depths. This diathermy treatment of ultrasound is used with the same intension as diathermy produced by high-frequency electromagnetic fields (see Sect. 4.7.2). It is mainly applied in the treatment of soft tissue injuries, the acceleration of wound healing, the resolution of edema, softening of scar tissue, bone injuries, and circulatory disorders. Raising the temperature by a few degrees may have a number of beneficial physiological effects, for example, an increase in blood circulation.

Recently, high-intensity focused ultrasound (HIFU) is used for *lithotripsy*, a noninvasive treatment of stones in the kidney and the gallbladder. It is possible to enhance the uptake of pharmacologically active drugs through the skin by application of ultrasound (*sonophoresis*). Parallel to the electroporation of cells (see Sect. 3.5.5), a temporary opening of the cell membrane is possible also by pulses of ultrasound (*sonoporation*). A number of experiments to stimulate healing of bone fracture are still not conclusively proven.

Although ultrasound, by definition, is a nonaudible sound, it was found that the human ear may sense tones even up to 40 kHz, although with very low sensibility. Nevertheless, it is argued whether the weighing scales, discussed in Sect. 4.3.2 (Fig. 4.7), must be extended up to this frequency.

To evaluate the intensity of the ultrasound radiation, usually the power density in $W\ m^{-2}$ is used. This, however, does not account for the real energy absorption in the body or in the tissue. The local sound pressure, for example, would be more convenient, but this is a not directly measurable parameter. The only measurable reference value is the temperature elevation during exposition. This safety parameter depends on the time of exposure. From nonhuman experiments, for example, a

threshold for tissue damage was found: if, at a duration of 0.1 s, the temperature was increased up to 18°C, for 5 min, an increase of only 4°C is possible.

The American Institute of Ultrasound in Medicine (AIUM) periodically examines the literature on ultrasound bioeffects and develops conclusions and recommendations related to diagnostic ultrasound. In general, diagnostic ultrasound has been in use since the late 1950s, and this has indicated that no independently confirmed adverse effects caused by exposure from present diagnostic ultrasound instruments have been reported in human patients. There has been no experimental evidence to suggest that inertial cavitation events occur from exposure-like conditions employed with diagnostic ultrasound equipment. In some cases, localized pulmonary bleeding has been reported, but the clinical significance of such effects is not yet known. Nevertheless, the ALARA principle ("as low as reasonably achievable") is recommended to obtain the necessary diagnostic information. The use of ALARA is an important consideration in all fetal examinations, and the dwell time may be overlooked as a means to reduce exposure.

WHO recommends a mean intensity limit of $3 \cdot 10^4$ Wm^{-2}. The real values applied in diagnostic methods are far below this limit. Therefore, no risk is involved in the common ultrasound diagnostics for health, especially regarding replacement of X-ray methods by ultrasound.

Further Reading

Primary mechanisms: Riesz and Kondo 1992; Takahashi et al. 2007; therapeutic applications: Frenkel 2010; ter Haar 2007; sonoporation: Ohta et al. 2008; safety recommendations of AIUM: Fowlkes 2008.

4.3.6 Biophysics of Sonar Systems

It has been known since the experiments of the Italian monk and scientist Lazzaro Spallanzani in 1794 that bats have the ability to orientate in complete darkness and to avoid obstacles. It had been demonstrated at that time that a bat could still fly safely when blinded but was quite helpless when its ears were plugged. Only in 1938 was D. R. Griffin able to show by direct measurements that bats are able to emit ultrasound and detect the echoes reflected from objects in their surroundings to determine their location. In the following years, many investigations had been carried out and it was found that not only bats but also rodents, aquatic mammals, birds, fish, and insects use echolocation by high-frequency sound, or ultrasound.

Because bats have been investigated in this respect more than other species, we will start with their example to explain the biophysical basis of echolocation. Figure 4.19 shows an oscillogram of a typical orientation signal of a bat. It is characterized by the following physical parameters: frequency (ν), amplitude, duration (Δt), and, of course, the distance between two signals.

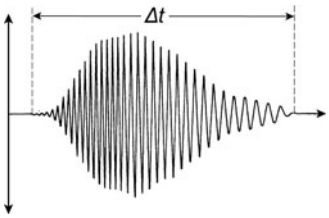

Fig. 4.19 Example of a typical FM-modulated signal of a bat

The frequency of the emitted sound depends on the size of the object which is to be localized. An effective echo can be expected only from targets that are equal or even larger in size than the wavelength of the sound. The relation between wavelength (λ) and frequency (v) is given by:

$$\lambda = \frac{\mathbf{v}}{v} \tag{4.15}$$

where $\mathbf{v}$ is the velocity of sound waves. In air under atmospheric conditions, $\mathbf{v} = 331\ \mathrm{ms}^{-1}$. A sound of 25 kHz, therefore, has a wavelength $\gamma = 331/25{,}000 = 0.01324$ m, i.e., 1.324 cm.

The frequencies emitted by bats differ from species to species (see Fig. 4.17). Usually, these amount to between 25 and 150 kHz. Bats that use their sonar system in order to catch insects emit signals of higher frequencies than those simply orientating in dark caves.

The amplitude of the signal, i.e., its intensity, is determined by the required range of the sonar system. Naturally, the auditory system of the bats must be sufficiently sensitive to receive the corresponding echo. The power of the emitted sound of the big brown bat (*Eptesicus fuscus*), for example, is about 10^{-4} W, whereas, as a minimum, a power of 10^{-16}–10^{-14} W corresponds to the auditory threshold. At a distance of 5–10 cm from the head of this bat, the sound pressure is 2–6 Pa. According to Eq. 4.13, this amounts to an intensity of 100–110 dB. We learned in Sect. 4.3.2, Fig. 4.8, that if transformed into audible sound, this would be a considerable noise.

This large difference between the emitted and the accepted sound causes problems for the animal in listening while crying. The maximal duration of a signal (Δt), therefore, is more or less limited by the time the sound needs to arrive at the target and come back, i.e., by the distance of the target.

Frequency (v), amplitude, and pulse duration (Δt), therefore, are the basic parameters of an echolocation signal. Looking at the sonogram in Fig. 4.19 carefully, however, more details can be noticed. The frequency, for example, as well as the amplitude of the signal is time dependent. It is a *frequency-modulated* sound, a so-called FM signal. In the case of the little brown bat (*Myotis lucifugus*), the signal starts with a frequency of 100 kHz and goes down by an octave at the end of the 2-ms-long-lasting signal. In contrast, the horseshoe bats use signals of 50–65 ms with constant frequencies (*CF signals*). Mostly, however, these CF signals have a

short final frequency-modulated part. The character of the emitted signals depends on the species, the situations, and even on the individual animal.

Frequency modulation seems to be an important property of the signal, especially for the measurement of distances. In some cases, it appears that by superimposition of the FM part at the end of the signal with the initial CF part of the returning echo, specific beat frequencies occur, which are evaluated by the animal. Furthermore, a principle known as the *pulse compression technique* in radar technology has been discussed. For this, short frequency components of the echo are delayed by a special acoustic filter, a so-called optimal filter, with respect to their frequencies. The higher frequency parts at the beginning of the signal are delayed to a larger extent than the lower frequency parts at the end of the signal. This process of impulse compression provides an instantaneous cross-correlation between the emitted and the received signals. Pulse depression explains the ability of the animal to measure the distance even in cases when the echo time is less than the duration of the emitted sound. Owing to this principle, disturbances by the Doppler effect are also minimized.

On one hand, the Doppler effect disturbs the bat when measuring distances, while on the other hand, it is used to measure relative velocities between the animal and its surroundings. For this, a Doppler-shift compensation occurs. If a flying bat approaches an object at a certain speed, the echo from that object will be Doppler-shifted upward to a higher frequency than the emitted signal. Subsequently, the bat lowers the frequency of the next emitted CF component by an amount that is nearly equivalent to the Doppler shift in the preceding echo. The amount of the required frequency is used by the bat to calculate its relative velocity.

Many questions on the information processing of the echolocation behavior in bats are still open. These concern mechanisms to determine the direction of the object as well as those regarding information about size, shape, and material of the target. Recently, it was found that a bat-pollinated rainforest vine lures the bats with specific disk-shaped leaves located near the ring of flowers which act as reflectors of ultrasound (Simon et al. 2011).

Echolocation is also seen in some birds. Alexander von Humboldt has described a South American cave-dwelling bird, the oilbird or guacharo (*Steatornis caripensis*), which flew around the head of the explorer uttering "screams of fear." It is now known that these cries serve as signals in an echolocation mechanism. The sound is pitched at frequencies of 6–10 kHz, which means that it can be heard by humans. These birds are herbivores, but they require their sonar system in order to orient in large dark caves. The frequency employed corresponds to wavelengths between 3 and 5 cm, which means that the sound can be reflected even from small rock projections.

Sonar systems are found not only in airborne species but also in several aquatic animals. There are, however, vast differences between these two kinds of echolocation. Due to the differences in the velocity of sound, the wavelength of a sound in water ($\mathbf{v} = 1{,}500\ \mathrm{ms}^{-1}$) is about 4.5 times larger than that of the same frequency in air (see Fig. 4.17). This diminishes the resolution of the aquatic sonar system at the corresponding frequency. On the other hand, the distance of the applied echolocation differs. Bats use their sonar system at short ranges up to approximately 3–4 m, whereas dolphins can detect small targets at ranges varying from a few tens of

meters, for the harbor porpoise, to over a 100 m, for the bottlenose and other large dolphins. Dolphins, for example, emit short click signals with a duration mostly of only 40–50 ms, having a frequency up to 130 kHz, with a repetition after 20–40 ms.

The mechanisms of sound production between bats and whales are also different. While bats use the larynx as the traditional mammalian kind for sound generation, dolphins have usurped and completely revamped the nasal apparatus for producing sonar sounds. Both power their sound-generation system pneumatically and produce their signals by pushing air past tissue gates or valves. Bats use subglotting pressure, while dolphins use intranasal pressure. The mechanisms in dolphins may be similar to the behavior of a human trumpet player's lips. Some animals are able to focus the beam of high-frequency clicks. This is the case of toothed whales, in which it is done by reflection at a dense concave bone of the cranium and by a large fatty organ known as the *melon*. This is a large forepart of the head containing triglycerol and wax esters, i.e., lipids of differing densities. It acts like an acoustic lens, focusing the beam in the direction in which their head is pointing.

In the case of aquatic sonar systems, the specific sound distribution in water must be taken into consideration. The transmission loss for a point source of sound in free space in general is:

$$\text{Transmission loss} = 10 \log \frac{I_0}{I_r} = 10 \log r^2 + \alpha\, r \tag{4.16}$$

where I_0 is the intensity at $r = 0$, I_r is the intensity at distance r, and α is the coefficient of absorption.

The first term of the sum describes the simple geometrical distribution of the sound, whereas the second term concerns the absorption of sound in the medium. Especially in seawater, because of its content of magnesium sulfate, the coefficient α is frequency dependent (Fig. 4.20). This means that in contrast to airborne animals, the frequency of the emitted signal for seawater animals is additionally a function of the distance. This coefficient also shows a dependence on pressure and temperature. So, for example, the 20°C value of 38.6 dB/km for 100 kHz diminishes to 28.9 dB/km for 5°C. The values in Fig. 4.20 correspond to surface

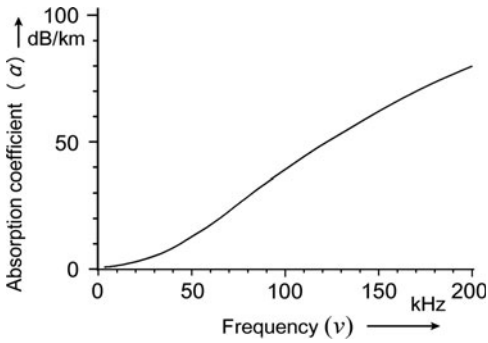

Fig. 4.20 The absorption coefficient (α) of seawater at 20°C as a function of frequency (ν) (Data from Ainslie and McColm 1998)

water. At 1,000-m depths, for example, the 100 kHz value for 5°C would shift from 28.9 to 24.8 dB/km.

Further Reading

Au 1994; Griffin 1958; Pollak und Casseda 1989; Thomas et al. 2004.

4.4 The Static Magnetic Field

The influence of magnetic fields on biological systems and human health is an ancient and contentious subject. It became topical with the introduction of clinical magnetic resonance imaging (MRI), where patients are exposed to an intense magnetic field of a strength not previously encountered by humans. On the other end of the scale (Fig. 4.21), the orientation of animals in the weak geomagnetic field is a permanent matter of discussion. In between these two regions of intensity, the field of magnetic healing quackery is positioned with its own history, starting with Anton Mesmer at the end of the eighteenth century.

The interaction of magnetic fields with biological materials is to be considered from two aspects: on the one hand a direct magnetic influence on molecules and supramolecular structures is possible, on the other hand, pulsed or alternating magnetic fields induce eddy-currents which finally may interact electrically. This leads to the topic of electromagnetic field effects on biological systems which will be discussed later (Sect. 4.6.1). Here, however, beside direct magnetic effects, we

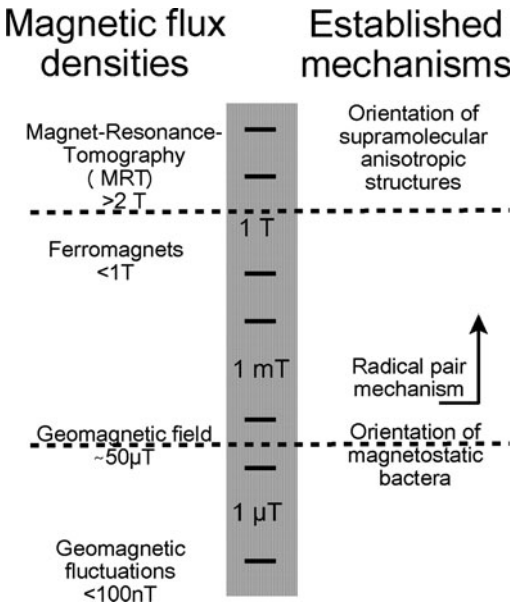

Fig. 4.21 The logarithmic scale of intensity of homogeneous static magnetic fields (magnetic flux intensity in Tesla), versus established mechanisms of possible biological interaction

Table 4.4 The magnetic susceptibility (χ) of air, water, and various biological materials (all: $\cdot 10^{-6}$)

	After Maniewski (1991)	After Khenia et al. in: Maret et al. (1986)
Air	+0.34	+0.264
Water	−9.05	−9.04
Arterial blood	−9.1	−9.3
Oxygenized erythrocytes		−9.03
Venous blood	−8.4	−7.8
Deoxygenized erythrocytes		+3.88
Lungs (breathed in)	−3.9	
Lungs (breathed out)	−4.1	
Lungs (15% air content)		−4.2
Muscle	−9.0	−9.03
Liver	−8.8	−8.26
Bone	−10	−10

must consider induction processes, generated in biological systems which are moving in a static magnetic field, for example in the case of blood flow, or animal locomotion.

Let's first explain some basic principles. A magnetic field with the *magnetic field strength* **H** (in A m^{-1}) causes in a body a *magnetic induction*, or *magnetic flux density* **B** (in Tesla: T = V s m^{-2}) of:

$$\mathbf{B} = \mu\mu_0\mathbf{H} \tag{4.17}$$

where $\mu_0 = 1.257 \cdot 10^{-6}$ V s $A^{-1}m^{-1}$ is the *magnetic permeability of vacuum*, and μ is the *magnetic permeability* – a dimensionless number in relation to vacuum, where $\mu = 1$. The deviations of the magnetic permeability for nonferromagnetic materials from 1 are extremely small. For practical use therefore another parameter is defined: the *magnetic susceptibility* $\chi = \mu - 1$.

Magnetic properties of various materials are classified according to their properties as being:

$$\begin{aligned} &\textit{diamagnetic}: && \mu < 1;\ \ \chi < 0 \\ &\textit{paramagnetic}: && \mu > 1;\ \ \chi > 0 \\ &\textit{ferromagnetic}: && \mu \gg 1;\ \ \chi \gg 0 \end{aligned} \tag{4.18}$$

As shown in Table 4.4, cells and tissue in general have diamagnetic properties. An exception is deoxygenized erythrocytes, which are paramagnetic due to the property of the central Fe-atom in the hemoglobin molecule. If it binds oxygen, it changes from paramagnetic to a diamagnetic state.

In contrast to the strong effects of electric fields, very strong magnetic fields show only subtle and hard to observe effects. The reason for this is the different deviations of the dimensionless dielectric constant (ε) on the one hand (see Sect. 3.5.3), and the magnetic permeability (μ) on the other hand, of the materials, from

the value 1 of the vacuum. For typical, nonferromagnetic materials, the electric susceptibility ($\varepsilon - 1$) is of the order of $10^5 - 10^6$ times larger than the magnetic susceptibility ($\chi = \mu - 1$).

This of course does not apply to ferromagnetic interactions, where the magnetic permeability (μ) may achieve the order of 10^4. Ferromagnetic materials form domains that exhibit a long-range ordering phenomenon at the atomic level which causes the unpaired electron spins to line up parallel with each other. Ferromagnetic materials, mostly consisting of Fe, Co, or Ni, remain magnetized after the external field is removed.

For some biotechnological and medical applications nanoparticles are used with *superparamagnetic* properties. These particles are magnetized by an external magnetic field like ferromagnetic materials, but unlike them they do not retain any significant amount of magnetization in the absence of the field. When the external magnetic field is applied all the domains are oriented in the same direction. If the field is removed, then they are mixed by Brownian motion. In contrast to ferromagnetic particles, these superparamagnetic nanoparticles, therefore, do not aggregate in the absence of an external magnetic field. This is the particular property that makes them applicable for biotechnological use. Coupling these particles with drugs, monoclonal antibodies, particular cells, or including them in liposomes opens a large field of biotechnological and medical application. These particles can easily be separated in moderate magnetic fields (*magnetoseparation, immunomagnetic cell separation*). Furthermore, magnetic drug targeting employing superparamagnetic nanoparticles as carriers is a promising cancer treatment.

In biological tissues various kinds of iron-containing ferromagnetic particles have been found; some of them concentrated in particular regions, others dispersed at very low concentrations. In some cases these particles are just absorbed from polluted external medium or they are the product of destruction of iron-containing proteins like hemoglobin or ferritin. In some cases larger ferromagnetic inclusions were observed. It is under discussion whether they play a role in magnetic field reception.

In many kinds of bacteria, ferromagnetic particles exist, so-called *magnetites*, which are synthesized by a particular mechanism from chelate bound iron. These are cuboidal crystals of Fe_3O_4 (a mixture of FeO and Fe_2O_3) with a size of 50–200 nm. The largest are surrounded by a membrane forming *magnetosomes*. The density of these particles is 5.1 g cm^{-3}. Because of their extremely small size, they consist of only one single magnetic domain which means that they represent a single elementary magnet.

These particles are arranged in a chain, several micrometers long, which is located along the axis of motility of the bacterium. The magnetic momentum of a single magnetosome is not large enough to resist the Brownian movement in the geomagnetic field of about 50 μT. The chain, however, forms a magnetic dipole which is sufficiently strong to orient the whole bacterium in the geomagnetic field.

Magnetostatic bacteria are usually anaerobic inhabitants of the sediment. Cells with appropriate polarization swim along the geomagnetic vectors, which in regions away from the equator are directed into the anaerobic depths (see Figs. 4.22 and 4.23). This oriented movement is called *magnetotaxis*. Bacteria

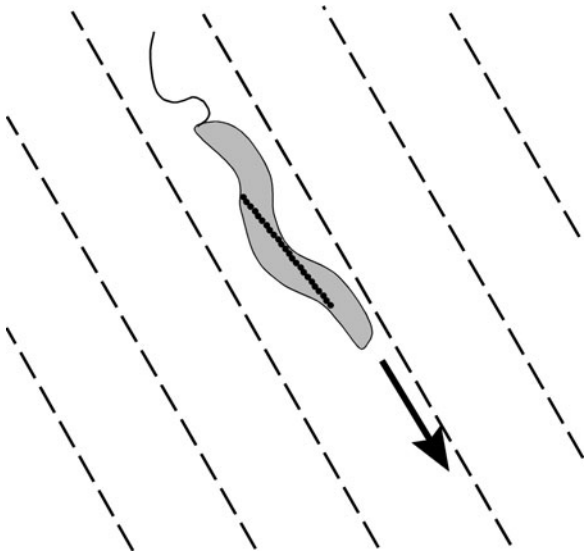

Fig. 4.22 Magnetospirillum moving down, oriented by its chain of magnetosomes along the geomagnetic field lines

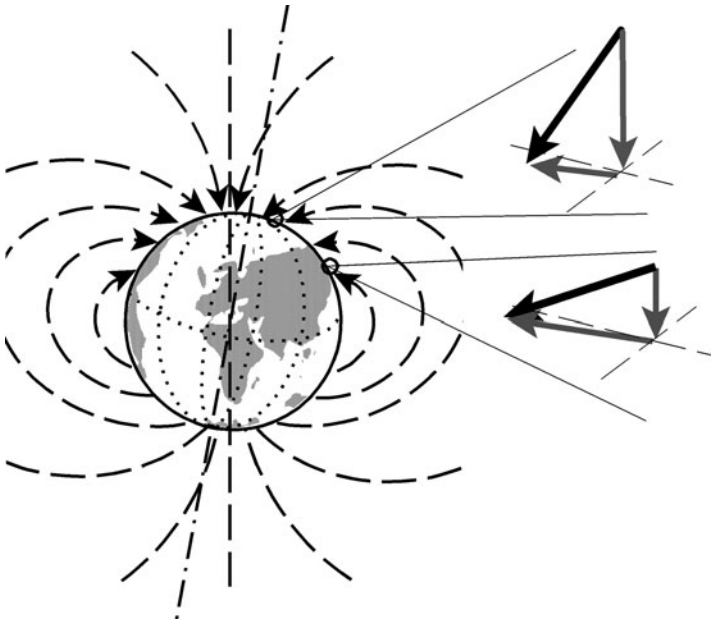

Fig. 4.23 Geomagnetic field lines, and their inclinations at two particular locations

with incorrect magnetic polarizations swim in the wrong direction and die in the oxygen-containing surface water. During division of the cells by mitosis, the magnetic chains will also be divided into two parts, and the daughter cells get a part of the correctly polarized chain. Such newly synthesized particles automatically become polarized according to the inherited part of the chain. It is possible to reverse the polarity of these chains in artificial magnetic fields of at least 10 mT.

The influence of magnetic fields on diamagnetic or paramagnetic molecules or structures requires much stronger field strengths. If during a chemical reaction a transformation occurs from diamagnetic to paramagnetic states or vice versa than according to Le Châtelier's principle (see Sect. 2.2.3) an influence of magnetic fields is possible (*magnetokinetics*). The magnetic contribution to the free enthalpy (ΔG) of reaction in a field with a magnetic flux density **B** can be considered as a further summand in the Gibbs equation (see Sect. 3.1.2, Eq. 3.29):

$$\Delta G = \frac{1}{2}\Delta\chi_m B^2 \tag{4.19}$$

where $\Delta\chi_m$ is the change of magnetic susceptibility during the reaction of one molar unit. Even assuming a rather high value of $\Delta\chi_m$, even at $\mathbf{B} = 1$ T, the change of the equilibrium constant will be negligible and amounts only to a factor of about 10^{-5}. Thus, even in very strong magnetic fields these kinds of effects should be difficult to detect.

In contrast to this, another possible mechanism of magnetic effect on chemical reactions is well established theoretically and experimentally, which is more sensible to magnetic field strength. It bases on the fact that in some cases in the course of chemical reactions pairs of radicals occur as short-living intermediates that quickly recombine. In the same way after photoexcitation, a donor molecule D^* may transfer an electron to an acceptor molecule A, resulting also in a radical pair $^{\bullet}D$ and $^{\bullet}A$. Usually, the unpaired electrons of these radicals will be in singlet states. Under the influence of a magnetic field, however, a singlet-triplet interconversion is possible. As the result, singlet-singlet and singlet-triplet reactions may occur to give distinct products, with respective rate constants k_S and k_T.

The sensibility of this *radical pair reaction* in respect of magnetic field intensity depends on the reaction time, i.e., on the probability that the singlet-triplet interconversion occurs faster than the recombination of the radicals. In fact, the energy of magnetic interaction involved in this radical pair process may be much smaller than the average thermal energy under normal temperature conditions because the spin of electrons bound to biomolecules is not coupled strongly to the thermal bath. Thermal motion, however, is important for the diffusion of the radicals from the region of generation. Clear effects of this mechanism are established at magnetic fields $\mathbf{B} > 1$ mT. The possibility of the occurrence of this effect at intensities of the geomagnetic field of 50 μT has been extensively discussed, and requires some hypothetical conditions.

The orientation of objects is a further possible use of magnetic field effects. It is based on the *magnetic anisotropy* of some materials, a direction dependence of their magnetic properties. This anisotropy $\Delta\chi$ is defined as follows:

$$\Delta\chi = \chi_{\parallel} - \chi_{\perp} \tag{4.20}$$

whereas $\chi_{\parallel}$ and $\chi_{\perp}$ are the corresponding susceptibilities parallel and perpendicular to a characteristic direction of the structure. For biological structures the magnitude of $\Delta\chi$ can be of the order of 1–10% of the mean susceptibility. Macromolecules with differing susceptibilities in different directions will experience a torque that will attempt to minimize the magnetic energy. This orienting torque is proportional to $\mathbf{B}^2$. For single molecules even in strong magnetic fields these torques are, however, too small with respect to the thermal energy. However, in supramolecular structures, such as membranes or protein filaments the alignment torque is proportional to the total number of molecules in the structure and to the volume.

This kind of orientation effect has been demonstrated in red blood cells in the case of sickle cell anemia in vitro already at 0.5 T. In this case the anisotropy is amplified by abnormal aggregates of oriented hemoglobin molecules. At a field strength of 8 T it was possible to orient the cleavage planes of the developing Xenopus embryo. This distortion of the third cleavage furrow of the developing egg, however, did not affect the postcleavage development.

In the case of gradients of magnetic fields, paramagnetic materials experience an attraction, and vice versa diamagnetic materials repulsion. In contrast to ferromagnetic effects, as noted earlier, these forces however, are very weak. It has been evaluated for example, that for a large diamagnetic protein even in strong field gradients, this force is about 10^8 times lower than the force of thermal movement. Again, only large organized supramolecular structures can be moved in extremely strong field gradients. So, for example, in strong field gradients *magnetophoretic movement* of paramagnetic deoxygenized erythrocytes occurs (see Table 4.4). Diamagnetic repulsion could be demonstrated for macroscopic objects. So, for example, a living frog with a magnetic susceptibility of the order of 10^{-5} could be levitated near a strong magnet of 16 T in a field gradient of $-1{,}400.9\ \mathrm{T}^2\ \mathrm{m}^{-1}$. Interestingly, no harm to the frog resulted from this exposure.

A highly controversial problem is whether, and how animals can sense the geomagnetic field. As demonstrated in Fig. 4.23, the vector of this field can be subdivided into a vertical (*inclination*), and a horizontal (*declination*) component. The inclination is at its maximum at the poles, achieving a magnetic flux density of 60–70 μT. The *declination*, has its maximum near the equator, with 34–40 μT. The intensity of the geomagnetic field shows various variations, which are caused chiefly by changes in sunspot activity. Furthermore, small variations during the day, during the month, and during the year occur. These astronomically caused fluctuations, however, amount to less than a tenth of a percent of the absolute value. Throughout history the magnetic pole of the earth has shifted a considerable

distance. Significant inhomogeneities of the geomagnetic field furthermore, are caused by geological factors.

Despite research over many decades and hundreds of papers, our knowledge of the reception of the geomagnetic field in animals is still controversial and fragmentary. We only have hints derived from behavioral experiments that show effects of magnetic orientation in nearly all classes of the animal kingdom. With the exception of magnetobacteria, where this effect is well established and the mechanism has been clarified, experiments with mollusks, insects and various other invertebrates, with fish, birds, and mammals suggest the existence of a magnetic sense without any reliable indications as to the responsible organs, before even beginning to think of reasonable biophysical mechanisms. Moreover, the results of these papers show a large diversity of phenomena suggesting that probably quite different mechanisms in different kinds of animals should exist. Some of them, like birds, do not estimate the declination, but rather the inclination of the field, and additionally require for this particular frequencies of light. Others, like turtles or subterranean rodents respond to declination without the necessity for light. In some cases, like in the movement of salamanders, light of different frequencies has been determined to change the angle of the field-orientated movement. Some authors even suspect that animals, like turtles or pigs, are able to achieve magnetic localization, i.e., to determine their position from the declination of the field and the local field gradient.

Unfortunately, in no case have reliable physiological or biophysical experiments led to a clarification of this issue. Nevertheless, a number of mechanisms have been proposed to explain these reactions. In the case of large quickly swimming fish like sharks the possibility of induction phenomena has been discussed. For birds the hypothesis has been formulated that the retinal rhodopsin or cryptochrome could be responsible using the radical pair mechanism. Other authors suggest magnetomechanical reactions caused by magnetosomes. Despite the lack of corresponding in vitro experiments, all of these mechanisms from a physical point of view are unrealistic in response to the required sensibility. Moreover, not only the high sensitivity of this hypothetical organ for the magnetic field strength must be explained by these mechanisms, but additionally the exact direction of the field lines must be known. In addition, the hypotheses of magnetic localization, or speculation about sensing of astronomically caused variations of the magnetic field by various animals lack any physical fundament.

We will now discuss the problem of induction processes for the strong magnetic field of MRI. During these diagnostic examinations, the patient is placed in a magnetic field with a flux density of more than 2 T. Even in a static magnetic field, it is necessary to consider the effects of patient motion within the field including the motion of the blood and other tissues within the patient. These kinds of induction processes in fact may provide the ultimate limitation in regard to the maximum magnetic strengths that can be tolerated by human beings. The largest magnetically induced current is associated with pulsating blood flow into the aorta during each cardiac cycle. Calculations have shown that at a field of 45 T the blood flow in the aorta will induce a current density of the order of 1.5 A m^{-2}

at the cardiac pacemaker site in the sinoatrial node, a 50% response level for ventricular fibrillation. Even at flux densities of about 1 T it is possible to measure these inductions in small deviations of the ECG.

During recent decades the method of *transcranial magnetic stimulation* has become available. In this case, stimulations occur by eddy currents, induced by magnetic millisecond pulses of an intensity of 1.5–2 T. In this way the primary motor cortex and the motor roots in conscious patients can be activated. This technique proved sensitive enough to illustrate early abnormalities of central motor conduction in various neurological diseases such as multiple sclerosis, amyotrophic lateral sclerosis, cervical spondylotic myelopathy, degenerative ataxias, or hereditary spastic paraplegias. At magnetic field pulses >10 mT an activation of the optical system is possible which results in so-called *magnetophosphenes*, i.e., visual sensations.

On the one hand eddy currents are induced in bodies moving in magnetic fields, on the other hand, currents in the body (see Sect. 3.5.2) induce magnetic fields themselves. To detect these fields sensitive measuring instruments using superconducting materials (SQUIDs = Superconductive Quantum Interference Devices) are used. To record magneto-cardiograms, -encephalograms, or -myograms, magnetic fields weaker than 1 pT must be measured. This is seven orders of magnitude lower than the geomagnetic field (not included in Fig. 4.21)! These methods are more costly than the corresponding ECG or EEG records, but they provide are much more instructive. As we already pointed out, the magnetic permeability (μ) of various materials does not deviate very much from $\mu = 1$. This means that the magnetic field in the body will not become significantly disordered, in contrast to the electric field. Therefore, it is much easier to localize the oscillating electric dipole in nerves and muscles by its induced magnetic field (see also the explanation of the ECG in Sect. 3.5.2, Fig. 3.38).

The application of highly sensitive measuring instruments for magnetic fields can also be used in occupational medicine to analyze the accumulation of iron dust in the lungs. Furthermore, the activity of the ciliated epithelium of the lung can be checked. For this purpose, a small amount of ferromagnetic labels are inhaled, and the rate of reorganization of these particles is recorded magnetically.

In conclusion: no dramatic influences of static magnetic fields are known, at least at flux densities $B < 10$ T. This is underscored by a large number of experiments with cells in vitro as well as with animals.

On the basis of established results on the influence of static magnetic fields, safety standards have been recommended by the International Commission on Non-Ionizing Radiation Protection (ICNIRP). According to this direct exposure of the general public to static fields should not exceed 400 mT. Because of potential indirect effects, for people with implanted electronic medical devices and implants containing ferromagnetic materials, a lower restriction level of 0.5 mT is recommended. Concerning MRI-diagnostics, a short-lasting exposition of humans without ferromagnetic implants and without cardiac pacemakers up to 8 T can be permitted if the environment is controlled, and if appropriate work practices are implemented to control movement-induced effects.

Further Reading

Influence of magnetic fields in general: Barnes and Greenbaum 2006; Glaser 2008; Miyakoshi 2005; Schenck 2005; magnetic applications in diagnostics and therapy: Andrä and Nowak 2006; magnetic orientation of animals: Rozhok 2008; Wiltschko and Wiltschko 1995; radical-pair reaction: Solov'yov and Schulten 2009; McLauchlan and Steiner 1991; magnetosomes: Bazylinski and Frankel 2004; magnetophoresis: Zborowski et al. 2003; immunomagnetic separation: Moore et al. 1998; Olsvik et al. 1994; magnetic stimulation: George et al. 1998; deNoordhout 1998; Wassermann 1998; Guidelines: ICNIRP 2009.

4.5 The Electrostatic Field

Aspects of bioelectricity have already been discussed in context with various other circumstances in previous sections of this book: After some basic parameters, and laws of electrostatics (Sect. 2.2.1), the principles of membrane electrostatics (Sect. 2.3.6) were explained. Subsequently, we came to transmembrane potentials (Sects. 3.4.3, 3.4.4) and to discussions of electric fields in cells and organisms (Sects. 3.5.1, 3.5.2). Finally, active, and passive electric properties of cells and tissues were considered (Sect. 3.5), as well as various techniques of cell manipulation using electric fields (Sect. 3.5.5). Now the question arises: how do electric fields in the environment influence cells and organisms? In this aspect one must distinguish between life in low conductivity air, and life in water or aqueous mediums with more or less high electrical conductivity.

In this section the effects of static, resp. DC-fields will be considered. However, it must be pointed out that a strong division between electrostatic fields and oscillating electromagnetic fields is artificial. In fact, there is a continuous transition, starting with static fields changing for example in a circadian rhythm or in periods of hours or minutes, up to extremely low-frequency electromagnetic fields (ELF-fields). The same holds for static fields switched on and off after some time, and pulsed forms. Using Fourier analysis, every kind of pulse can be considered as a sum of sine fields of various frequencies. Some aspects discussed in this chapter therefore, are important also for low-frequency electromagnetic fields.

Let us start with the conditions of organisms in air. Terrestrial animals live in the electrostatic field of the earth which is caused by astrophysical, as well as meteorological processes. Our globe can be considered as a negatively charged sphere. This results in a field strength near the earth's surface at sea level of approximately 100–200 V m^{-1}. For astrophysical reasons, the electric field of the earth changes during day and night and also through the year. Additionally, various meteorological processes lead to charge separations, for example in between clouds, as well as between clouds and the earth's surface. Below a thundercloud the electric field strength on the surface can rise up to 20,000 V m^{-1}.

These electrostatic fields, as well as those in the vicinity of various technical devices, are not very important from the point of view of health protection. They could, however, lead to a considerable charge of objects acting as capacitors. This, for example, includes car bodies or other isolated metal surfaces. Touching such electrically charged surfaces can produce painful discharges.

The specific conductivity (g) of dry air near the earth's surface amounts to about $2.5 \cdot 10^{-14}$ S m^{-1}. According to Ohm's law ($j = g \cdot E$), at a field strength of $E = 200$ V m^{-1} a current density of $j = 5 \cdot 10^{-12}$ A m^{-2} results. This conductivity depends on the presence of charged particles. These particles have the misleading name *air ions*. In fact, these are particles, charged with both polarities, which have quite heterogeneous nature and size, beginning with true ions of nitrogen or sulfate compounds, up to various microscopic dust particles containing surface charges. The concentration of such "ions" in air at high altitudes amounts to approximately 10^9 ions per m^3. This varies across a broad range depending on various meteorological situations. It increases near cascades or breakers. To measure this parameter, so-called *Gerdien tubes* are used. These are coaxially arranged capacitors, and their discharge over time is recorded during a particular air flow.

There has been much discussion of a possible biological role of these charges. A number of attempts have been made to construct various artificial sources of air ions for therapeutic reasons. *Electro-aerosol therapy* (EAT) was proposed to cure various bronchial afflictions. However, in fact no correlation with any kind of disorder, and no true indications of its therapeutic efficiency have been established yet.

The biological influence of environment fields in air depends on their penetration into the body. The electric conductivity of the human body is about 10^{14} times larger than that of air. The dielectric constant exceeds that of air by a factor of 50. This leads to considerable distortion of the field lines around the body (Fig. 4.24). The electric field strength near the surface of the body can significantly increase, especially at the head or at the end of a raised hand.

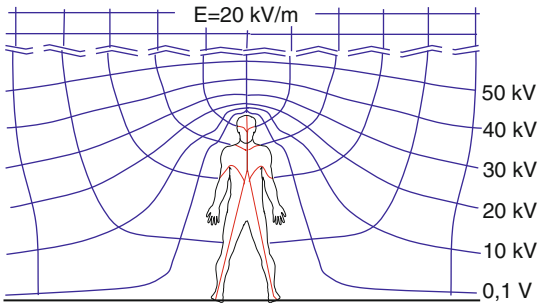

Fig. 4.24 Distortion of an electrostatic field near a standing man (After Leitgeb 1990 redrawn)

The external electric field leads to a displacement of internal charges in the body. An external electrical field $\mathbf{E}_e$ in air ($\varepsilon_e = 1$) induces in a spherical, nonconducting body ($g_i = 0$) the following internal field $\mathbf{E}_i$:

$$\mathbf{E}_i = \frac{3\,\mathbf{E}_e}{2 + \varepsilon_i} \qquad \text{for:} \quad g_i = 0 \tag{4.21}$$

If the body is conducting ($g_i > 0$), this internal field immediately will be neutralized by an internal current. Taking this process into account, one gets the real field strength $\mathbf{E}_i$ as a function of time (t):

$$\mathbf{E}_i = \frac{3\mathbf{E}_e}{2 + \varepsilon_i} \mathrm{e}^{-\frac{g_i t}{\varepsilon_i \varepsilon_0}} = \frac{3\mathbf{E}_e}{2 + \varepsilon_i} \mathrm{e}^{-kt} \qquad \text{where:} \quad k \equiv \frac{g_i}{\varepsilon_i \varepsilon_0} \tag{4.22}$$

Using appropriate parameters ($g_i = 0.6$ S m^{-1}, $\varepsilon_i = 50$, $\varepsilon_0 = 8.84 \cdot 10^{-12}$ C V^{-1} m^{-1}), a corresponding rate constant $k = 1.35 \cdot 10^9$ s^{-1} can be obtained. This means that an internal electric field which is induced by a single rectangular pulse will vanish by a half life time of $(\ln 2)/(1.35 \cdot 10^9) = 5.13 \cdot 10^{-10}$ s. A significant field in the body therefore, can be induced only in the case of higher frequency AC, or frequently pulsed fields. We will come back to this point in Sect. 4.6.

This consideration indicates that an electrostatic field in the air environment may influence only the surface of the body. This concerns, for example, electrostatic erection of hairs. In the case of low-frequency AC fields, a vibration of hairs can be sensed. The threshold where humans sense electrostatic fields in the environment is near 10 kV m^{-1}.

In contrast to the conditions in air, the field interaction in aqueous media between organisms and the environment is much stronger, leading to the electric field becoming an important element in the behavior of some aquatic organisms. In this respect, animals that live in water developed electroreceptors with an enormous sensibility. Behavioral experiments suggest that the lowest field perceived by freshwater fish is of the order of 0.1 V m^{-1}, and 2 μV m^{-1} by marine fish. These sense organs are used for active, as well as for passive electrolocation. "Active" means the measurement of distortion of the electric field pulses which are generated by the fish itself, caused by dielectric bodies in the neighborhood. This is a mechanism of orientation in weak electric fish (see Sect. 3.5.2). "Passive" electrolocation denotes the reception of electric fields from extrinsic sources and is used, for example, for the localization of living prey, or for communication with other individuals in a shoal. Furthermore, it is possible that some fishes are able to sense inorganic sources of electric fields, like electric potentials generated by streaming water, or even eddy currents induced in the body of large, fast-swimming fish by the geomagnetic field.

There is a large diversity in organs of electroreception in various aquatic animals. In general, two types of organs have been found (Fig. 4.25). *Ampullar organs*, which are cavities more or less deeply embedded in the body, connected with the surrounding water by a canal, filled with a highly conducting mucous jelly. The cavities contain the sensory epithelium. The wall of the canal is composed of

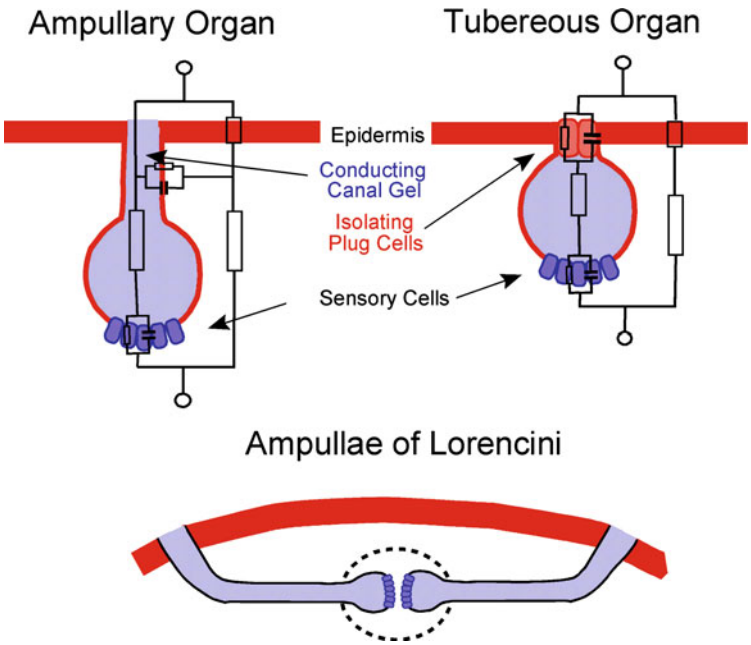

Fig. 4.25 Schematic illustration of electroreceptors in the skin of fishes. *Ampullary organs* are coupled by conducting gel to the surrounding water, whereas *tubereous organs* are connected just capacitively to the environment. The *ampullae of Lorencini* are centimeter-long canals, open to the surface at distant locations via a pore in the skin, and ending with many sense organs in a common capsule

flattened cells, connected by tight junctions and therefore indicating a high electrical resistance. *Tuberous organs* are similarly constructed organs, but without an electrically conducting connection to the surrounding water. In this case the pore is covered by a plug of epidermal cells. These tuberous organs therefore are not able to measure static potential differences, but as they are coupled capacitively to the environment, they therefore respond to time-dependent voltage changes. Tuberous organs have so far been demonstrated only in teleost fishes.

In the same way as for field-generating electrical organs (Sect. 3.5.2), also in the case of electroreceptors the different conductivity of seawater and freshwater is very important. Furthermore, the high skin resistances in freshwater fishes effectively exclude external fields, and the receptors only need to measure the potential drop across the skin, in relation to the nearly isopotential body interior. In marine fishes external fields can pervade the internal tissues. In this case centimeter-long canals are required to permit sampling of a significant portion of shallow uniform voltage gradients (Fig. 4.25). Such structures were first described by Stefano Lorenzini in 1678, and later called *ampullae of Lorenzini*. Dielectric measurements of the glycoprotein gel in these canals show that they are too sluggish for frequencies above 1 kHz, and therefore may act as antennas for extremely low frequencies. These long canals permit the clustering of the ampullae from many different receptors, with skin pores

widely distributed across the body surface. Recently it has been found that the glycoprotein gel in the ampullae of Lorenzini has electrical characteristics similar to those of semiconductors, exhibiting strong thermoelectric effects. This therefore also qualifies them for temperature sensibility.

In fact, the electroreception in fish emerged as a highly sophisticated system which is still far from being decoded. On the one hand the unbelievable sensitivity, at high noise–signal ratio must be explained, while on the other hand its ability for detailed analyses of signal information must be elucidated. Some of these phenomena can be explained as the result of averaging the response of a large number of sense organs. Additionally, mechanisms of stochastic resonance seem to optimize the noise–signal relation (see Sect. 3.1.5). The different properties of ampullar and tuberous organs allow particular responses to DC and AC fields. Furthermore, it has been found that the tuberous organs contain P (probability)- and T (time)-receptors; the first respond to amplitude characteristics, the second to the time of zero-point crossing of the potential. This complex net of different primary sensors is part of a sophisticated system of neurological data processing.

In context with biological influences of electric fields in aqueous media galvanotaxis and galvanotropism must be mentioned. *Galvanotaxis* represents the movement of cells directed by a static electric field with field strengths of about 100–500 V m^{-1}. These kinds of orientation have been observed not only in various protozoans, sperms, and zoospores, but also in many other kinds of cells, moving slowly on the substratum, like granulocytes, fibroblasts, osteoblasts, and nerve cells, etc. This effect must not be confused with electrophoresis, which means a passive transportation of charged particles in an electric field (see Sect. 2.3.5). In contrast to electrophoresis, galvanotaxis predicts an active movement of the cell. In the case of galvanotaxis, the electric field does not act as a driving force, but just as a parameter for orientation of the actual movement. In contrast to electrophoresis, galvanotaxis, being an active biological process, needs a much longer lag phase. Galvanotactically moving cells may still drive in one direction for many seconds or even minutes, even if the polarity of the applied field has already been changed. Most cells, even if negatively charged, move by galvanotaxis toward the cathode, i.e., in the direction opposite to that electrophoresis would move them.

The mechanism leading to galvanotaxis of tissue cells is rather unclear and probably not consistent for all kinds of cells. Whereas in ciliata the orientation of their motion is apparently controlled by the modified transmembrane potential, for other cells other mechanisms are proposed. Using fluorescent labels it is possible to indicate that membrane-bound receptors shift under the influence of an external field laterally in the cell membrane, and concentrate on one side of the cell. This does not seem to be the result of individual electrophoresis of these molecules but rather a reaction to local electro-osmotic flow, induced by the interaction of the external field with all charges of the membrane surface (for electro-osmosis, see Sect. 2.3.5, Fig. 2.45).

A further property of cells in electrostatic fields is *galvanotropism*. This means the influence of an external DC-field on the direction of cell growth. So, for example, nerve cells in electric fields of 0.1–1 kV m^{-1} form dendrites, preferentially

at the side of the cell which is directed toward the cathode. In this case, local modifications of the membrane potential are probably responsible for these reactions, but the above-mentioned lateral translation of membrane proteins can also be responsible for this. This property has been applied in therapy to stimulate nerve regeneration.

We already pointed out that there are various biogenic electrical fields in the human body which probably are not simple passive concomitant phenomena of some electrophysiological processes, but which may have functional relevance. In this context we already mentioned wound potentials, which can create local electric fields of hundreds of V m^{-1}, or electric fields in loaded bones (Sect. 3.5.2, Fig. 3.36). This formed the basis for various attempts at using electrotherapy to control biological processes like cell motion, cell differentiation, or cell growth, etc., through the application of applied electric fields.

Further Reading

Electric fields in the environment: Barnes and Greenbaum 2006; Glaser 2008; Reiter 1992; air ions: Charry and Kavet 1987; electroreception: Brown 2003; Bullock et al. 2005; Fortune 2006; Kalmijn et al. 2002; Peters et al. 2007; galvanotaxis: Mycielska and Djamgoz 2004; Ogawa et al. 2006; wound healing: Zhao et al. 2006.

4.6 Low-Frequency Electromagnetic Fields

In this section we begin consideration of the biophysical aspects of electromagnetic fields starting with the low-frequency range (ELF – "extremely low," ULF – "ultra low," VLF – "very low," LF – "low" frequency). The classification of the frequency regions is arbitrary and defined by engineers just for technical use (see Fig. 4.26). By chance, however, this division between "low" (L), and "high" (H) frequency in a positive way also matches differences in the dielectric behavior of living cells. As explained in Sect. 3.5.3, the cell, surrounded by a membrane, can be described as an electrical RC-circuit (Fig. 3.43), whereas at frequencies above a level of 10^5–10^6 Hz the membrane will be capacitively short-circuited. This means that biophysically the "low" frequency can be defined as the frequency region where the externally applied fields more or less are able to influence the membrane potential of living cells.

4.6.1 Physical Background and Dosimetry

In the low-frequency region particular physical properties of electromagnetic fields must be considered. According to Maxwell's equations, electromagnetic fields have a magnetic and an electric vector. With increasing frequencies, it is more and more difficult to separate experimentally the magnetic from the electric component. At ELF

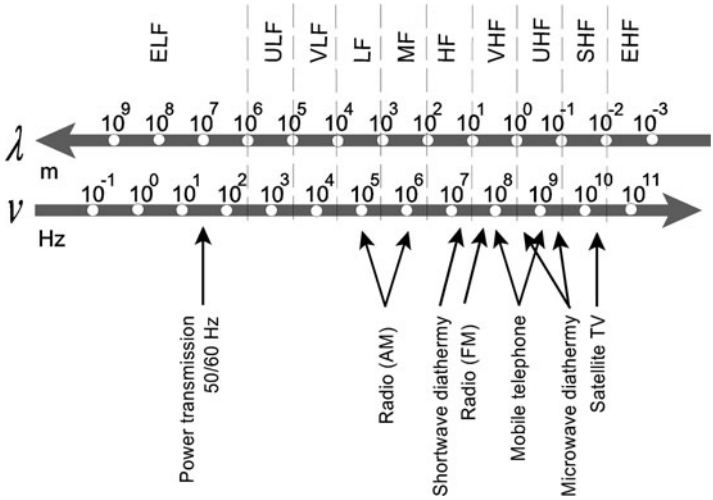

Fig. 4.26 The spectrum of technically used frequencies of electromagnetic fields (HF = high frequency, LF = low frequency, E = extremely, S = super, U = ultra, V = very, M = mean)

and ULF fields however, it depends on the techniques of field application, whether mostly an electric, or preferentially a magnetic interaction will occur. To illustrate this, three methods are shown in Fig. 4.27 to apply low frequency fields as examples. If, for example, the object is positioned between the two poles of an iron core, it is influenced mainly by the magnetic component of the field, induced in the core by the current in the coil (Fig. 4.27a). If the object is between two plates of a capacitor in air, not being in touch with them, almost only electric influences occur (Fig. 4.27c). In the same way, alternating current (AC) can be applied by electrodes connected directly with the biological object. Using coils (Fig. 4.27b), the magnetic, as well as the electric component of the field interacts with the object. There is no difference, whether the object is positioned inside the coil or in its vicinity. This situation resembles the general kind of exposition of humans near technical devices.

If humans are exposed to technical facilities, additional circumstances have to be considered which may lead to a dominance of the magnetic or the electric vector of the field. The electric field of a particular position near a power line, for example, depends on the construction of the line, i.e., on the voltage of the transported energy, which is constant for a given construction. The magnetic field, emitted by this line however, varies depending on the current flowing through it, which is always changing during the day. Furthermore, usually several wires are combined in one line, carrying different currents with phase differences. The magnetic field of a power line therefore can vary considerably. Similar aspects must also be taken into account in cases of other electric devices.

Furthermore, it must be considered that electric fields are shielded by buildings, trees, etc. Magnetic fields, in contrast to this penetrate the walls of houses and

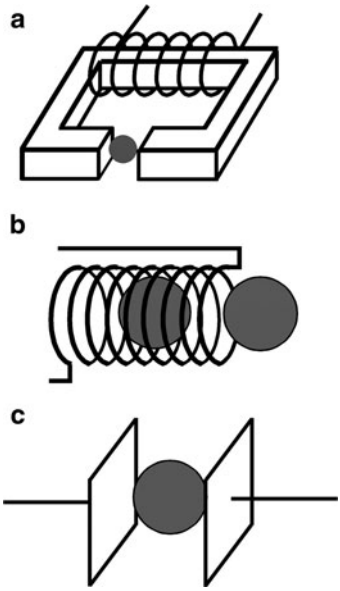

Fig. 4.27 Examples of three possibilities to apply low-frequency electromagnetic fields: (**a**) Iron core techniques with dominating magnetic field influences; (**b**) influences of magnetic and electric component; (**c**) capacitive arrangement with dominating electric field component

diminish only with increasing distance from the source. This leads to the dominance of the magnetic field in buildings and at places shielded in other ways.

Before discussing possible biological effects of electromagnetic fields, its penetration into the body must be explained, i.e., the particular conditions near the real site of interaction. From the physical point of view, low-frequency electromagnetic fields can generate electric current in the human body in two ways: by *influence* and by *induction*. The influence has already been explained in the previous Sect. 4.5 (Fig. 4.24). It is governed by Eq. 4.22, whereas the rate constant (k) of the neutralization phenomenon is compensated for by the frequency of electric field variation. Therefore, the current density increases with the frequency.

The second way to generate currents and electric fields in the body, induction, profits from the fact that the magnetic component freely penetrates the body. In this way it induces eddy currents in the tissues. The current density produced in this way depends on the frequency of the field, on its intensity, and on the geometrical parameters of the induction loop. The latter is determined by the size or diameter of the body in a projection plane perpendicular to the magnetic field vector, but also by anatomical factors and the impedance of the corresponding tissue.

Differences in the conductivity of the organs in the body can lead to preferential conductivity loops. Such loops may occur via special arrangements of blood vessels or even between electrically communicating cells. The cell itself as a space of high conductivity, surrounded by an isolating membrane, can act as a conducting loop, whose diameter however, is very small. All these circumstances in fact complicate the calculation of the real field conditions, and the local current densities in the body even if the environmental field parameters are known.

In the case of an undisturbed electromagnetic field, for example in a human under, or near a high-voltage power line, the currents generated in the body by processes of influence or of induction are quantitatively similar to each other. Qualitatively, however, the directions of these currents are different, and therefore also the appearance of current densities. Various model calculations and measurements on equivalent phantom objects are used to evaluate these parameters.

To assess safety standards, two types of parameters are used: *basic restrictions*, which refer to the current density at the site of the biological interaction in the body, and *reference levels* describing the corresponding electric or magnetic field strength in the environment which probably will induce these conditions. In contrast to the parameters of basic restrictions, these reference levels are easily measurable, and therefore used in safety control. They are evaluated from the basic restrictions by the above-mentioned models. If a measured value in the human environment exceeds the reference level, it does not necessarily follow that the basic restriction will also be exceeded. However, in such cases, model calculations are necessary to evaluate the actual reference level.

Besides technically induced fields, humans are also exposed to natural electromagnetic fields in the environment. These fields have wide-spread frequencies, starting with weak variations of the electrostatic field of the earth, as discussed in Sect. 4.5, in a region far below 1 Hz. Furthermore, pulses induced by lightning produce frequencies above 10 Hz. These world-wide discharges induce permanent low-frequency electromagnetic oscillation in the atmosphere, which can be measured even in clear weather conditions. In this case the so-called *Schumann resonance* is important, an electrical resonance frequency of the globe of 7.8 Hz with corresponding harmonics at 13.8, 19.7, 25.7, and 31.7 Hz. At higher frequencies, so-called *atmospherics* (or *spherics*) can be measured. These are pulses induced by various discharges in the atmosphere, containing electromagnetic frequencies up to tenths of kHz. The intensity of these atmospherics decreases with increasing frequency, and depends on various atmospheric conditions. Their magnetic flux density does not exceed 20 nT. It is speculated that the weather sensitivity of humans could be based on this influence, but this hypothesis has no scientific support.

Further Reading

Dosimetry and safety standards: ICNIRP 1998; Barnes and Greenbaum 2006; natural fields and spherics: Glaser 2008; Reiter 1992; Schienle et al. 1997.

4.6.2 Biological Effects and Biophysical Background

The question as to how electromagnetic fields may affect biological systems is of particular interest for problems of health protection, and also it opens new possibilities of therapeutic use. Basically, the quantum energy of electromagnetic fields in the frequency region below UV-light is insufficient to break chemical

bonds (see Sect. 4.8, Fig. 4.32). Each kind of absorbed energy is finally transformed into heat. Therefore, at higher field intensities, thermal effects occur, but the real threshold at which low frequency fields affect various membrane processes, like transport and reaction rates, and finally cause excitations of corresponding cells, is much lower.

As already mentioned in the previous section and explained in detail in Sects. 3.5.3 and 3.5.4, low-frequency electromagnetic fields and field pulses modify the transmembrane potential proportional to the external field strength, and to the diameter of the cell in the direction of the field vectors (Eq. 3.219). As shown in Fig. 3.45, caused by its low conductivity, the external field increases in the membrane. This can be considered as a considerable effect of field amplification in the membrane (cf. Fig. 3.49).

Assuming for example a cell with an elongation in the field direction of 10 μm = 10^{-5} m, and a membrane thickness of 10 nm = 10^{-8} m, then the field strength in the membrane, in relation to a low-frequency external field, will be enlarged by a factor of 10^3. In fact the effective extension of the cell in the direction of the electric field vector can be much larger. For neurons elongations in field direction of up to 1 mm are assumed. Furthermore, the word "effective" means that not only the length of the single cell, but also the extension of the conductive area surrounded by the isolating membrane must be considered. If two cells, for example, are connected by gap junctions with a high electric conductivity, then the "effective" length means the extension of this whole system.

The real effect of low-frequency electromagnetic fields, i.e., their interaction with essential molecules, therefore occurs preferentially in the membrane. As already explained in Sects. 3.4 and 3.5 there are various membrane properties which are governed by the internal field strength. This of course concerns predominantly the excitable membranes of nerves and muscles.

Experimentally, neuronal sensitivity has been detected for field strengths in the tissue as low as 0.1 V m^{-1}. To explain this high sensibility, in addition to the above-mentioned amplification effect of the field in the membrane, other circumstances must also be considered. Firstly, it is assumed that the field-sensitive channels, mainly Ca-channels, are positioned at both ends of these long cells. Furthermore, these channels as a kind of electric rectifier can accumulate the gating charges during several cycles of alternating field. Finally, the mean response of a large number of field-sensitive channels in a single cell is essential, as well as processes of stochastic resonance (see Sect. 3.1.5).

Figure 4.29 shows simplified functions of threshold values for various effects based on experimental data. The minimal range of observed biological effects of 0.01 A m^{-2} corresponds to the above-mentioned field strength of 0.1 V m^{-1}, taking into account a conductivity of tissue of 0.1 S m^{-1} (see Fig. 3.41).

In this figure an increase of the threshold is shown at frequencies >300 Hz. This is caused simultaneously for two reasons. First, as explained in Sect. 3.5.5 (see also Fig. 3.49), the influence of low frequency fields on the membrane potential decreases with increasing frequency, and nearly vanishes at frequencies above 1 MHz. This is caused by the increasing capacitive conductivity of the membrane,

i.e., by its RC behavior. The second reason concerns the mechanism of membrane excitation itself. As shown in Fig. 3.29, the action potential of nerve or muscle cells lasted several milliseconds. This means that an excitation with a frequency of several 100 Hz, which is faster than 10 ms, becomes ineffective because of the refractory period of the cell after an actual excitation.

At the frequency range of electromagnetic fields, and of alternating currents up to about 100 kHz, the dominant mechanisms of interaction therefore, are excitations of nerves and muscles. These excitation properties, shown in Fig. 4.29, led to the recommendation that in the frequency range between 4 Hz and 1 kHz the basic restriction level of occupational exposure should be limited to current densities less than 10 mA m^{-2} in the body. For the general public an additional factor of 5 is applied. This corresponds to the reference level as listed in Fig. 4.28.

Comparing Figs. 4.28 and 4.29 it strikes one that in one case the functions step up with increasing frequency, while in the other case, they decline. The reason for this is that even if the sensibility of nerve and muscles to electric excitations decreases with increasing frequency (restriction level) (Fig. 4.29), the current density of induction, i.e., the efficiency of the induction process, increases at the same time, and will eventually dominate the function of the reference levels (Fig. 4.28).

To evaluate thermal effects of low frequency fields the resulting power density (P) must be calculated. This parameter in W m^{-3} can easily be translated into the *specific absorption rate* (SAR) in W kg^{-1} using a mean density of tissue of about 1,000 kg m^{-3}. For low frequency fields, using Ohm's law, this means:

$$P = j\mathbf{E} = \frac{j^2}{g} = \mathbf{E}^2 g \tag{4.23}$$

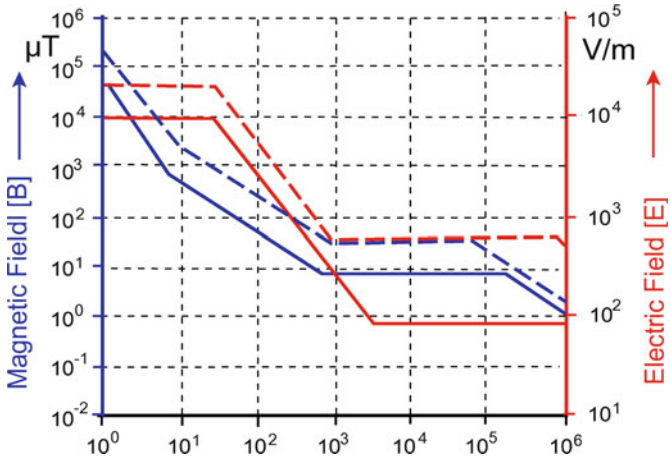

Fig. 4.28 Reference levels for magnetic and electric field for the general public (*solid lines*) and occupational exposure (*dashed lines*) (After ICNIRP 1998)

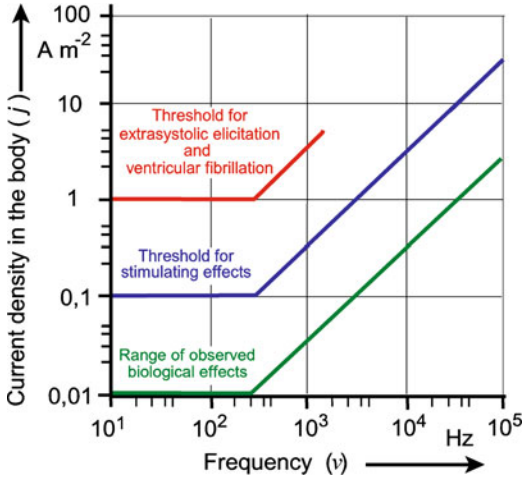

Fig. 4.29 Threshold values of the electric current density in the human body in the low frequency region (After Bernhardt 1988, simplified)

where j is the current density in Am^{-2}, g is the specific conductivity in $S\ m^{-1}$, and **E** the field strength in $V\ m^{-1}$.

Using the parameters of Fig. 4.29 and inserting them into Eq. 4.23 one can easily see that for low frequency fields even at the highest threshold, namely absolute danger to life, the SAR amounts to only about 0.001 $W\ kg^{-1}$. This is negligibly small in relation to the basic metabolic rate, i.e., the heat production of the resting human body which amounts to 1 $W\ kg^{-1}$, and which furthermore often increases in the case of active movement by a factor of ten (see Sect. 3.8). This can be directly related to the dissipation function (Φ) (see Sect. 3.1.4, Eq. 3.64) which for small mammals is even larger (see Fig. 3.7).

Because of its relevance to safety standards for the population, the biological effects of low-frequency electromagnetic fields, even below the threshold of excitation, have been the subject of many investigations in recent decades. Experiments have been carried out on all levels of biological organization, and completed by epidemiological studies. Consistent with biophysical considerations, however, no reproducible effects below the level of excitation could be found. Therefore, there is no good reason to decrease the safety levels as discussed above.

Low frequency currents and electromagnetic fields have also been applied for various therapeutic uses. This includes implanted stimulating electrodes, like cardiac pacemakers, and various kinds of externally applied electrodes for electrostimulation of nerves (TENS = Transcutaneous Electric Nerve Stimulation), as well as attempts to influence biological processes using eddy currents, induced by external coils. As already mentioned in Sect. 4.4, neuronal electric stimulation in this way is possible, using very strong millisecond magnetic pulses (1.5–2 T). In some cases implanted electrodes are used, combined with small coils, which receive their current by induction processes in external magnetic fields. Furthermore, various PEMF-techniques (Pulsed Electro-Magnetic Field) with external coils have been proposed for the treatment of various diseases.

As a criterion for the real efficiency of these methods a calculation must be made as to whether the induced current density is really large enough to affect the biological system. This not only depends on the intensity and frequency of the applied field, but additionally on the edge steepness, if rectangular pulses are applied. Not only for public health protection, but moreover for possible therapeutic effects the values depicted in Fig. 4.29 are important. As no biological effects have been found below these levels, no therapeutic results would be expected below these intensities. In fact, many of the advertized therapeutic machines must be classed as placebo therapy.

Further Reading

General aspects of low-frequency field effects: Barnes and Greenbaum 2006; biological sensibility: Francis et al. 2003; Weaver et al. 1998; aspects of health protection: ICNIRP 1998; history of medical applications: Rowbottom and Susskind 1984.

4.7 Radio- and Microwave Electromagnetic Fields

As already mentioned in Sect. 4.6, the classification of the frequency regions of electromagnetic fields is rather arbitrary (see Fig. 4.26), but there are a number of physical and biophysical peculiarities which makes it reasonable to distinguish between "low" and "high" frequency. The frequency bands which in Fig. 4.26 contain the Letter "H," in their lower part, are mostly called "radio frequency." In the region above about 3 GHz on the other hand the term "microwaves" is used.

4.7.1 Physical Background and Dosimetry

In contrast to low frequency fields, in the HF region a splitting into the magnetic and electric field vector is impossible. Although up to UHF frequencies it is technically possible to apply fields at least with pronounced electrical or magnetic components, in the practical use of technical devices, both components are connected.

In this frequency region the so-called *skin effect* becomes important. This is the result of the eddy currents, induced in the conductor, cancelling the current flow in the center, and reinforcing it at the surface. With increasing frequency the tendency for an alternating electric current to distribute itself within a conductor increases so that the current density near the surface of the conductor is larger than that at its core.

This effect also determines the depth of penetration of high-frequency electromagnetic fields in a homogeneous body. It is characterized by the *skin depth* (δ) which can be calculated for practical use by:

$$\delta = \sqrt{\frac{1}{\pi \mu \mu_0 g \nu}} \tag{4.24}$$

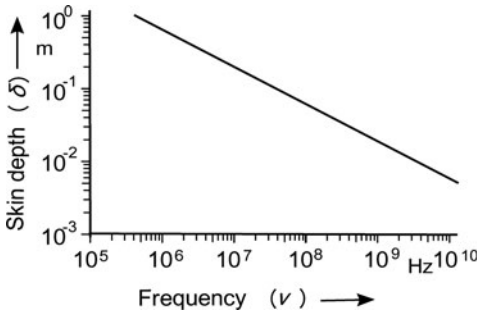

Fig. 4.30 Skin depth (δ) according to Eq. 4.24 for a homogeneous body with a specific conductivity $g = 0.6$ S m^{-1} as a function of frequency (ν)

This skin depth (δ) is the distance over which the field intensity decreases to a factor of 1/e = 0.368. Figure 4.30 indicates the function $\delta(\nu)$ for the following conditions: magnetic permeability of vacuum $\mu_0 = 1.256.10^{-6}$ V s A^{-1} m^{-1}, the magnetic permeability number $\mu = 1$, and the mean conductivity of the tissue: $g = 0.6$ S m^{-1} (see Fig. 3.41). It shows that this effect will become important only at high frequencies ($\nu > 10^6$ Hz).

The distribution and penetration of high-frequency electromagnetic fields in the living body is an important factor in therapeutic applications, as well as in all safety considerations. However, calculations using Eq. 4.24, and correspondingly Fig. 4.30 only represent a rough estimation of field penetration because they assume a body with homogeneous dielectric properties. After all, it shows that in the frequency range from about 20 to 300 MHz a relatively high absorption can occur in the whole body. At higher frequencies, the field does not penetrate deeply, but will be absorbed mainly at the surface. It is possible, for example, to estimate in this way that the electromagnetic field of a mobile telephone with a frequency of around 1 GHz fully penetrates the body of small laboratory animals, but affects in humans only a certain part of the surface. At frequencies above about 10 GHz the absorption occurs primarily at the skin.

For detailed dosimetric considerations, particular anatomic and dielectric peculiarities of the body must be taken into account. As already shown in Sect. 3.5.3 (Fig. 3.41), the dielectric parameters of different tissues vary to a large extent. Furthermore, in contrast to the assumptions leading to the graph in Fig. 4.30, the conductivities themselves are functions of the frequency. To establish a realistic dosimetry for high-frequency field exposition, various model calculations have been proposed, using the finite-difference time-domain (FDTD) method. In this case, based for example on detailed MRT-pictures of the body, analyses have been done with pixel volumes down to 1 mm^3.

In general the dosimetric calculations are based on the intensity of the field which is characterized by the *plane power density* (W m^{-2}) emitted by an external source. In the case of far-field exposure, i.e., at a distance from the antenna more than twice the wavelength, plane wave conditions can be expected. Furthermore, in dosimetric considerations resonance phenomena of the whole body or of parts of it (e.g., the head) must be considered. The human body, if not grounded, has a resonant absorption frequency close to 70 MHz. For small laboratory animals, such as rats or mice, the resonance frequency is correspondingly higher.

As already mentioned in the introduction to Sect. 4, according to the Grotthus–Draper principle, not the energy penetrating the organism, but only that part which is actually absorbed into the system can be effective. Therefore, a *specific absorption rate* (SAR) in W kg^{-1} is defined to characterize the dose of high frequency exposition (see Eq. 4.23). In contrast to the plane power density (in W m^{-2}), which just depends on technical parameters of the field-emitting device, the SAR is the energy, which per unit of time is absorbed in a unit of mass or volume of the body. Knowing the SAR and the heat capacity of the tissue, thermal effects of absorbed electromagnetic fields can be calculated. In this way SAR is also directly measurable by sensitive thermistors. Because of the inhomogeneity of the tissue, the SAR values can differ at various locations. For this reason SAR values are evaluated for an average mass of 10 g, or in some cases even for 1 g. In the case of time varying radiation, time-averaged values are used.

At frequencies greater than about 10 GHz, because of the limited depth of field penetration, the SAR is proofed not as a good measure for assessing absorbed energy. This is the reason where as at microwave frequencies up to UV-light the incident power density (W m^{-2}) is used as a more appropriate dosimetric quantity.

4.7.2 Biophysical Aspects of High-Frequency Field Interaction

In the previous section (Sect. 4.6.2) we explained that in the frequency range up to about 100 kHz excitations of nerves and muscles, but not thermal effects, are the dominating mechanisms of interaction. At higher frequencies, however, this situation reverses. In the frequency region $\nu > 10^5$ Hz, diathermal heating becomes dominant. *Diathermy* means an inhomogeneous heating of the body corresponding to the inhomogeneity of field absorption, i.e., the inhomogeneous distribution of the SAR-value, as discussed in Sect. 4.7. This word, combined from the Greak words *διά (through)* and *δέρμος* (heat), denotes heat generation inside the body. This inherent difference of diathermy in contrast to conventional heating by thermoconduction from outside makes it useful for various kinds of therapy.

In the discussion of safety aspects of radiofrequency irradiation, it was hypothesized that beside diathermal heating, additionally, there may exist nonthermal effects. In fact the terms *thermal* and *nonthermal* (or *athermal*) are used in different ways. From the empirical point of view, effects are usually called "nonthermal" in situations where the irradiation intensity is so low that changes in temperature of the exposed body are not predictable or not measurable, or if some observed effects do not correspond to such, which appear to the same degree after conventional heating.

Contrary to this, the biophysical definition of this term is based on the types of mechanisms of field interaction. A mechanism is considered as nonthermal if the interaction of the electrical (or magnetic) vector of the electromagnetic field with charges or dipoles of molecules in the living system directly leads to specific

effects, other than heating, or if the system changes its properties in a way that cannot be achieved simply by a temperature increase.

According to this biophysical definition a number of nonthermal effects are well known. This includes, for example, dielectrophoreses or the electrorotation of cells as described in detail in Sect. 3.5.5 (see Fig. 3.47). In these cases the electric field induces dipoles which directly lead to cell movements or deformations. Actually, these effects require field intensities, which cause considerable heating. A field of about 10^4 V m^{-1}, which for example is necessary to induce dielectrophoretic cell movement in a medium with a conductivity of about 0.1 S m^{-1} according to Eq. 4.23 produces a SAR of 10^7 W m^{-3}, or approximately 10^4 W kg^{-1}. This of course leads to an intense heating of the system. As already mentioned in Sect. 3.5.5, the application of these dielectric techniques in biotechnology requires special precautions of thermal protection.

In contrast to these effects at extremely large field strength, nonthermal effects at low field intensities, i.e., without a measurable temperature increase, are biophysically not imaginable, and experimentally not convincingly demonstrated in this frequency region. Occasionally described results of this type are either nonreproducible, or after all a result of local heating.

For this reason the recommendation of exposure limits is based on the circumstance that no established biological and health effects could occur at a rise in the body temperature $>1°C$. This temperature limit resembles an amount, which corresponds to everyday heating of individuals under moderate environmental conditions. It will arrive at a whole body SAR of about 4 W kg^{-1}. This corresponds to the magnitude of the basic metabolic rate, whereas not the mean metabolic rate of the whole body must be considered to evaluate health risk, but rather that of the most active organs like muscles or brain which may be higher by one order of magnitude. Using an additional safety factor, for whole body irradiation with frequencies between 100 kHz and 10 GHz an average whole body SAR limit of 0.08 W kg^{-1} is recommended. Note, that this is 5 orders of magnitude lower than the above-mentioned SAR in biotechnological applications, allowing cells to live and develop even under permanent exposition for days without observable damage!

The recommendation of the exposure limit is therefore based exclusively on thermal effects of HF radiation. This is justified because "nonthermal" effects in the empirical definition, i.e., without an increase in the temperature, have not been established, as already mentioned. The comparison of effects of diathermal heating with heating to the same temperature in a conventional way, appears to be an unrealistic approach because the resulting temperature gradients are quite different for both cases.

In fact, all of these considerations of the system of thermoregulation of the living body must be taken into account. This has already been described in Sect. 4.1, where in the bioheat equation (Eq. 4.4) the SAR as a generalized heat input from outside is included. Considering the system as illustrated in Fig. 4.2, it cannot be excluded that thermoreceptors can be activated as the result of low-intensity field interaction without a measurable increase in the body temperature, which could

lead to local effects like modifications of blood circulation or EEG. This, however, is comparable with other everyday effects without noxious implications.

The absorption of HF fields in biological systems is basically determined by its water content. In contrast to free water, the dipoles of which are oscillating in the frequency of 18.7 GHz (Sect. 3.5.3), the resonance frequency of bound water can be shifted down, up to tenths of MHz. The broad dispersion of dielectric properties of the biological material (Fig. 3.41) makes it impossible, to find sharp absorption maxima or resonance peaks, and therefore no frequency windows of HF-field interaction are to be expected.

At strong high frequency pulses a *microwave auditory effect*, or *RF-hearing* occurs which is caused by abrupt heating of tissue water in the head. The sudden expansion which is generated in this way, launches acoustic waves which can elicit low intensity sound like a buzz, click, hiss, or knock. RF-hearing has been reported at frequencies ranging from 2.4 MHz to 10 GHz. This effect depends on the energy of the single pulse, and not on the average power density.

These considerations lead to the problem of *microdosimetry*, and the question whether *microthermal* heating is possible as the result of field exposure. In fact, the heterogeneity of dielectric parameters is not only established in anatomical dimensions, as demonstrated in Fig. 3.41 (Sect. 3.5.3) but moreover down to the cellular, subcellular, and even molecular magnitudes. What could the minimal size of a hotspot, i.e., a region with particularly increased temperature caused by increasing absorption of high frequency energy, be?

In the simplest approach, this question can be checked on the basis of heat dynamics of a sphere in an environment with different dielectric properties. Assume that a spherical object of radius r is subject to heating at a given SAR, and is surrounded by unheated material. The maximum temperature increase (ΔT), and the thermal time constant [τ (s)] can be found as a solution of the heat equation (Eq. 4.4 in Sect. 4.1), ignoring the blood flow term, and the heat production by metabolism:

$$\Delta \mathrm{T} = \frac{\mathrm{SAR}}{\mathrm{C}}\tau \tag{4.25}$$

$$\tau = \frac{\rho \mathrm{C}\ \mathrm{r}^2}{\lambda} \tag{4.26}$$

where C is the specific heat capacity, ρ the density, and λ the thermal conductivity.

These equations show that the time constant (τ), and therefore also the steady-state temperature increase (ΔT), are proportional to the square of the dimension of the sphere (r^2). As shown in Fig. 4.31, in fact the temperature fluctuations produced by selective heating of very small structures, as well as the time scale in this dimension are negligible. According to these calculations, points of local temperature increase, i.e., so-called *hot spots*, can occur only in regions of dielectric inhomogeneity with a size at least in millimeter dimensions.

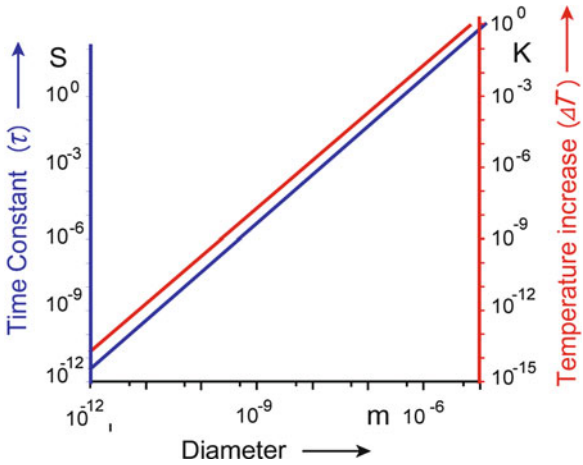

Fig. 4.31 Time constant (thermal response time) and maximum steady-state temperature increase of a sphere as a function of its diameter exposed at a SAR of 10 W kg^{-1} in an unheated medium. For the thermal properties of the spheres the parameters of brain tissue were used (Data from Foster and Glaser 2007)

It should be mentioned, however, that these equations are hardly applicable to processes in molecular dimensions where the phenomenological concept of temperature changes into that of statistical thermodynamics. Conversely, as explained in Sect. 2.1.6 (see Fig. 2.8), the frequencies of vibrational and rotational movements of molecules are above 10^{10} Hz, i.e., essentially in the Terra-Hertz region.

To analyze possible biophysical mechanisms of high-frequency effects of weak fields on biological systems, a number of hypotheses had been proposed. Some of them are based on the idea that high-frequency electromagnetic fields could exhibit classical resonance phenomena, and in this way might absorb energy in excess. The particular analyses, however, suggest that the vibratory motion by biological fluids is severely restricted by the damping properties of water. The absence of a reliable biophysical theory for possible low-intensity, nonthermal effects of high-frequency electromagnetic fields in fact corresponds to the unavailing experimental results. Therefore only thermal, or possibly microthermal effects are to be proposed below electrorotation or dielectrophoreses as nonthermal effects at strong field intensities.

Further Reading

General effects: Barnes and Greenbaum 2006; microthermal effects: Foster and Glaser 2007; RF-hearing: Elder and Chou 2003; mechanisms and resonance phenomena: Adair 2002; guidelines and limits: ICNIRP 1998.

4.8 Visible and Nonvisible Optical Radiation

The spectrum of technically used frequencies of electromagnetic radiation, as discussed in the previous sections, ended in Fig. 4.26 with the "Extremely High Frequency" (EHF) region corresponding to a wavelength of 1 mm. In continuation, the "Terra Hertz Frequency" region follows, which reaches into the infrared region.

Table 4.5 Characteristic parameters of optical radiation

		Wavelength (λ)	Frequency (ν) in Hz	Quantum energy (E) in eV
Terahertz-radiation	<1 mm	3.10^{11}–3.10^{12}	$<1.24 \cdot 10^{3}$	
Infrared	IRC	3,000 nm–1 mm	$3 \cdot 10^{11}$–$1 \cdot 10^{14}$	$1.24 \cdot 10^{3}$–0.41
	IRB	1,400–3,000 nm	$1 \cdot 10^{14}$–$2.1 \cdot 10^{14}$	0.41–0.89
	IRA	700–1,400 nm	$2.1 \cdot 10^{14}$–$4.3 \cdot 10^{14}$	0.89–1.77
Visible light		400–700 nm	$4.3 \cdot 10^{14}$–$7.5 \cdot 10^{14}$	1.77–3.09
Ultraviolet	UVA	315–400 nm	$7.5 \cdot 10^{14}$–$9.5 \cdot 10^{14}$	3.09–3.94
	UVB	280–315 nm	$9.5 \cdot 10^{14}$–$1.1 \cdot 10^{15}$	3.94–4.42
	UVC	100–280 nm	$1.1 \cdot 10^{15}$–$3.0 \cdot 10^{15}$	4.42–12.4
Ionizing radiation		<100 nm	$>3.0 \cdot 10^{15}$	>12.4

Here the nomenclature of high frequency engineers on the one hand, and the specialists in optical spectroscopy on the other hand overlap. The THZ region from 0.3 to 3 THz, corresponding to a wavelength (λ) from 0.1 to 1 mm, overlaps with the far infrared, the so-called IRC, which is defined in the large region between 3 μm and 1 mm (see Table 4.5). Therefore, the THz range spans the transition from radio-electronics to photonics.

In contrast to Fig. 4.26, in Fig. 4.32, the quantum energy of the radiation is additionally included (E in eV) as a third coordinate. The relation between E and the frequency (ν) is given by Planck's constant $h = 6.626 \cdot 10^{-34}$ J s $= 4.136 \cdot 10^{-15}$ eV s, corresponding to the relation $E = h\nu$.

In the lower frequency region the quantum energy of radiation is far too low to be considered as a possible reason for interactions with matter. But if it rises up to the levels of molecular vibrations, this parameter becomes of increasing importance. At first it exceeds the energy of thermal noise (kT). Finally, it achieves the energy of covalent bonds, and therefore the energy of ionization. Therefore, in Fig. 4.32 two remarkable points in the scale are included: First the value of 0.026 eV, which corresponds to the energy of thermal noise at 300 K ($E = kT = 8.617 \cdot 10^{-5} \cdot 300$ eV $= 0.026$ eV), and then the energy of ionization, i.e., the quantum energy which is sufficient to break a covalent bond of water, which amounts to around 12 eV. This second point in the frequency spectrum is considered as the border line to ionizing radiation (see Sect. 4.9).

It is important to note that these two points indicate the general range of energetic transformations in biological processes. From the point of view of thermodynamics, effective mechanisms of energy transformation are possible only above the level of thermal noise. Conversely, the quantum energy must not be as large, as it could destroy the machinery itself. Therefore, the upper limit of biological existence is the quantum energy of ionization, where the quantum energy of the radiation starts to break the covalent bonds of proteins and other biologically important molecules. In fact, only the tiny frequency region of "visible light" between 400 and 700 nm, i.e., 1.77–3.09 eV is suitable to be used by biological systems to extract energy from sunlight, and to recover optical information.

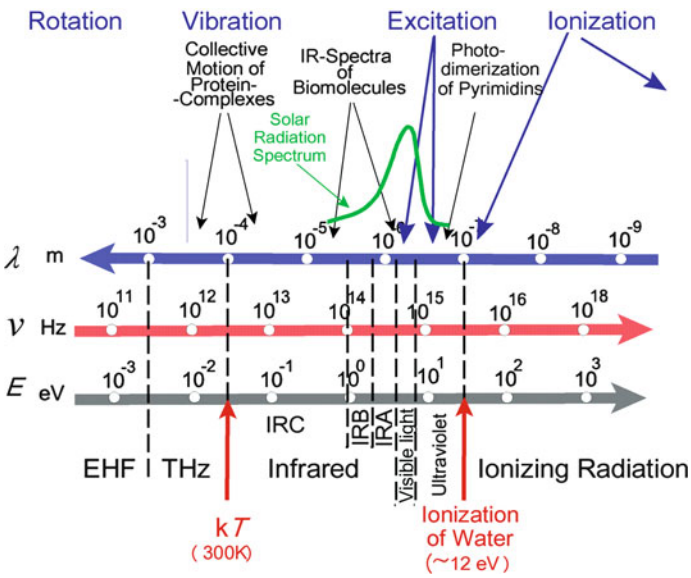

Fig. 4.32 The spectrum of optical frequencies and ionizing radiation (continuation of technical-used frequencies shown in Fig. 4.26)

The scientific literature for this frequency spectrum is largely dominated by spectroscopic investigations. This aspect is quite important for research on the structure and functions of molecular systems, and presented in a number of excellent monographs. Corresponding to the aim of this textbook, the following explanations, however, will concentrate on the mechanisms of molecular interactions, and on aspects of biological influences of this kind of radiation.

It should be noted here that in optical spectroscopy, as a peculiarity, the parameter *wave number* is used to characterize absorption spectra. This parameter is reciprocal to the wavelength. The wavelength (λ) of 3,000 nm $= 3{\cdot}10^{-4}$ cm, for example, corresponds to the wave number of: $1/3{\cdot}10^{-4} = 3{,}330\ \mathrm{cm}^{-1}$. Unfortunately, this parameter is sometimes called "frequency" by spectroscopists, which of course has the correct dimension: 1/s = Hz. Furthermore, the abscissae of absorption spectra are sometimes plotted in a decreasing, and sometimes in an increasing version. In the following text we will only use the three parameters λ (m), ν (Hz), and E (eV) as depicted in Fig. 4.32, plotting them always in the same orientation.

4.8.1 THz and Infrared: The Vibration-Inducing Frequencies

The frequency spectrum which will be considered in this chapter can be characterized in general as thermal radiation, emitted by the sun, by heated materials, and also by the human body. As shown in Figs. 4.32 and 4.37 the thermal

radiation which arrives at the earth's surface from the sun occurs mainly at frequencies $>10^{14}$ Hz, i.e., in the frequency region of IRA, and to a lesser extent at IRB. This also corresponds to the warm sensation of animals, which, however, is considered a temperature sensation according to the Arrhenius law (Sect. 2.1.5), rather than a perception of photons of the infrared radiation. Even the infrared orientation of some snakes, which helps them in the hunting of warm-blooded animals, are not based on particular quantum processes but rather on a temperature-sensitive membrane inside a particular pinhole camera (see Sect. 4.1).

Only in the last decennium has the technical possibilities been developed to produce and to indicate radiation in the THz-frequency range. The THz technologies now receive increasing attention, and various devices use this wavelength. Therefore this frequency band becomes increasingly important in diverse applications. It opens the way to extend infrared spectroscopy into these parts of the spectrum. Because the THz-radiation is strongly absorbed by water molecules, it penetrates just several millimeters of fatty tissue with low water content. This also complicates the THz-spectroscopy of biomolecules in their natural water environment. Conversely the dependence of THz absorption on the water content of the tissue may become important for some diagnostic methods, for example to detect some kinds of epithelial cancer. Some frequencies of terahertz radiation can be used for 3D imaging of teeth and may be more accurate and safer than conventional X-ray imaging in dentistry.

The frequency dependence of absorption of infrared radiation by water and CO_2 is best illustrated by the absorption spectrum of the normal atmosphere, not loaded with fog or rain (Fig. 4.33). It shows a maximum in the frequency region between 10^{12} and 10^{13} Hz. Therefore, it is somewhat unsuitable for use in technical telecommunications, at least under outdoor conditions.

The molecular mechanism of direct interaction of THz and infrared radiation with biological systems can finally be deduced from the data of absorption spectroscopy and by inelastic scattering of photons (*Raman spectroscopy*). The absorption of photons leads to vibrational movements of the molecules and their components. Depending on the structure of the molecule, a more or less large number of vibrational modes are possible. The vibrational modes of proteins are mostly influenced by their secondary structure, and furthermore by their kinds of hydration.

As already discussed in Sect. 2.1.6 (see also Fig. 2.8) the vibration frequency of a C–C bond is in the infrared frequency range of 10^{14} Hz which corresponds to a wavelength of 3 μm. The modes of rotation of these bonds, in contrast, are much lower, and correspond to a frequency below 1 THz. As shown in Fig. 4.32, this is below the energy of thermal movement (kT). The vibration modes, however, may also shift to lower frequencies if collective molecular motions or those of strongly hydrated macromolecules are considered. Collective motions of proteins can involve subdomains of hundreds of atoms with corresponding frequencies up to the THz regime. In these complexes the vibrational energy may flow in a concerted manner, to produce conformational changes.

Recently methods of THz time-domain spectroscopy have been developed. In this case short THz-pulses are applied to the sample material. This allows one to

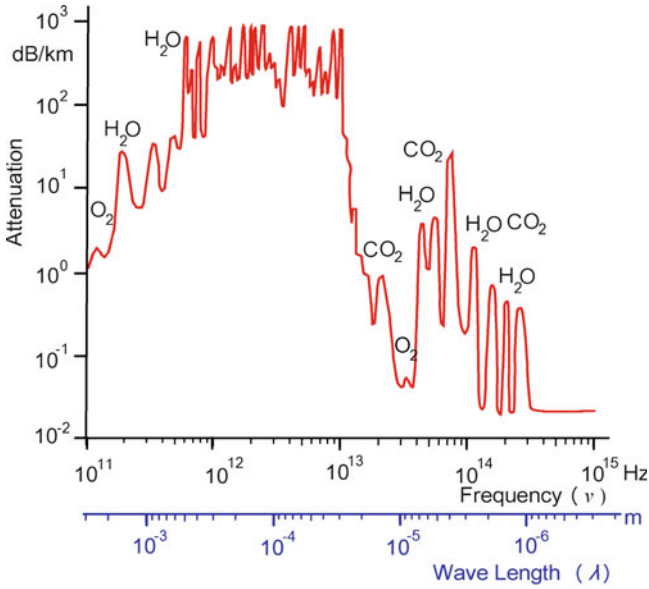

Fig. 4.33 Light absorption in the earth's atmosphere (Data from Sizov 2010)

register both the amplitude and the phase shifts, which contain far more information than a conventional image formed with a single-frequency source.

Exposure of human skin to infrared radiation resulting from solar irradiation, or from IR-emitting devices is used in medical treatments, as a preventative measure, and more recently in the "wellness" sector. Terahertz radiation is nonionizing, and thus is not expected to damage tissues and DNA, unlike X-rays. Single overexposures to IR radiation, however, can lead to acute damage in the form of skin burns, or collapse of the circulatory system. In cases of chronic or frequent repeated exposure, squamous cell carcinoma can result, especially in combination with other sources, like UV radiation. To date the recommendations for protecting humans from the risks of skin exposure to IR are only defined in terms of acute effects.

Further Reading

IR-spectroscopy: Siebert and Hildebrandt 2008; THz-spectroscopy: Plusquellic et al. 2007; Balu et al. 2008; safety aspects: Piazena and Kelleher 2010.

4.8.2 Visible Light: Processes of Excitation and Energy Transfer

The wavelength of visible light lies between 400 and 700 nm. This corresponds to quantum energies between 3.09 and 1.77 eV (see Fig. 4.32 and Table 4.5). This

quantum energy therefore, is far below that of ionizing radiation, a value, which is arrived at only in short-wave ultraviolet light (UVC). Conversely it is larger than that of thermal noise (k*T*), which at temperatures of biological importance amounts to only about 0.026 eV. As already mentioned in the preface to this Sect. (4.8) the organism uses exactly, this gap between the quantum energy of thermal noise, and the quantum energies causing ionization for photosynthesis and communication with the environment. The photons of light are strong enough for electron excitation, i.e., to lift electrons into a higher energetic state. This is the basic step for effective photochemical processes of energy conversion and photoreception, whilst not endangering the stability of biomolecules.

To understand the basic biophysical processes of photon absorption, let us first consider briefly the process of molecular excitation as illustrated in the so-called *Jablonski diagram* (Fig. 4.34). In a first step, the absorption of a photon leads to the raising of an electron to an orbit of higher quantum number. This can occur in the framework of the following two series of energetic states, which are qualitatively different: S_0, S_1, S_2,..., and T_1, T_2, T_3,.... Between these steps with increasing quantum numbers additionally, small energetic steps of thermal excitations are positioned. In the case of *singlet states* (*S*), the electrons of a pair have antiparallel oriented spins. The spin quantum numbers, therefore, have different signs. In the case of *triplet states* (T), the spins of the electrons of the pair are oriented in parallel, thus their spin quantum numbers are identical. The occurrence of electrons in which all quantum numbers are equal is ruled out by *Pauli's exclusion principle* stating that it is impossible for two electrons with identical quantum numbers to occur in the same atom. Thus, if the triplet state represents an electron pair with identical spin quantum numbers, these two electrons must differ with regard to other energy parameters although their orbitals can be energetically very similar. A triplet is a so-called *degenerated state*.

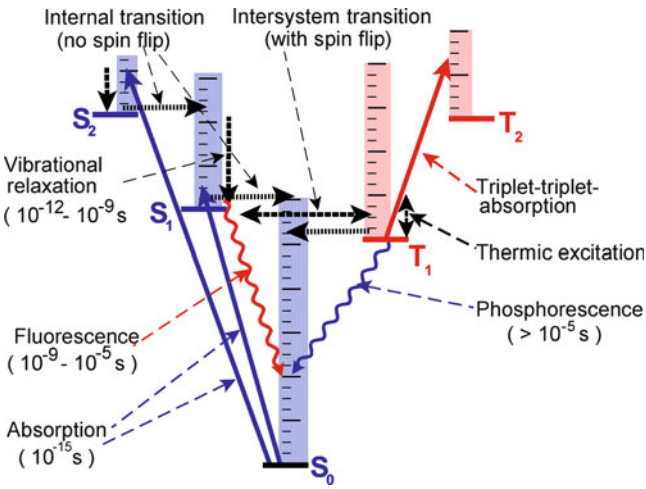

Fig. 4.34 Jablonski diagram of molecular excitations

These two states of excitation differ substantially in their life span. Figure 4.34 shows that the transition $S_1 \rightarrow S_0$ occurs under emission of *fluorescent light* within 10^{-9}–10^{-5} s, whereas the transition $T_1 \rightarrow S_0$, recordable as *phosphorescence*, will occur at a much slower rate. Consequently, triplet states are characterized by an increased stability when compared with excited singlet states.

In photobiological systems of energy harvesting, as well as in photoreceptor processes the light energy absorbed by the chromophores must be transferred, in order to produce an excitation of the corresponding effector molecules. This transfer from a donor to an acceptor molecule occurs either by charge carriers, i.e., in an electron transfer as a redox-process, by way of fluorescence, or by Förster resonance energy transfer (abbreviated FRET transfer).

The mechanism of this *resonance transfer* can be envisioned as some sort of coupling between oscillating dipoles. It is a process in which a $S_1 \rightarrow S_0$ transition in the donor molecule induces an $S_0 \rightarrow S_1$ excitation in the acceptor. The excited electron of the donor molecule undergoes oscillations and returns to its basic state thus inducing excitation of an electron in the acceptor molecule. This process requires an overlapping of the fluorescent bands of the donor with the absorption band of the acceptor, i.e., the resonance of both oscillators. The smaller the difference of the characteristic frequencies between donator and acceptor, the faster the transfer will be. These so-called strong dipole-dipole couplings are possible to distances of up to 5 nm. This distance is in fact much smaller than the wavelength of emitted light. Therefore a real photon is undetectable, and this mechanism is classified as radiation-less. The term *Förster resonance energy transfer* (FRET) therefore seems to be more appropriate than *fluorescence resonance transfer*.

In general, an *energy transfer by radiation* is also possible. In this case the energy transfer occurs actually by fluorescent radiation emitted by one, and absorbed by the neighboring molecule. Such mechanisms are capable of transferring energy over distances which are large when compared with the other processes described in this context. However, the efficiency of this process is quite low. In fact, such mechanisms do not play a significant role in biological processes.

In contrast to FRET, which usually occurs as a radiation-less singlet-singlet transfer, the *Dexter electron transfer* is a mechanism which allows the energy transfer from triplet states. This is a particular case of electron transfer, in which an excited electron transfers from one molecule (the donor) to a second (the acceptor), maintaining its spin. Typically it may occur at distances below 10 nm.

In the most common metabolic reactions the energy transfer occurs by charge carriers as a classical example of a redox reaction. It consists basically of the transfer of one or two electrons from the donor, to the acceptor molecule. In this way, the donor becomes oxidized, and the acceptor reduced.

For these processes of electron transfer, donor and acceptor molecules must be in exactly defined positions to each other, and at a minimum distance, so that overlapping of respective electron orbitals can occur. In the first place, donor and acceptor will form a complex of highly specific steric configuration, a so-called *charge transfer complex*. This process of complex formation occasionally requires steric transformations of both molecules. It takes place at lower rates when

compared with the energy transfer by induction as discussed earlier. Hence, the charge-transfer complex is an activated transition state which enables redox processes to take place between highly specific reaction partners in the enzyme systems of the cellular metabolism. Because of the oscillating nature of electron transfer, this coupling of two molecules is strengthened by additional electrostatic forces sometimes defined as *charge-transfer forces*.

Further Reading

Montali et al. 2006.

4.8.3 Visible Light: Photobiological Processes

Electromagnetic radiation in the wavelength between 400 and 700 nm is called "visible light" because it is used in cells and organisms at all levels of evolution for information transfer, i.e., as photoreceptors as well as for bioluminescence, and furthermore in the kingdom of eutrophic organisms even as a source of energy.

About 0.05% of the total 10^{22} kJ energy which reaches the earth every year from the sun is assimilated by photosynthesis. This is the general energetic pool for all living processes of the earth. The efficiency of primary reactions of photosynthesis is very high, compared with our recent technical equipment. During subsequent metabolic processes of energy transfer, however, an additional loss of energy occurs. The total efficiency of the process of photosynthesis, in fact, is assumed to vary from 0.1% to 8%, depending on various environmental conditions.

The efficiency of photosynthesis is established by the system of energy transfer from light-harvesting antenna complexes to the entire photosynthetic reaction center. In plants, for example, one reaction center corresponds to nearly 300 antenna molecules. The antenna system, in fact, enlarges the diameter of optical effectiveness of the photoactive pigments by nearly two orders of magnitude. Depending on the species of plant, chlorophyll and various pigments (e.g., carotenoids such as xantophylls) are part of these antennae (see Fig. 4.35). Size, composition, structure, and absorption spectra of the antennae are quite different for bacteria, algae, and various higher plants. This is understandable, considering the large differences in intensities and in spectral characteristics of the light leading to photosynthesis, in organisms ranging from submarine algae, up to tropical plants.

In eukaryotic plants the process of photosynthesis occurs in the chloroplasts, especially in the thylakoids located there. *Thylakoids* are flat vesicles with a diameter of about 500 nm, which form an ordered complex of a large number of thylakoids, so-called *grana*. One chloroplast contains about 10^3 thylakoids. Every thylakoid contains about 10^6 pigment molecules.

In general, photosynthesis can be considered as a reaction during which water is split, driven by the energy of photons, producing O_2 and transferring hydrogen to the redox system NADPH/$NADP^+$, the nicotinamid-adenin-dinucleotid phosphate. Simultaneously, a proton gradient across the thylakoid membrane is generated.

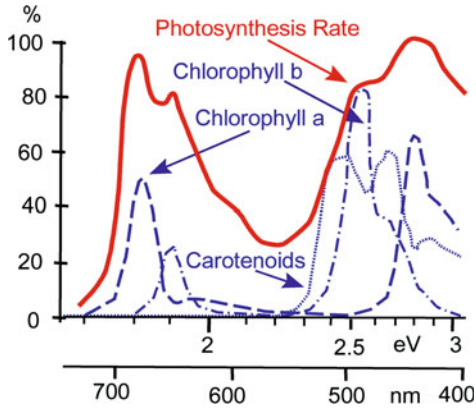

Fig. 4.35 Estimated absorption spectra of chlorophyll a, chlorophyll b and carotenoids in chloroplasts, and action spectrum of photosynthesis (oxygen evolution/incident photon) (Data from Whitmarsh and Govindjee 1999)

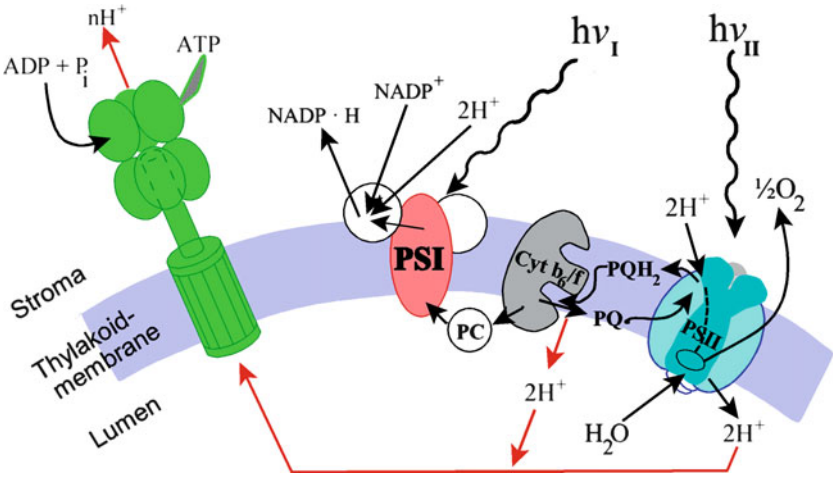

Fig. 4.36 Structural and functional organization of primary processes of photosynthesis in the thylakoid membrane. For an explanation see the text (From Renger 1994, redrawn)

Within a separate process, this leads to the synthesis of ATP. Subsequently, an ATP-consuming synthesis of carbohydrates occurs. This process is usually called the *dark reaction* of photosynthesis occurring in the stroma of chloroplasts.

The energy absorbed by the antenna molecules is transmitted by processes of nonradiant energy transfer to two reaction centers: photosystem I and photosystem II. The antenna molecules of these two photosystems are interconnected to each other. If photosystem II, for example, is overloaded, the absorbed energy will be transferred to photosystem I by a so-called *spillover process*. There are further mechanisms to protect the photosystem from over exposition.

In Fig. 4.36 the primary process of photosynthesis is depicted schematically. The complexes: photosystem I (PSI), photosystem II (PSII), as well as the cytochrome b/f complex (Cyt b/f) are seen as components of the thylakoid membrane.

The light-induced splitting of water occurs in the so-called water oxidizing multi-enzyme complex, structurally connected to photosystem II, where the molecular oxygen becomes free, but the hydrogen, in contrast, is bound by plastoquinon (PQ), forming plastohydoquinon (PQH2). The cytochrome b/f complex mediates the electron transport between PSII and PSI, reducing two molecules of plastocyanin (PC), using the hydrogen of PQH2. This light-independent process at the same time extrudes two protons into the internal volume of the thylakoid. In a second photochemical process, photosystem I (PSI), using the redox potential of plastocyanin, transfers one proton to NADP+, producing in this way NADPH, one of the energy-rich products of photosynthesis.

In addition to photosynthesis, as the primary process of energy conversion, light furthermore is an essential source of information. There are a number of photobiological processes, which do not end in the gain of chemical or electrochemical energy, but in signal cascades, triggering various kinds of biological response. These photoreceptors can vary from diffusely distributed photoreceptive cells, to complex organs in discrete locations.

The highest level of organization is arrived at in various organs of visual perception. In these the photoreceptor molecules, for example the visual purple rhodopsin, with a highly organized arrangement, are able to localize the source of light, or even reproduce the environment in detailed pictures. Other light-induced processes are *phototaxis* (the movement of an organism by orientation towards light), *phototropism* (orientation of parts of an organism, for example leafs of plants, to optimize received illumination), *photomorphogenesis* (light-controlled differentiation). Irrespective of the differences in location and function, photoreceptors show intriguing similarities in their basic structure and function.

The precondition of all photobiological processes is an effective absorption of corresponding photons. As the polypeptide backbone of the amino acid side chains do not absorb photons in the visible light range, the photoreceptor proteins contain one or more nonprotein components, i.e., chromophores, bound to the protein covalently or noncovalently. These chromophores are color tuned to their environment.

In general the photoreceptor molecules can be classified in the following groups: light-oxygen-voltage (LOV) sensors, xanthopsins, phytochromes, blue-light-using flavin adenine dinucleotides (BLUF), cryptochromes, and rhodopsins. Except for the rhodopsins, which for example are localized in the membrane of photoreceptors, all others are water-soluble, and have quite different cellular locations. The initial changes in the excited state of the chromophore must be very fast. Mostly, beginning with an $S_0 \rightarrow S_1$ excitation, an isomerization process occurs about one or more double bonds.

The mechanisms of photoreception require optimization in the same way as the energy-harvesting processes of photosynthesis. For this the initial process of photon absorption, as well as the transfer of the absorbed photon energy to the protein must be efficient and specific. In this way it is necessary to minimize the energy dissipation into nonproductive processes of vibrational and thermal movement, as well as a fluorescence de-excitation. For this in the receptor proteins various functional domains are localized directly, for example, some for binding the

chromophore, others to promote association with another protein or membrane, or output domains to exhibit light-dependent catalytic activity.

Beside reception, in some organisms even systems for emission of photons occur. *Bioluminescence* is distributed across a broad range of the major groups of organisms from bacteria and fungi to various animals. In insects and some other organisms it is realized by bacterial symbionts, mostly, and particularly in sea water inhabitants, it is produced by the organisms themselves. Bioluminescence is a kind of chemiluminescence typically produced by the oxidation of light-emitting molecules of the luciferin classes in conjunction with luciferase, a corresponding catalyzing enzyme. During the course of this reaction, an electronically excited intermediate is generated that emits a photon of light upon relaxation to the ground state. Because the ability to make light has evolved many times during evolution, a large number of modifications of these molecules occur. The wavelength of the emitted light depends on the chemical structure of the molecule emitter, along with influences of the conditions of the internal microenvironment. The emission spectrum of a particular luciferin-luciferase system can therefore vary.

This property of living organisms has recently been widely used in the so-called *bioluminescence imaging techniques* (BLI). In this case the light-emitting properties of luciferase enzymes are applied to monitor cells and biomolecular processes in living subjects. Luciferases and other proteins which are required for biosynthesis in luminescent bacteria for example, are encoded within a single *lux*-operon. In this way these light-emitting molecules can be introduced into a variety of nonluminescent hosts to track cells, to visualize gene expression, and to analyze collections of biomolecules.

Not only bioluminescence but also the fluorescence of particular marker molecules is used today as a powerful method for microscopic and submicroscopic research. In many cases this method even replaces the radiotracer method. The availability of many kinds of fluorescent tracers together with the technical development of confocal laser microscopes establishes its success.

Especially the discovery of the *green fluorescent protein* (GFP) and related proteins boosted this application. This protein was purified from the jellyfish *Aequorea victoria* by Osamu Shimomura in the 1970s (Nobel Prize 2008). It is supposed that this fluorescent protein (GFP) is colocalized with a bioluminescent counterpart and therefore is important for communication between these animals. The prevalent use of this protein and its modifications in research is because of the possibility to introduce the corresponding genes into any cellular DNA. In this case the cells themselves produce this fluorescent protein. Furthermore, the GPF gene can be fused to genes of particular proteins; the expressed molecules become fluorescent and their position in the cell can be localized.

Further Reading

Photosynthesis: Singhal et al. 1999; Orr and Govindjee 2010; Santabarbara et al. 2010; photoreception: Hegemann 2008; Möglich et al. 2010; energy transfer: Ritz and Damjanovi 2002; bioluminescence: Haddock et al. 2010; bioluminescence imaging: Prescher and Contag 2010; GFP: Nienhaus 2008.

4.8.4 Ultraviolet: The Transition to Ionizing Radiation

As depicted in Fig. 4.32, at the maximum of ultraviolet frequencies, the quantum energy of photons of UV-light forms the border to ionizing radiation. Formally, the UV spectrum is divided into three regions: UVA (315–400 nm), UVB (280–315 nm), and UVC (100–280 nm). UV-radiation in sunlight that reaches the earth's surface is mostly UVA, and partly UVB (Fig. 4.37). The short-wave part of UVB ($\lambda < 290$ nm) is completely screened out by the ozone in the atmosphere, and by the stratospheric ozone layer. The interaction of short-wavelength UVB, as well as UVC with biological systems is therefore only of interest in relation to some technical sources.

All three spectral regions of UV-radiation in different ways affect human health. On one hand UVB exposure induces the production of vitamin D in the skin. On the other hand, UVA, UVB, and UVC can all damage collagen fibers, and therefore induce photo-aging of the skin. Furthermore, it causes skin cancer, and many other detrimental health effects like sunburn, ocular damage, or immune suppression. Because of the absorption of UV from various chromophores in the skin, it penetrates only a few cell layers. Nevertheless, UVA reaches the hypodermis and therefore affects all layers of the skin. In contrast, UVB acts mainly in the epidermis including cells of the basal layer, whereas UVC is mostly absorbed by the *stratum corneum*.

Considering just the normal environmental UV-radiation spectrum, UVB is primarily responsible for most biological effects. In fact, it appears to be three to four orders of magnitude more effective than UVA. However, considering the sun's emission spectrum as depicted in Fig. 4.37, and weighting the spectral intensity, this effectiveness reduces to only the tenfold. UVA may negate or enhance the effects of UVB and vice versa. UVA is also known to affect different biological endpoints which are influenced by UVB. For example, UVA contributes towards photo-aging but mainly causes skin sagging rather than wrinkling, which is largely caused by UVB.

The genotoxic effect of UV-radiation is based on its direct interaction with the DNA molecule as well as indirectly by other photochemical reactions (Fig. 4.37). In contrast to sugar and phosphate residues, the absorption of UV by the DNA molecule is due to the pyrimidine bases. The *direct mechanism* of UV-interaction consists chiefly of the formation of 6,4-pyrimidine-pyrimidone and cyclobutane pyrimidine dimers (Fig. 4.38).

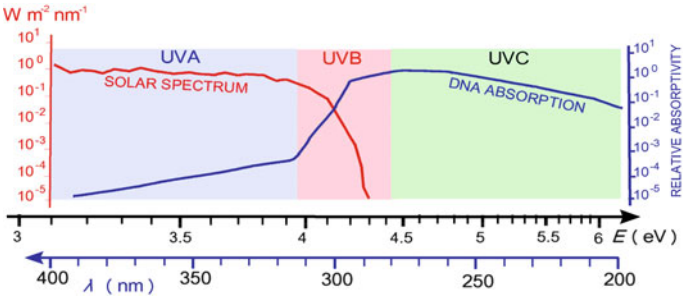

Fig. 4.37 Solar spectral irradiance measured at sea level on a clear day in July (Data from Godar 2005) and absorption spectrum of DNA (Data from Sutherland and Griffin 1981)

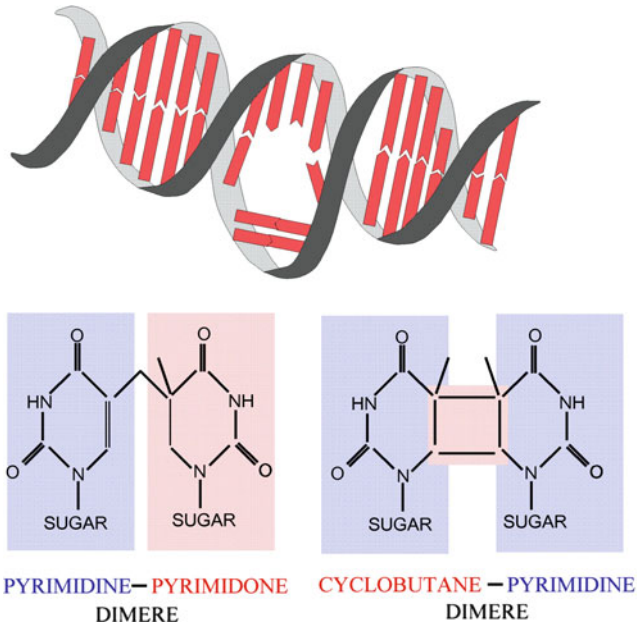

Fig. 4.38 Formation of a thymin-dimer as an example of a 6,4-pyrimidine-pyrimidone, and a cyclobutane pyrimidine dimer, and the consequences to the structure of a DNA double helix

In this case two adjacent pyrimidines of the same strand connect across 5–6 double bonds, and are in this way bound together, or form a cyclobutane ring structure. The yields of the various photoproducts depend on the wavelengths of the radiation. Mostly, thymine dimers appear, but even other combinations are found like cysteine-thymine, cysteine-cysteine, as well as thymine-uracil and cysteine-uracil. These dimers are extremely stable and they can therefore easily be indicated analytically.

The formation of these dimers requires an extensive rotation of the neighboring pyrimidines from their usual position. They were formed more easily in melted and in curved DNA. Conversely, increased DNA rigidity may interfere with this kind of photodimerization, probably by preventing the optimal alignment of the double bonds involved in dimer formation.

These dipyrimidine photoproducts alter the structure of DNA, and consequently inhibit polymerases. In this way they disturb normal replication. Even if they are normally excised by the system of nucleotide repair enzymes, the amount of unrepaired lesions is not negligible, and results in mutations. These are called "*UV-signature mutations*," which are almost only the result of UV-radiation. They falling into the mutation type of *transition*, i.e., a change from one pyrimidine (cytosine or thymine) or purine base (guanine or adenine) to the other, for example a C:G pair to T:A.

The *indirect mechanism* of UV-interaction is generally caused by the generation of various reactive oxygen species (ROS). These include the superoxide anion radical ($^{\cdot}O_2^{-}$), hydroxyl radical ($^{\cdot}OH$) and many others. To some extent ROS are natural byproducts of the normal metabolism of oxygen, and have important roles

in cell signaling. Their concentration is normally controlled by a system of redox enzymes, such as superoxide dismutases, catalases, lactoperoxidases, glutathione peroxidases, etc. However, some environmental influences like UV, ionizing radiation (see. Sect. 4.9.2), or ultrasound (Sect. 4.3.5) can increase these levels dramatically with detrimental consequences.

It should be emphasized, however, that the mechanisms of generation of these radicals are quite different in these three causes. In contrast to the sonolysis of water by ultrasound, where the ROS production is the result of a strong local increase of temperature, the UVB-induced formation of ROS is mediated by various photosensitizers, i.e., components of the cells absorbing the corresponding wavelength in the UVB range. The ground state photosensitizer absorbs UVB, and is excited to the singlet state which is very short-lived (<1 ns). By intersystem crossing (see Fig. 4.34) the triplet state occurs with much longer lifetime (~1 μs). This triplet photosensitizer transfers its triplet energy to molecular oxygen to form singlet oxygen while the photosensitizer returns to the ground state.

Because UVA in contrast to UVB is only weakly absorbed by DNA itself, the damage induction in this case occurs via this indirect mechanism. These ROS induce DNA damage for example by the formation of the mutagenic modified base, 8-oxoguanine. This can cause G to T transversion mutations by mispairing of template 8oxoG with adenine, or alternatively T to G transversions via incorporation of 8oxodGTP opposite adenine during replication.

Irradiated cells may emit signals which induce DNA and other cellular damage in other cells which are not directly hit by the radiation. This is the so-called *bystander effect* which was first determined as a result of ionizing radiatin. The agents of these bystander signals can be some kinds of ROS, as well as various stress response proteins, or byproducts of lipid peroxidation. They can be transferred via gap junctions between adjacent cells, or diffuse over larger distances in the tissue which can lead to effects even deeper in the tissue than the radiation could penetrate.

The intensity of UV-radiation is usually measured as a power density in $W\ m^{-2}$. In the distribution spectrum in Fig. 4.37, the dose is applied to a spectral slot, therefore defined as $W\ m^{-2}\ nm^{-1}$. According to the so-called *Bunsen–Roscoe reciprocity rule* (Bunsen and Roscoe 1859), taking into account the possibility of accumulation of photolytic products, a photochemical reaction is directly proportional to the total energy dose, and is independent of the particular dose distribution. Therefore, the term $W\ s\ m^{-2} = J\ m^{-2}$ is applied. Considering the subsequent biological effects, however, the processes of repair in biological systems must be taken into account. Consequently, the biological effect depends not simply on the total dose, applied in a period, but additionally on the dose rate.

Because of differences in interaction mechanisms of various frequency windows of UV-radiation, and sensibility according to various biological reactions (e.g., erythema, photocarcinogenesis, tanning, melanogenesis) sometimes an *effective dose* is used, by multiplying the measured intensity with a corresponding factor.

Further Reading

Kiefer 1990; Nishigori 2006; Ridley et al. 2009; Svobodova and Vostalova 2010.

4.9 Ionizing Radiation

Studies on effects of ionizing radiation on living organisms have become necessary following the introduction of X-rays in medical therapy and diagnostics at the beginning of the twentieth century, and have acquired a special relevance in the so-called nuclear age. In this book only a few important aspects of radiation biophysics can be focused on.

In the spectrum of electromagnetic waves (Fig. 4.32), ionizing radiation begins at a quantum energy of the order of 10 eV. Usually the energy of ionization of the water molecule, which amounts to 12.46 eV, is taken as a borderline. This corresponds to a range of wavelengths in the upper limit of UVC (see Sect. 4.8).

The term "ionizing radiation" includes the photons of the corresponding part of the electromagnetic spectrum as well as various kinds of corpuscular radiation. These are accelerated elementary particles as well as ions of various mass numbers. Depending on the source of the photon radiation, it is usually called *γ-radiation* if it is the result of an atomic decay process. In 1895 the German physicist Wilhelm Röntgen detected a mysterious radiation, emitted by a cathode tube, which penetrates various materials. He termed it *X-rays*, using the mathematical designation for something unknown. This term is used even now for photon radiations emitted by various technical devices. In general, the terms γ-radiation and X-rays are synonyms for the same kind of photons, characterized solely by their wavelength resp. their photon energy.

4.9.1 Nature, Properties, and Dosimetry of Radiation

Ionizing radiation in our environment is emitted by extraterrestrial sources, by various technical devices, and by radionuclides. Even if the quality and quantity of human exposition to ionizing radiation has been altered by technical development, a natural exposition of all biological organisms has always existed and has been a part of environmental conditions during evolution.

In general ionizing radiation occurs as photons like X-rays or γ-radiations, as a part of electromagnetic waves (see Fig. 4.32), or as corpuscular radiation. Let us now characterize some properties of corpuscular radiations.

α-rays are the product of atomic decay of several naturally occurring isotopes of radium, uranium, thorium, etc. These are fast-moving helium nuclei with a mass number of 4 and an atomic number of 2 $\left({}^{4}_{2}\mathrm{He}\right)$. The helium nucleus consists of two neutrons and two protons and thus carries two positive charges. Because of this strong charge, there is a correspondingly strong interaction between α-rays and the elementary particles of matter. The energy of α-rays emitted by radionuclides is generally quite high, namely of the order of several millions of electron volts (MeV). As the α-rays pass through matter, this energy is dissipated as a result of ionizing processes and the particles are slowed down. For example, the energy which is required to generate one pair of ions in air is 34.7 eV. It can easily be

calculated that a radiation energy of several 10^6 eV is sufficient to induce about 10^5 ionizations. Consequently, α-particles will leave behind a straight-line track of limited length in irradiated matter which consists of the ionization products. This can be visualized by special methods.

β-rays consist of fast-moving electrons. These particles carry a single negative charge and an extremely small mass. Although it is possible to generate β-radiation of very high energy by means of particle accelerators, the energy of the β-radiation from radioactive nuclides on average is lower than that of α-radiation. In contrast to α-radiation, the energies of electrons of β-emitting radionuclides are not at all equal to each other but are spread across a specific range. Therefore, the terms *mean energy* and *maximum energy* are used when referring to the β-emission of radionuclides. The distance to which a β-particle penetrates matter will, naturally correspond with its energy. The ionization tracks of β-particles in contrast to those of α-particles, do not follow a straight line but their path becomes increasingly curved towards the end. In addition, the density of ionization increases as the energy of the particle decreases so that ionization is more densely packed with low energy radiation than with high energy radiation and, for the same reason, this effect can also be seen towards the ends of the tracks.

Neutron radiation as the result of nuclear fission, occupies a rather special position in the classification of corpuscular radiation. Its particles are electrically neutral and possess a considerable mass when compared with β-particles. For this reason they are able to penetrate an atom and reach the nucleus where they can cause nuclear transformations. In this way the irradiated substance itself becomes radioactive. Neutron emission does not occur when a radionuclide decays spontaneously but takes place during nuclear fission or in the wake of other, externally induced reactions.

Recently various kinds of nuclides have been used in cancer therapy. In this case ions like protons or carbon ions have been used, accelerated by synchrotron- or cyclotron-based facilities up to kinetic energies of several hundreds of MeV.

The process of energy dissipation that occurs during the absorption of electromagnetic radiation by matter follows the same pattern as that during the absorption of corpuscular radiation in that it is not continuous but takes place in steps, i.e., in quantum leaps. The size of energy quanta absorbed in this way depends on the type of interaction. In general, three types of absorption processes may be distinguished according to the relation between the required ionization energy and the available quantum energy:

- With low quantum energies, the *photo effect* is produced. In this, a γ-quantum (i.e., a *photon*) is absorbed and this causes a displacement of an orbiting electron from the shell of an atom. The excess energy, above that which is required for the ionization process, serves to accelerate this so-called *photoelectron*.
- The *Compton effect* occurs at a quantum energy of about 10^5 eV. In this case not only a *Compton electron* is ejected from the atom but this is accompanied by the scattering of secondary γ-radiation. This latter radiation has a quantum energy lower than that which was originally absorbed.

– If the quantum energy of the γ-radiation is above 1.02 MeV then *electron-pair formation* can occur. The quantum energy disappears producing a negative and a positive electron. Such formation of an ion pair can only take place close to the nucleus of an atom, i.e., it can only occur in an absorbing material and not spontaneously in a vacuum.

As ionizing energy moves through the material, a number of secondary particles can be created, at smaller or greater distances. The direct energy loss in the radiation as it moves through a material is called the *linear energy transfer* (LET). It is defined as the energy loss of the radiation per unit length.

To evaluate the dose of ionizing radiation, however, not only the LET, but the total energy is considered which is absorbed in the material, including also the effects of the secondarily produced particles and photons. For this the unit *gray* (abbreviated to Gy) is defined as the energy absorbed per unit mass:

$$1\ \mathrm{Gy} = 1\ \mathrm{J\ kg^{-1}}$$

In earlier papers the units *roentgen* (R) and *rad* (rd) were used. One roentgen was defined as the amount of radiation which is required to liberate positive and negative charges of one electrostatic unit in 1 cm^3 of dry air at standard temperature and pressure. Therefore, in contrast to the unit gray, it is not a physical equivalent for the dose of absorbed radiation, but rather a representative of the radiation effect. The unit rad is based on the CGS-system of units and is defined as equal to 100 erg g^{-1}. It can be converted as follows:

$$1\ \mathrm{rd} = 100\,\mathrm{erg\ g^{-1}} = 10^{-2}\mathrm{Gy}$$

To convert roentgen into gray, the properties of the particular absorbing matter must be considered. For the case of water and tissue it is:

$$1\,\mathrm{R} = 0.93 - 0.98\,\mathrm{rd}$$

In addition, as a measure of the *dose rate* the unit Gy s^{-1} = W kg^{-1} is used. This corresponds to the SAR-parameter as explained in Sect. 4.7.1.

Different kinds of radiation have different effects in biological interactions. So, for example the *relative biological effectiveness* (RBE) of α-rays amounts to 20. In the case of neutron radiation, the RBE obviously depends on the actual dose but not on the energy distribution. An average of the maximum RBE of neutrons in relation to γ-rays of ^{60}Co amounts to 86 at the low-dose limit. For carbon ions the RBE is also variable and depends on the actual energy loss in the tissue.

This parameter is the *dose equivalent* with the unit *sievert* (Sv). It is named after the Swedish medical physicist Rolf Sievert. Considering the stated biological effectiveness values gives the following relations: for X-rays: 1 Gy = 1 Sv, for α-rays, however: 1 Gy = 20 Sv.

Considering the penetration of ionizing radiation into the body, some peculiarities need to be taken into account. For photon radiation, like X-rays, an

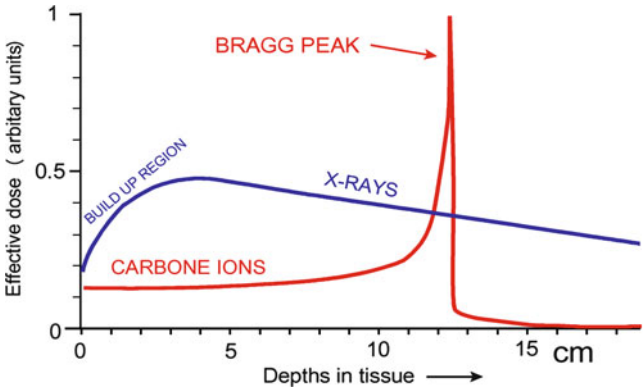

Fig. 4.39 Depth profile of the radiation dose in tissue for photons of X-rays (about 20 MeV) compared with carbon ions of about 300 MeV per nucleon (Modified after Durante and Loeffler 2010)

exponential decay of the intensity occurs, depending on the photon energy, and the density of the medium. Considering, however, the depth dose function it is found that the maximum dose is found at a certain distance from the surface (Fig. 4.39). This effect reflects the difference between the LET and the real doses which takes into account the fluence of the secondary particles. This so-called *build-up phenomenon* is caused by the fact that immediately at the surface access to a number of secondary products of interaction is limited. In the case of high photon energy radiation, the maximum of the curve is shifted several centimeters inside the body, an effect which is used in high voltage therapy.

In the case of beams of accelerated heavy ions the situation is even more complicated. The LET, and the release of secondary products, in this case is inversely proportional to the kinetic energy. The function which indicates the stopping power of the beam, i.e., the amount of ionization, is called the *Bragg curve*. As indicated in Fig. 4.39 this function shows a typical peak deeper in the body. In this way accelerated ions like protons or carbon are a useful tool in radiotherapy to affect particular tumor regions deeper in the body.

Further Reading

Karger et al. 2010; Kiefer 1990.

4.9.2 Primary Processes of Radiation Chemistry

The field of *radiation chemistry* represents the chemical consequences of the physical interaction of ionizing radiation, and it can be distinguished from *radiochemistry*, which is the study of particular chemical properties of radionuclides. As mentioned earlier, at quantum energies of photons, or correspondingly the kinetic

energy of particles for radiation greater than 12 eV, the interaction of the radiation leads to ionization of atoms and molecules. In contrast to the photons of visible light which reversibly raise electrons into a higher excited state (see Fig. 4.34), as explained in Sect. 4.8.2, in the case of ionizing radiation the electrons are fully ejected from the atomic orbitals. The results are on the one hand positively charged radicals, i.e., ions with an unpaired electron, and on the other hand free electrons. Both are short-living unstable products. As a consequence of this alteration, and as a result of the interaction of these primary products of radiolysis, even covalent chemical bonds could be broken.

The entire biological effect starts with interference in a biological cascade of information transfer, i.e., with a DNA molecule or an important enzyme. This can either be the result of a *direct* interaction with the radiation quantum, or the consequence of an interaction with another product of radiolysis (*indirect effect*).

Because water is by far the most common molecule in biological systems, its radiolysis products are of particular interest in the generation of indirect effects. In Fig. 4.40 some steps of radiolysis of water and recombination reactions are illustrated schematically. In a first step within a time span of 10^{-18}–10^{-16} s an electron is pulled out of the molecular binding, leaving a positively charged water radical ($H_2O^{\bullet+}$), and a free electron.

The released electron (e_{aq}) as a charge in an aqueous environment, immediately becomes hydrated, similar to ions in aqueous solutions (Sect. 2.2.2). As an example of this H_2O^- is depicted schematically in Fig. 4.40. Because of this shell of bound water the life span of this free electron, depending on the pH of the solution, can achieve 600 s. It can interact with various other molecules. Reactions with other water molecules in the hydration shell are possible in the following way:

$$e_{aq} + H_2O \rightarrow H_2O^- \rightarrow OH^- + H$$

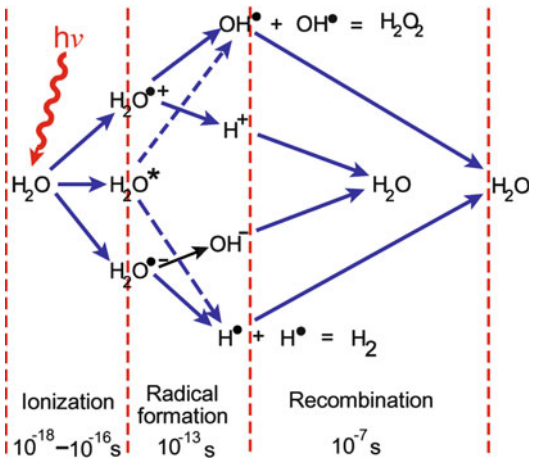

Fig. 4.40 Schematic illustration of the most important reactions of water radiolysis (* – excited states, • – radicals)

The other primary product of radiolysis, the unstable charged radical $H_2O^{\bullet+}$, breaks up as follows:

$$H_2O^{\bullet+} \rightarrow H^+ + OH^\bullet$$

Furthermore, as a primary result of the interaction, an electronically exited water molecule H_2O^* may occur which in a far slower reaction (10^{-13} s) produces two radicals:

$$H_2O^* \rightarrow H^\bullet + OH^\bullet$$

The probability of the appearance of these products can be expressed by the so-called *G-value*. It is defined as the number of molecules which become altered per 100 eV absorbed energy. At a pH of the solution in the range between 3 and 10, the following G-values are obtained as a result of ^{60}Co-γ-radiation:

$$G(e_{aq}) = 2.65; \qquad G(H^\bullet) = 0.55; \qquad G(OH^\bullet) = 2.7$$

This unit corresponds to:

$$1\ \text{molecule}/100\,\text{eV} = 1.036 \times 10^{-7}\text{mol J}^{-1}$$

As shown in Fig. 4.40 various combinations of radicals may occur, produced by proximate reactions of radiolysis, for example:

$$OH^\bullet + OH^\bullet \rightarrow H_2O_2$$
$$H^\bullet + H^\bullet \rightarrow H_2$$
$$H^\bullet + OH^\bullet \rightarrow H_2O$$

Furthermore, various recombinations of these radicals with oxygen are possible, solved in the aqueous phase, which eventually leads to an additional production of H_2O_2. Furthermore, the oxygen is able to facilitate the transfer of radical sites between molecules or molecular components. As a consequence, oxygen-rich tissue suffers more from irradiation than that with low oxygen content (*oxygen effect*).

It should be noted that these kinds of water radiolysis represent the third way to generate reactive radicals. First, the thermolysis of water was mentioned as the result of local heating through ultrasound cavitation (Sect. 4.3.5). Secondly such radicals were explained as a result of UV-radiation, mediated by photosensitizers (Sect. 4.8.4). These reactive species are together frequently summed up in the all-encompassing designation ROS (*reactive oxygen species*), all being highly reactive due to their content of unpaired valence electrons. This phrase, however, seems to be too imprecise because a greater diversity exists in reactive radicals involved in biological reactions, i.e., those that contain also nitrogen, sulfur, halogens, and carbon.

In fact, free radicals, especially the superoxide radical, are byproducts of the normal cellular metabolism. They are produced inside the mitochondria in the process of oxidative phosphorylation, by membrane-bound NADPH oxidase, or by the nitric oxide synthases. A number of enzymes such as superoxide dismutases, catalases, lactoperoxidases, glutathione peroxidases, or peroxiredoxins are able to regulate this concentration and defend the cells against damage. In fact, this is a complicated system of radical metabolism which by the way is also the subject of cancer research, and many other biomedical topics.

Furthermore, there are a number of intercellular signaling pathways which are based on free radical processes, including ROS and similar species. This explains observations of the so-called *bystander effect*. In this case cells which have not been irradiated, nevertheless show radiation effects, caused by information transfer from irradiated neighboring cells.

In contrast to radicals occurring in normal metabolism, the particular effect of radical species produced by ionizing radiation is caused by the circumstance that they occur directly in the vicinity of biologically important molecules. This especially concerns DNA as a highly charged polyanion, strongly hydrated by water molecules. As a signature of DNA alterations through ionizing radiation, *tandem lesions*, or clusters of DNA lesions occur as the result of various radical-transfer reactions. This means that two or more defects are formed in close proximity on the same DNA strand or even double strand breaks. Even a single $OH^{\bullet}$ radical is able to induce complex tandem lesions. Because this kind of DNA lesion is untypical in the endogenous processes the efficiency of the cellular repair mechanism is lower.

The hydrated electron reacts primarily with those parts of an organic molecule that have high affinity for electrons such as SH-, CO-, NO_2-, or NO-groups. Either it simply becomes attached to the molecule, thus imparting a negative charge to it, or a dissociative electron capture takes place which, similar to the instances described above, leads again to the formation of a free radical.

In general, two cell defense systems must be considered to cope with free radical DNA damage. They work on very different time scales. On one hand there is a very fast *chemical repair* which occurs at the stage of DNA free radicals. This means that other molecules, so-called *scavengers*, like various thiols containing SH-groups transfer the electron by oxidation. On the other hand an enzymatic repair is possible which is slow, and active if the damage is fully settled. In this respect the double strand helix can be considered as a construction of higher stability against irradiation in relation to the single-stranded DNA helix. This is supported by experiments showing that if the hydrogen bridges between the two molecular filaments are broken by placing the DNA in a solution of urea, then the fragmentation of the DNA by irradiation becomes easier.

Further Reading

Kiefer 1990; Mozumder 1999; O'Neill and Wardman 2009; Sonntag 2006.

4.9.3 Radiobiological Reactions

In this section we leave the narrow region of biophysics and come to the biological effects that are a consequence of the primary processes of radiation chemistry as depicted in the previous section. This leads to the assumption that basically the radiation influences are *stochastic effects*, namely the generation of accidental molecular alterations which are randomly distributed. This in fact is the fundamental problem of low dose irradiation, which may generate genetic defects and cancer. At higher doses of ionizing radiation, leading to acute radiation syndromes, the multitude of these stochastic effects merge to phenomenological, i.e., *nonstochastic* reactions.

Anyway, quantum processes at the molecular level, rather than the total amount of absorbed radiation energy are the reason for the sensitivity of biological systems to ionizing radiation. This can be illustrated easily by considering the real amount of energy which is absorbed in the human body at the lethal dose (LD_{50}) of ionizing radiation which amounts to about 5 Gy, or correspondingly 5 J kg^{-1} (see Fig. 4.42). Considering the specific heat capacity of biological tissue of 4 Jg^{-1} K^{-1} this energy absorption therefore leads to a temperature increase of about 0.001 K, an amount that is completely negligible.

Let us first consider the stochastic effects of radiation as the primary biological reactions. As pointed out already in the previous section, the most important effect consists of alterations of the DNA, especially in the generation of double strand breaks. With sequencing of the human genome, the general technological advances in molecular biology, and finally the development of methods of human cell culture, the screening of individual cells for gene defects after irradiation became possible. This allowed detailed investigations of cellular responses even at the low dose range.

It must be emphasized that ionizing radiation induces not only isolated DNA lesions, but also clusters of lesions formed within a few tens of base pairs by a single radiation track. Even a single hydroxyl radical ($OH^{\bullet}$) may induce such complex tandem lesions. This in fact seems to be the most biologically relevant DNA damage induced by radiation whereas in contrast to this such clustered lesions do not occur endogenously in significant numbers.

As a measure of the radiation effect on DNA, various types of radiation-induced chromosome aberrations are commonly used. These studies indicate that the development of these aberrations in response to ionizing radiation, and the dose–response kinetics appear as a combined effect of radiolysis, and errors in the repair pathways. There are different mechanisms of repair which in fact appear in all phases of the cell cycle. At least for higher radiation doses, nearly all chromosome aberration types show a linear dose effect dependence. At the region of low dose interaction this linearity, however, is a matter of discussion. It may be deflected in both directions mainly by the so-called bystander effect.

As already mentioned in the previous section, the *bystander effect* was established in experiments indicating that radiation effects occur in unirradiated cells in the vicinity of others, hit by radiation. Obviously there exists a direct cell–cell

communication via gap junctions, as well as a mutual influence by the release of various factors from irradiated cells into the medium. This includes reactive oxygen species (ROS), as well as other signaling molecules such as for example various reactive nitrogen compounds. Some of these communications may be effective even over larger distances because several of these species are active for a longer time period. In some cases even removing the medium from irradiated cells, and transferring it to nonirradiated cells induces a corresponding bystander response.

These interactions can be either damaging or protective. Consequently the dose–response curves at low dose may deflect up or down from its linear behavior. In some cases even adaptive responses have been observed, where a small dose of priming radiation reduces the effect of a larger dose, typically when given several hours later.

To evaluate the stochastic, i.e., the genetic or carcinogenic effects caused by ionizing radiation, the dose of irradiation must be integrated over the whole life span of an individual, or even over the whole population. The reason for this is not a biophysical, but a genetic mechanism of accumulation. Especially recessive mutations, i.e., such which become effective only in the case where two of them occasionally meet by arbitrary combinations, become dangerous if they become accumulated in the population. The same holds for radiation-induced cancer as a result of somatic mutations.

Radiation effects at the cellular level and even in organs must be characterized as *nonstochastic*, because of the multitude of regulatory processes which respond to ionizing radiation. Already comparatively low doses of radiation reversibly stop the process of cell division. Immediately after irradiation by a sublethal dose the number of dividing cells is reduced. Later these cells undergo mitosis together with the undamaged cells, leading sometimes to a small overshoot of the number of proliferating cells.

In this respect in addition to the influence on the genetic or epigenetic system of the cell, even radiation-induced structural and functional alterations of proteins must be taken into account, especially the behavior of enzymes. The sensitivity of enzymes to radiation shows great variations. Among the most sensitive enzymes are ATPases and catalases. This depends to a large amount on their composition. We already mentioned that proteins with a high percentage of sulfur-containing amino acids are particularly sensitive to radiation. As a consequence of an alteration of protein structures, a number of transport properties of membranes are impaired. These reactions occur only at relatively high doses of radiation, but may have a profound influence on physiological processes, especially on the function of the central nervous system.

All these considerations suggest that juvenile organisms, particularly those in the embryonic phase, are particularly sensitive to irradiation. Damage to the genetic and mitotic apparatus in this period of life can lead to severe malformations or even death of the individual. There are some phases during the development of an organism that are particularly critical in relation to the radiation damage. This, for example, concerns the early stages of cleavage of the ovum up to the morula formation. Radiation damage in these states, however, does not necessarily lead to malformations because the injured cells either die, or are successfully repaired.

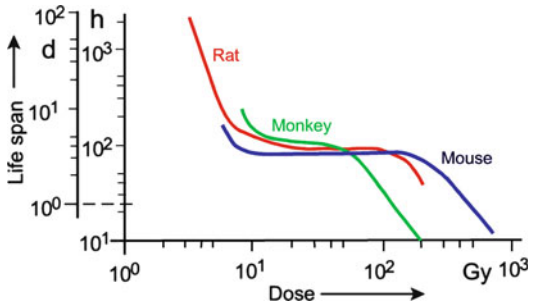

Fig. 4.41 Average life span of various mammals as a function of the dose of a single whole-body irradiation with X-rays (After Grodzenskij 1966 redrawn)

Irradiation during the stage when the organs are being laid down is substantially more critical. Exposure during these stages frequently causes malformations. In this context, the development of the central nervous system is particularly sensitive, in contrast to the completely developed brain which is one of the most resistant organs in relation to ionizing radiation.

The complexity of radiobiological reactions helps one to understand the course of acute radiation sickness. Figure 4.41 shows the average life span of some animals as a function of an applied radiation dose. All of the curves similarly show a decline at doses below 10 Gy, then there is a plateau followed by a second decrease at about 80–100 Gy. The shape of these curves reflects two different types of radiation sickness. At low doses the radiation sickness is mainly caused by pathologic alterations in blood-forming organs, which is reflected in dramatic changes in the blood picture. A considerable deficiency of lymphocytes occurs which reduces the resistance of the body to bacterial infections. This can eventually lead to a situation where even the intestinal bacteria become pathogenic. This type of radiation sickness lasts from several days up to weeks and can eventually lead to the death of the individual. The pathological course of this type of radiation sickness is already maximal at a dose of about 10 Gy. A further increase in radiation intensity does not accelerate this process. But if the animals are irradiated with doses over 80 Gy, the central nervous system becomes damaged by a direct influence on the excitation properties of neuronal membranes. In this case the animals die much faster.

Because of the complexity of radio-biological reactions it is difficult to find benchmark figures as a measure of the resistance of different organisms to irradiation. Similar to the characterizations of poisonous drugs, the parameter LD_{50}^{30} (*mean lethal dose*) is used, i.e., the dose of radiation that causes 50% of the irradiated animals to die within 30 days.

Figure 4.42 indicates that the sensitivity to radiation varies over several orders of magnitude for different species. A comparison of the sensitivity at different ages and stages in the development of a given species clearly shows the embryonic organism to be more sensitive than the adult one.

Further Reading

Heintz et al. 2012, Kiefer 1990; Kogel and Joiner 2009.

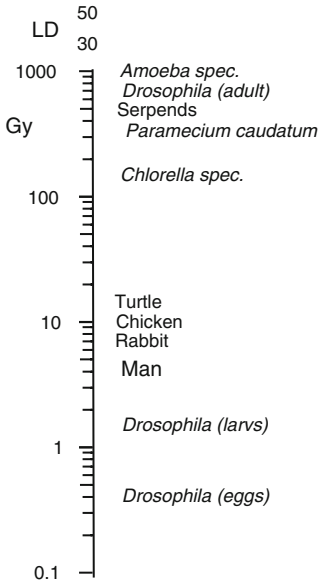

Fig. 4.42 Examples for the mean lethal dose LD_{50}^{30} of various organisms after single irradiation with X-rays (Data from Graevskij and Šapiro 1957)

4.9.4 Some Aspects of Radiation Protection

Radiation protection must consider both irradiation from sources outside of the body, as well as from incorporated radionuclides within it. In fact, it is more complicated to evaluate the dose of irradiation caused by accumulated radionuclides, than those from external sources. This concerns on the one hand the diversity of biological effectiveness of the emitted α-, β-, or γ-rays, and on the other hand the pattern of distribution of the corresponding radionuclides in the body, its organs, cells, and molecules.

The investigation of the distribution of natural and man-made radionuclides in the biosphere falls within the field of *radioecology*. This includes their accumulation in various products of the food chain, and finally the degree of resorption, accumulation, distribution, and excretion by man. Empirically obtained data of their distributions, and parameters of their biological half-life times are determined and concentration limits of these nuclides in air, water, and various foods are suggested for legal regulations.

The most important natural radionuclide in the body is the radioisotope ^{40}K, a β-, and γ-emitting nuclide with a half-life time of $1.25 \cdot 10^9$ years. There are 1.2 atoms of ^{40}K for every 10^4 of nonradioactive atoms of potassium. Considering the total potassium content in the human body, this results in about $4.4 \cdot 10^3$ disintegrations per second, i.e., 4.4 kBq.

Another natural radionuclide is the radiocarbon ^{14}C which is continuously produced in the upper layers of the stratosphere by the impact of space radiation. It emits weak β-radiation, and its specific radioactivity, i.e., the relation to the amount of

nonradioactive carbon is lower than that of ^{40}K. Conversely, in contrast to potassium, it is part of all organic molecules, including DNA. The UNSCEAR (United Nations Scientific Committee on the Effects of Atomic Radiation) calculated the annual dose of radiation from ^{40}K as an inherent element of the human body as 0.17 mSv, as a part of the 0.29 mSv of radiation from total ingested radionuclides (Fig. 4.43).

As shown in Fig. 4.43, the largest radiation dose of about 2.4 mS a^{-1} comes from various natural sources. This concerns the ingestion and inhalation of products of natural radioactive decay, especially the inhalation of the radioactive noble gas radon (Rn) as a decay product of uranium, the radioactive decay products of which eventually, are accumulated in the lung. The data of Fig. 4.43, in fact are global averages, and therefore vary more or less strongly in different regions. The mean value of 1.26 mSv a^{-1} from radon inhalation for example indicates a variation between 0.2 and 10 depending on geological conditions. The value for medical diagnosis also varies between 0.03 and 2 mSv a^{-1}, corresponding to differences in health care. Irradiations from various therapeutic treatments are greater for the individuals concerned, and not included in these data.

This figure indicates the predominance of natural, in relation to that of technical sources of radiation, where the irradiation caused by medical treatments dominates by far. The doses from sources of atomic energy devices are negligible in this relation.

The protection of man against ionizing radiation is based on recommendations of the International Commission of Radiological Protection (ICRP), a nongovernmental organization founded in 1928. The philosophy of these recommendations is the exclusion of any nonstochastic radiation effects, and the minimization of inevitable stochastic effects. These stochastic effects really are the critical point of radiation

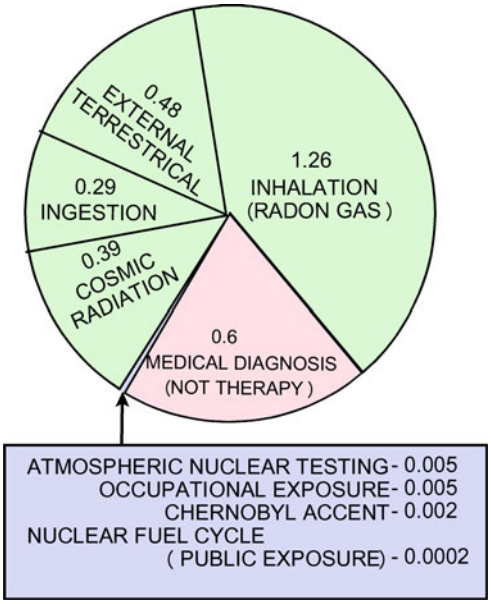

Fig. 4.43 Estimated global annual average dose of humans from natural (*green*), and artificial (*red* and *blue*) sources in mSv a^{-1} (Data from UNSCEAR-Report-2008)

damage. It includes possible genetic aberrations or induction of cancer. In general, one can assume that any increase of irradiation exceeding that of the natural dose of radiation will lead to an increase of the mutation rate. There is no threshold, below which no influence of the mutation rate can be expected. Therefore, all exposure should be kept "as low as reasonably achievable," a philosophy which is commonly known as the *ALARA-principle*.

Because of the possibility that stochastic effects will be integrated over the whole life span, the limits of maximal exposure are formulated over longer periods of time. Persons with occupational exposure and patients receiving radio-therapeutic treatment are under special supervision. For occupational exposure a maximum yearly irradiation dose of 20 mSv is laid down. For the general population 1 mSv per year is considered to be acceptable. As seen in Fig. 4.43 this is below the amount of natural irradiation which amounts to a mean value of 2.4 mSv a^{-1}, and varies worldwide between 1 and 13 mSv a^{-1}, thus the dose limit applies only to any additional exposure.

Further Reading

UNSCEAR-Reports, recommendations of the ICRP.

4.9.5 Mathematical Models of Primary Radiobiological Effects

Since the first investigations of biological effects of ionizing radiation as early as the 1920s, efforts were made to formulate theoretical approaches, helping to understand the observed phenomena. At this time quantum physics was being developed, which opened up new ways of understanding the interaction between ionizing radiation and biological systems. The starting point was the realization that the total amount of absorbed energy was by far too low to understand the resulting biological effects (see Sect. 4.9.3). Even before anything was known about molecular genetics, biological repair mechanisms, or details of primary molecular reactions the idea was born that particular target effects should occur.

J. A. Crowther, a pioneer of the target theory suggested the picture of "...firing at a swarm of midges with a machine gun," and he came to the conclusion: "It seems possible, today at least, that the quantum theory must be taken into account in biology as well as in physics, and that a single cell may have a much more direct and painful appreciation of the existence of quanta than is possible to our grosser senses" (Crowther 1926).

This *target theory* can be considered as the first attempt to explain biological phenomena on the basis of stochastic reactions in parallel with the newly developed quantum theory of physics. This eventually proved to become a powerful stimulus to the development of molecular genetics. Even if the knowledge of primary radiation effects, including cellular repair mechanisms indicates a much more complex picture of radiobiological effects, the ideas of these early attempts should not only be seen from a historical perspective but they can still be applied today to solve problems of microdosimetry, and some quantum biological processes, like photosynthesis or scotopic vision, and even for the determination of molecular weights of enzymes.

The starting point of these approaches was the realization that radiation effects are characterized by the following particularities:

- The effects not only depend on the total amount of the absorbed energy, but additionally on the quality of the applied radiation.
- When comparing biological effects obtained by irradiation with rays of the same quality, a dose dependence was found, but not a proportionality between effects and irradiation dose.

These observations have led to the following conclusion: Apparently, there are molecules in living organisms, which must be considered as "neuralgic" points in the system, the destruction of which would produce a sequence of reactions, finally leading to the death of the individual. This sort of primary event which is caused by a reaction with a single energy quantum of radiation was called a "hit" and the corresponding location where the process occurs, a "target." This leads to the name *target theory*, first applied to suspensions of single cells.

Let as assume that a population consists of n identical individuals, each of them organized physiologically in such a way that a single "hit" would set off a sequence of reactions, leading to death (*single hit process*). According to the laws of probability, with increasing time of irradiation, an increasing amount of individuals would become killed by this *single hit* process. The rate at which the number of living individuals decreases in this way can be expressed by the differential quotient $-\mathrm{d}n/\mathrm{d}t$. It should be proportional to the number of still-living individuals (n), the time of irradiation (t), and an irradiation constant (σ) which depends on quantity and quality of irradiation:

$$\frac{\mathrm{d}n}{\mathrm{d}t} = -\sigma n \tag{4.27}$$

Using the initial conditions, where $t = 0$ and $n = n_0$ results in:

$$n = n_0\,\mathrm{e}^{-\sigma t} \tag{4.28}$$

The reduction of the number of living cells therefore follows a simple exponential function.

In the same way, the number of killed cells (n') can be calculated. Because of the relation: $n' + n = n_0$, we obtain:

$$n' = n_0(1 - \mathrm{e}^{-\sigma \mathrm{t}}) \tag{4.29}$$

or:

$$\frac{n'}{n_0} = 1 - \mathrm{e}^{-\sigma t} \tag{4.30}$$

In Fig. 4.44 the curve for $m = 1$ represents this function. At $t = 0$, $n' = 0$ and therefore: $n'/n_0 = 0$. With increasing irradiation time and doses (σt) the value $n'/n_0 = 1$ will be approached.

In a similar way another model can be calculated. In this case it is assumed that the sequence of processes leading to the death of the individual is only triggered off if the organism has received a minimum number (m) of hits. Blau and Altenburger have calculated the following equation describing this *multi-hit process:*

$$n' = n_0 \left\{ 1 - \mathrm{e}^{-\sigma t} \left[1 + \sigma t + \frac{(\sigma t)^2}{2!} + \frac{(\sigma t)^3}{3!} \right] + \ldots + \frac{(\sigma t)^{m-1}}{(m-1)!} \right\} \tag{4.31}$$

Some of the curves corresponding to this equation are shown in Fig. 4.44. These functions help to explain experimentally obtained dose-dependent effects.

This theory was extended by J. A. Crowther who introduced a *target area* into this concept. This means he transformed this formal target into a concrete area where the "hits" occur. For this he used the results of experiments with radiation of different wavelengths. As already stated, radiation leaves an ionization trail as it passes through an object. The density of ionizations along this path depends on the character of the radiation, i.e., of its quantum energy. Suppose a "hit" means an ionization of a quite specific molecule or a molecular configuration, then a certain volume must be sensitive to the radiation, which is called the *target area*.

Figure 4.45 schematically illustrates two experiments where a biological object with a given target area is irradiated by two kinds of ionizing radiation. In case A a radiation is used inducing a lower ionization density than in case B. Let us suppose that the biological reaction in this case is triggered by a single hit process, then in

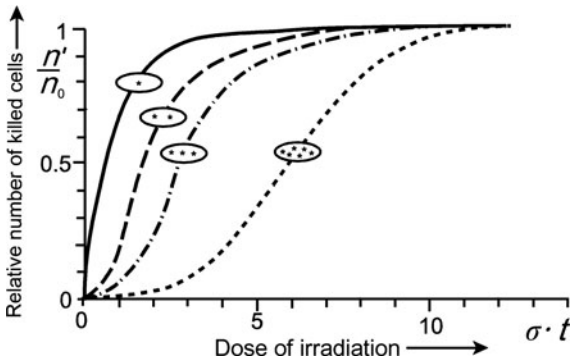

Fig. 4.44 Theoretical curves for one- and multi-hit processes (m corresponds to the number of stars in the "cell") (After Dessauer 1964)

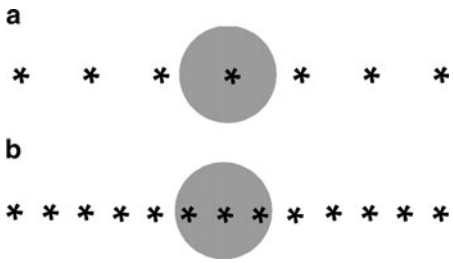

Fig. 4.45 Schematic illustration of the irradiation of a single target area (*circular area*) with a radiation of lower (**a**), and higher (**b**) ionization density. The points mark the locations of ionizations

case B the energy will be squandered because the diameter of the target area is larger than the mutual distance between two points of ionization. This theoretical prediction has been verified by experiments, relating particular dose-effect curves obtained in experiments where different types of radiation were applied.

In a similar way the target theory has been modified step-by-step in adaptation to experimental results. Meanwhile, a considerable number of additional factors have been taken into account influencing the course of radiobiological reactions. For example, it is possible to calculate a multi-hit process, the targets of which have different sensibility. Furthermore, it is possible to take into consideration also some processes of repair. For example, one can assume that in the course of a multi-hit process the efficiency of subsequent "hits" depends on the time period in between. Processes of energy transfer, including for example indirect effects, can be included. Of course any extension of the model leads to the introduction of additional parameters. This finally leads to ambiguous interpretation of experimental results. This seems to be the limit of the extension of these types of calculations.

Nevertheless, the target theory has achieved a certain importance in the analysis of various kinds of radiobiological effects. So, for example, mortality curves for bacteria have been characterized as multi-hit processes. Induction of mutations as a result of irradiation has also been analyzed by this formalism. Some mutations, even those of chromosomes, could be characterized as single-hit processes.

Further Reading

Dessauer 1964; Hug and Kellerer 1966; Kiefer 1990; Zimmer 1961.